Title

Understanding the paleoecology and niche dynamics of mammals in the Mascall Fauna (Middle Miocene), Oregon

Permalink

https://escholarship.org/uc/item/4vj6h69n

Author

Maguire, Kaitlin Clare

Publication Date

2013

Peer reviewed|Thesis/dissertation

Understanding the paleoecology and niche dynamics of mammals in the Mascall Fauna (Middle Miocene), Oregon

By

Kaitlin Clare Maguire

A dissertation submitted in partial satisfaction of the

requirements for the degree of

Doctor of Philosophy

in

Integrative Biology

in the

Graduate Division

of the

University of California, Berkeley

Committee in charge:

Professory Anthony D. Barnosky, Chair
Professor David D. Ackerly
Professor Ronald Amundson
Professor Joshua X. Samuels

Fall 2013

Understanding the paleoecology and niche dynamics of mammals in the
Mascall Fauana (Middle Fauna), Oregon

Abstract

Understanding the paleoecology and niche dynamics of mammals in the Mascall Fauna (Middle Miocene), Oregon
by
Kaitlin Clare Maguire
Doctor of Philosophy in Integrative Biology
University of California, Berkeley
Professor Anthony D. Barnosky, Chair

Understanding species-environment interactions through time is important for studying evolutionary processes such as taxonomic turnover. Studying this ecological interaction in the past sets a baseline for expected changes to occur given future environmental changes. Here I study species-environment interactions at the local and continental scale to understand how faunal composition, dietary niches, and climatic niches of species shift during periods of climatic and environmental change. A thorough revision of the Barstovian Mascall Fauna in Oregon provides an up-to-date faunal list and new ages for tuffs in order to examine faunal change at a local scale across a major climatic event, the mid-Miocene Climatic Optimum. Fifteen species are added and six synonymies are incorporated into the original faunal list. The Mascall Tuff, the most fossiliferous layer of the Mascall Formation, is dated at 15.3 Ma and the Kangaroo Tuff in the upper unit of the formation is dated at 13.6 Ma. Faunal comparisons to other Barstovian localities in North America reveal patterns of provinciality during this time. Faunal composition is consistent through the formation except for a turnover from browsing to grazing equids.

To examine this turnover in more detail, the dietary niches of four equid genera are reconstructed using stable carbon isotopes. Dietary niche partitioning is evident based on $\delta^{13}C$ values and tooth morphology: *Archaeohippus* was a small brachyodont equid with a narrow dietary niche most likely consuming crown leaf vegetation in the clearings of a woodland habitat; *Parahipppus* and *Desmatippus* were medium sized browsing equids with a broad dietary niche eating C3 browse in an open environment; and aff. *Acritohippus* was a larger grazer also with a broad dietary niche eating C3 grasses in an open environment. The dietary niches of these four genera did not change through time across the mid-Miocene Climatic Optimum. Extinction of the browsing genera, especially *Archaeohippus* with its narrow niche breadth, is most likely to do opening of habitats as C3 grasses spread after the mid-Miocene Climatic Optimum. There is no evidence of C4 vegetation in the diet of aff. *Acritohippus* suggesting it was not a dominant part of the vegetation in the Pacific Northwest during the Barstovian, in contrast to other regions of North America during that time.

Although the most common method of reconstructing niche space of extinct mammals is using stable isotopes to reconstruct their dietary niche, given other potential environmental proxy data, a more complete niche space of a species can be reconstructed in the fossil record. It is often difficult to obtain sufficient data to reconstruct entire environmental layers to study niche dynamics through time but proxy data can be obtained to examine the species niche in multivariate space. I test the potential for using this data to test for niche instability through time by studying the climatic niches of 15 mammalian species from the Last Glacial Maximum to the Recent. I find evidence supporting species niche shifts, primarily along the temperature axis, however the shifts are not greater than the shift in climate from the Last Glacial Maximum to the Recent. Therefore, species are shifting their realized niche space and are not evolving their

fundamental niche space. When studying niche dynamics in multivariate space in the fossil record, tests for realized niche stability are possible, however tests for niche evolution require background environmental layers and information on the size and shape of the fundamental niche space.

TABLE OF CONTENTS

1 The fauna and chronostratigraphy of the Middle Miocene Mascall type area, John Day Basin, Oregon.

2 The diets of equids across the mid-Miocene Climatic Optimum in Oregon, USA.

LIST OF FIGURES

LIST OF TABLES

ACKNOWLEDGMENTS

There are many people that made this research possible and helped me along the way. First and foremost, I would like to thank my committee: Tony Barnosky, David Ackerly, Ronald Amundson and Joshua Samuels. Their guidance and suggestions made me push harder and made the work better. I also want to thank my labmates: Jenny McGuire for orienting a new graduate student to such a large department; Susumu Tomiya for great paleoecology discussions and help with analyses through the years; Allison Stegner for endless amounts of statistical help and making me laugh through the process; and Natalia Villavicencio for stable isotope discussions and moral support I needed during the “crunch”. I owe a very special thank you to Pat Holroyd. Her endless patience with me as I bounced ideas off of her and her invaluable knowledge on everything “paleo” made my work better and my time at Berkeley extremely fulfilling.

I can’t thank the staff of John Day Fossil Beds National Monument enough for taking me under their wing and supporting my field research. I want to especially thank Joshua Samuels who taught me everything I know about taxonomic identification and was always happy to help me solve the mysteries of the Mascall formation and fauna. Thank you to Chris Scheirup for access to the collections and showing me proper curation techniques and thank you to Jennifer Cavin for help in the prep lab. And lastly, Liz Lovelock for encouraging me to work there and finding various grants to support my research. The John Day Fossil Beds is where I cut my teeth on paleontology and I appreciate all the opportunities they provided me.

There are too many people to thank for help with fieldwork but I would like to especially thank Paul Newsom and Tony Huynh for volunteering their summers to help me. I would also like to thank Samantha Hopkins, Edward Davis, Win McLaughlin and the entire Oregon University paleo crew for help in the field and letting me tag along on their field work. And a special thanks to my brother John; Tony, Emma and Clara Barnosky; and Rayaan and Mehdi Mohtashemi for bearing the heat and helping me in the field. I would also like to thank the many people on the John Day Fossil Beds paleo crew over the years for joining me in the very boring Mascall deposits.

I worked in many labs and museums across the western U.S. to complete this research. At Berkeley, I would like to thank Diane Erwin for help with the chemical lab in the UCMP; Alan Shabel for showing me how to prepare isotope samples; Todd Dawson and Stefania Mambelli for help in the Center for Stable Isotope Biogeochemistry at UC Berkeley; Wenbo Yang for running my isotope samples in the Laboratory for Environmental and Sedimentary Isotope Geochemistry at UC Berkeley; Liz Lovelock, Mark Schmitz and James Crowley of the Isotope Geology Laboratory at Boise State University for dating the tuffs in the Mascall Formation. For museum visits I would like to thank Edward Davis for access to the collections at University of Oregon, Sam McLoed for access to the collections at LACM and Ron Eng for access to the collections at the Burke Museum.

I would like to thank the following funding sources: The Evolving Earth Foundation, University of California Museum of Paleontology, Department of Integrative Biology, GeoCorps, NPS George Melendez Wright Climate Change Fellowship, Geological Society of

America, and Society of Vertebrate Paleontology. Without their generosity, I could not have completed any of the work presented here.

This work would not have been possible without my amazing support team. Thank you Chris for feeding me, reminding me why I love what I do, and most importantly always believing in me. Thank you Eve for always being there and for your delicious treats. And thank you to my parents; you may not know what I am doing or why I am doing it but you are always understanding and supportive.

To sum it up, I can't thank Tony enough for the support and encouragement through the years. And I feel so lucky to have been part of the wonderful UCMP community. The graduate students, staff and faculty have made my PhD experience rewarding. And like they say: "If you can survive presenting at Fossil Coffee, you can make it anywhere".

CHAPTER 1: THE FAUNA AND CHRONOSTRATIGRAPHY OF THE MIDDLE MIOCENE MASCALL TYPE AREA, JOHN DAY BASIN, OREGON

INTRODUCTION

The Mascall Formation, located in central Oregon amongst the well-known John Day Basin deposits, contains a robust Barstovian fauna (Fig. 1.1). Collection of the fauna dates back to the 1870s when field crews were sent by E.D. Cope and O.C. Marsh (Merriam, 1901; Prothero et al., 2006). J.C. Merriam of the University of California was the first to both describe the Mascall Formation and to do significant collecting therein (Merriam, 1901; Merriam and Sinclair, 1907). Theodore Downs, also of the University of California, continued focused fieldwork and analysis of the fauna during the 1940s and 1950s (Downs, 1956). By the time the Wood Committee (1941) published their treatise on the North American Land Mammal Ages, the Mascall fauna was considered to be a typical Barstovian assemblage. Later, with the establishment of the John Day Fossil Beds National Monument (JODA), park employees began to systematically collect the deposits, adding to and refining the faunal list, an activity that is still underway.

While the composition of this Pacific Northwest fauna shares similarities with other early Barstovian North American fauna, it exhibits some important differences that have caused some to regard the Pacific Northwest faunas to be different from other middle Miocene faunas (Pagnac, 2005; Tedford et al., 2004). In general, comparison of Barstovian faunas across North America suggests provincialism during this time. However, recent studies comparing Barstovian faunas have not drawn solid conclusions regarding the Mascall fauna because it has not been thoroughly studied since Downs (1956) (Pagnac, 2005). Complicating the comparison of the Mascall fauna to other Barstovian faunas is the fact that many published specimens have not been reported with adequate stratigraphic data, nor have their published identifications been updated with current taxonomy. Therefore a key goal of this paper is to provide the stratigraphic and taxonomic refinement needed to adequately compare the Mascall fauna with other Barstovian faunas, locally, regionally, and on the continental scale, which is a prerequisite to gaining insight into biogeographic patterns, paleoecological patterns, and evolutionary relationships. In addition, the Mascall fauna was one of the key faunas used in characterizing the Barstovian (Wood, 1941), making it all the more important to have an accurate stratigraphic and taxonomic framework.

Since the last comprehensive review of the Mascall Fauna was compiled by Downs (1956), systematic collecting by the staff at JODA has resulted in a much larger collection of fossils which I have included in this analysis. To build a more secure stratigraphic framework, I have attempted to date tuff layers from throughout the section; here I present dates for the Mascall Tuff, from which most of the fossils in the Mascall Formation have been recovered, and the KangarooTuff, the uppermost tuff in the type section (Bestland et al. 2008).

Geological Context

The stratigraphy and description of the Mascall Formation, which is about 610m thick and contains a series of paleosols with sporadic tuff and diatomite deposits, was recently reviewed by Bestland and others (2008). They subdivided it into three units (lower, middle and upper), based on stratigraphic marker beds (Fig. 1.2). The boundary between the lower and

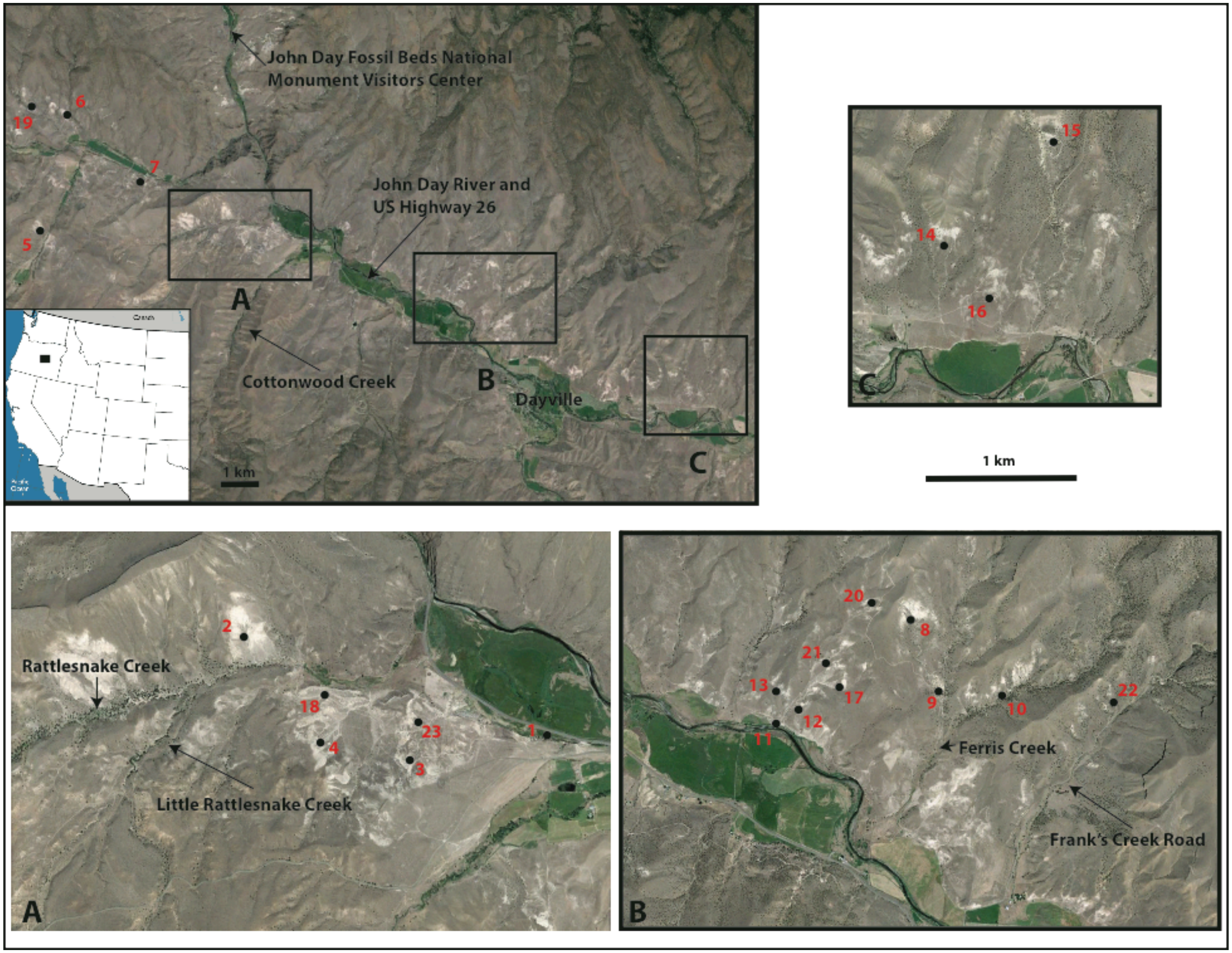
John Day Fossil Beds National Monument Visitors Center
John Day River and US Highway 26
Cottonwood Creek
Dayville
A
B
C
1 km
19
6
7
5
15
14
16
Rattlesnake Creek
Little Rattlesnake Creek
2
18
23
4
3
1
20
8
21
13
17
9
10
22
12
11
Ferris Creek
Frank's Creek Road

Figure 1.1 (Previous page). Map of the Mascall Formation type area with localities. Numbers correspond to localities in Table 1.1.

middle units is the base of the Mascall Tuff layer. The middle and upper units are separated by a prominent conglomerate interval. The majority of fossils are found in the lower and middle units with only fragmentary, well-worn specimens coming from the upper units. The Mascall Tuff, a reworked massive tuffaceous siltstone, preserves the majority of fossils known from the entire Mascall Formation (Bestland et al., 2008). This is Downs's (1956) unit 5 from which he recovered most of his material. The Mascall Tuff can itself be divided into two lithostratigraphically distinct beds, with only the lower one being fossiliferous. The upper, nonfossiliferous bed of the tuff is highly bioturbated and indurated, with sections of it containing loosely horizonated Inceptisols. Above the Mascall Formation in its type section is the late Miocene Rattlesnake Formation.

Chronostratigraphic Context

The Mascall Formation sits on top of the Dayville Basalt Formation of the Picture Gorge Basalt Subgroup. The Dayville Basalt Formation has been dated between 16.5 and 16.3 Ma paleomagnetically and radiometrically (Long and Duncan, 1982; Hooper and Swanson, 1990) and a tuffaceous paleosol within the Dayville Basalts was dated as 16.0 ± 0.2 Ma (dated by C.C. Swisher, presented in Sheldon 2006). These basalts are part of the larger Columbia River Basalt regime. A tuff in the lower part of the Mascall Formation was dated by Fiebelkorn et al. (1983) at 16.2 ± 1.4 Ma. Swisher (1992) dated a tuff (unit 2 of Downs (1956)) low in the Mascall Formation at 15.77 ± 0.07 Ma. Thus the base of the Mascall Formation seems to be about 16 Ma old (Bestland et al. 2008). Prothero et al. (2006) analyzed the magnetostratigraphy of the lower and middle Mascall and determined its correlation with Chrons C5Bn1n-C5Br giving the fauna an age of 14.8-16 Ma. The overlying Rattlesnake Formation has a prominent tuff bed, the Rattlesnake Ash Flow Tuff, dated at 7.05 ± 0.01 Ma (Streck and Gunder, 1995; Streck et al., 1999).

Environmental and Regional Context

The Mascall Formation begins at the height of the mid-Miocene Climatic Optimum (Zachos, 2001), a period of globally warmer temperatures and wetter conditions (e.g. Wolfe, 1981). Bestland et al. (2008) hypothesized the paleosols spanning all units of the Mascall Formation represent climatic optimum conditions. The mid-Miocene Climatic Optimum was followed by global cooling, beginning at 15 Ma, which appears to have been stepwise and regionally variable (Vincent and Berger, 1985; Flower and Kennett, 1993). It has been suggested that this cooling led to more open and presumably arid habitats, which in turn supported grazing mammals in heightened abundance (Wolfe, 1981; Downs, 1956). However, the paleosols of the Mascall Formation during this global cooling phase indicate wetter conditions than in other parts of the continent, such as the Great Plains. This may suggest that the Pacific Northwest received more rainfall during the post Mid-Miocene Climatic Optimum interval (Bestland et al. 2008).

There is a rich paleobotanical record in the lower horizons of the Mascall Formation. Chaney (1925) originally described the flora as an oak-madrone forest similar to those in Northern California today. He later revised this interpretation (Chaney, 1956), comparing the Mascall Flora to the deciduous forests of the Ohio River Basin and Szechuan China. Krull (1998)

Table 1.1 Recorded localities in the Type Mascall Formation area.

UCMP loc. no.	Loc. synonym	Name(s)	Notes	Map No.
-816	-	Cottonwood Creek 1	Possibly YPM “Cottonwood Creek”	
-882	-	Mascall Misc. 1		
-884	-	Mascall Misc. 2	See V4825	
-885	-	Mascall Misc. 3		
-886	-	Mascall Misc. 4		
-903	-	Old Sneider Ranch	See V4830-4835	
-3043	JDNM-262 UO 2993	Mascall Roadcoat		1
-3047	-	Mascall		
-3048	-	Mascall		
-3049	-	Mascall	See V4827	
-3059	JDNM-179	Mascall Bowl		2
-3063	-	Mascall	See V4823	
-3064	-	Mascall		
-3066	-	Mascall		
V4823	-	Mascall	Possibly UCMP -3063, possibly YPM “Mascall Ranch”, possibly YPM “1 mile west of Cottonwood Creek”	3
V4824	-	Mascall 10	Possibly YPM “Mascall Ranch”, possibly YPM “1 mile west of Cottonwood Creek”	4
V4825	JDNM-30	Mitchell Road, Confusion	Possibly UCMP -815, -817, -884, -887, -3042	
V4826	-	Mascall 12	No specimens	
V4827	JDNM-70	Mascall 13, Birch Creek	Possibly UCMP -3049	5
V4848	-	Mascall 14		6
V4829	JDNM-71A	Rock Creek		7
-	JDNM-71B	Rock Creek Southwest		7
-	JDNM-71C	Rock Creek South		7

Table 1.1 Continued.

UCMP loc. no.	Loc. synonym	Name(s)	Notes	Map No.
-	JDNM-71D	Rock Creek Southeast		7
V4830	JDNM-201	Mascall 16, Ferris Creek Bowl, Old Sneider Ranch, North of Dayville	Part of UCMP -903 (Old Sneider Ranch), part of LACM 1869 (North of Dayville)	8
V4831 (=V4913)	JDNM-264	Mascall 17, Old Sneider Ranch, North of Dayville	Part of UCMP -903 (Old Sneider Ranch), part of LACM 1869 (North of Dayville)	9
V4832 (=V4914)	JDNM-202	Mascall 18, Ferris Creek North, Old Sneider Ranch, North of Dayville	Part of UCMP -903 (Old Sneider Ranch), part of LACM 1869 (North of Dayville)	10
V4833 (=V4915)	-	Mascall 19, Old Sneider Ranch, North of Dayville	Part of UCMP -903 (Old Sneider Ranch), part of LACM 1869 (North of Dayville)	11
V4834	JDNM-260	Mascall 20, Old Sneider Ranch, North of Dayville	Part of UCMP -903 (Old Sneider Ranch), part of LACM 1869 (North of Dayville)	12
V4835	-	Mascall 21, Old Sneider Ranch, North of Dayville	Part of UCMP -903 (Old Sneider Ranch), part of LACM 1869 (North of Dayville)	13
V4941 (=V4912)	-	Mascall 22, Van Horn Ranch, Mackay Ranch		14
V4942	-	Mascall 23, Van Horn Ranch, Mackay Ranch		15
V4943	-	Mascall 24, Van Horn Ranch, Mackay Ranch		16
V4944	-	Mascall 25, Old Sneider Ranch, North of Dayville	Part of UCMP -903 (Old Sneider Ranch), part of LACM 1869 (North of Dayville)	17
V4945	-	Mascall 26		18
V4946	-	Mascall 27, McDonald Ranch		19
V6440	-		"Dayville 9.8 miles east", no specimens.	
V65400	-	Cottonwood Creek 5, YPM "*Ticholeptus* beds of Cottonwood Creek"		
V65405	-	Rattlesnake Creek Mascall		

Table 1.1 Continued.

UCMP loc. no.	Loc. synonym	Name(s)	Notes	Map No.
V67153 (=V6403)	JDNM-4	Mascall General, YPM John Day River/Valley	Includes -3506 (Rattlesnake Misc.) in part	
-	JDNM-261	Ferris Creek Below BLM Road		20
-	JDNM-263	West Mascall 20		21
-	JDNM-265	Frank's Creek Road		22
-	JDNM-266	Mascall Red Hills		23
-	CIT 113	Dayville	Unclear what area this encompasses	
-	CIT 183	Mascall Type Area, Near Rattlesnake Creek, West of Weatherford Ranch	Possibly -3059	
-	CIT 184	Mascall	Unclear what area this encompasses	
-	LACM 1869	North of Dayville and West of John Day Highway	Some of this locality overlaps with V4830-V4831, some of this locality overlaps with localities near Cottonwood and Rattlesnake Creeks. Specimens purchased from the Weatherfords were also assigned this locality number.	
-	LACM 5535	Mascall Area General	Unclear what area this encompasses	
-	LACM 3178	Rattlesnake Creek, Wheeler County	Unclear what area this encompasses	

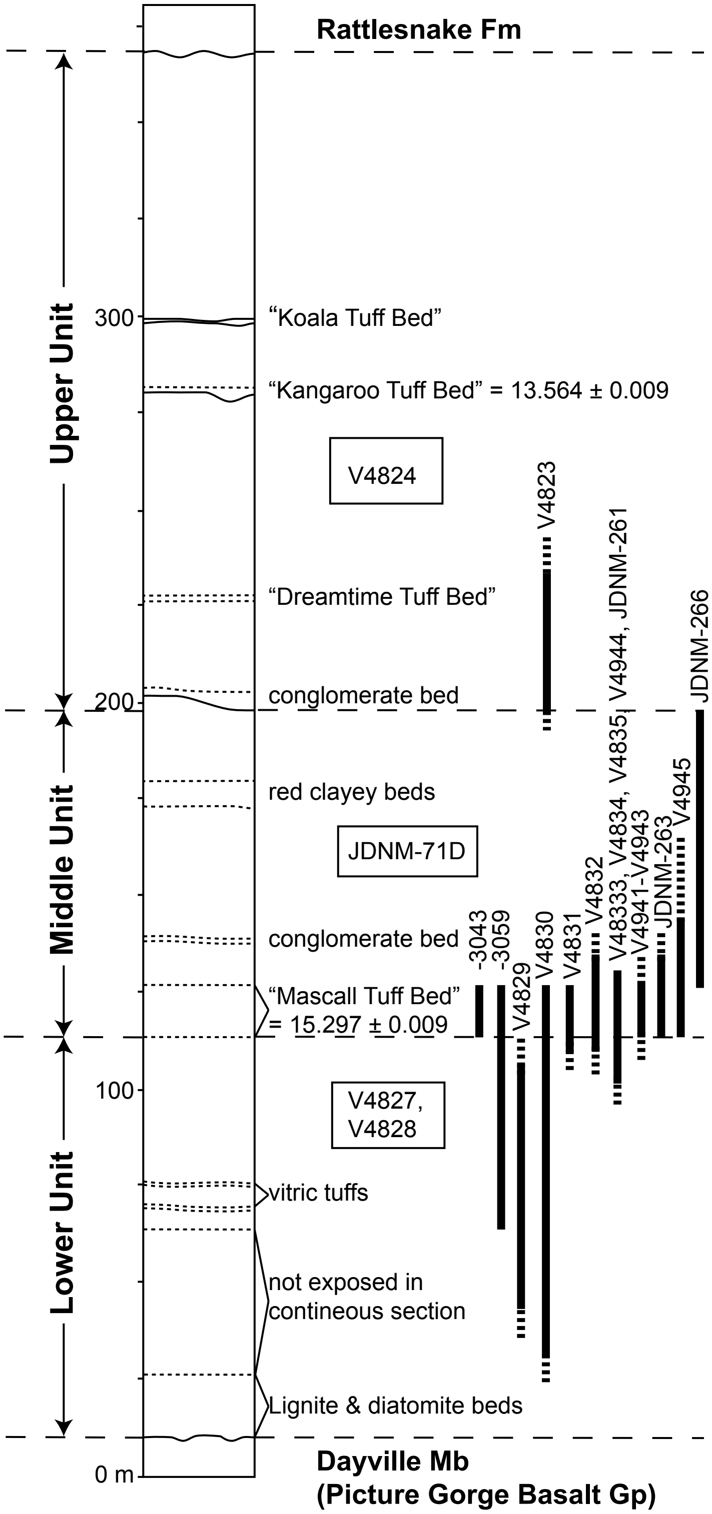

Figure 1.2 Stratigraphy of the Mascall Formation in the type locality (modified from Bestland et al., 2008). Stratigraphic ranges of localities are indicated by vertical lines. Dashed lines indicate uncertainty. Localities in boxes have unknown stratigraphic coverage but are known from the unit they are within. New radiometric dates are given for the Mascall and Kangaroo Tuff Beds.

comprehensively studied all the stratigraphic layers with paleobotanical material, and concluded that the Mascall "flora" is not a single, contemporaeous flora, but rather many stratigraphically, and thus temporally, separated samples of the plants growing in the area. In conjunction with the paleosol record which contains sequences of maturing and fining upward soils, the superposed plant horizons reveal shifts between a Mediterranean-like climate and a more humid subtropical climate with leaf size and diversity increasing upsection as paleosol units become more developed (Krull, 1998). Combining the paleobotanical record and the paleosol record, Bestland et al. (2008) concluded the Mascall Formation shifted back and forth through section between "a humid, temperate climate with both Mediterranean climatic aspects (dry, warm summer) and continental climate aspects (cool to cold winter)".

There are several deposits in the Pacific Northwest that may be similar in age and depositional environment to the Mascall Formation. The Simtustus Formation in the Deschutes Basin of central Oregon, approximately 100 km due west of the John Day Basin, overlays and interstratifies the Columbia River Basalt Group like the Mascall Formation and contains a similar fauna. Downs (1956), in fact, included the Gateway Locality (CIT 368 and V-3427) of the Simtustus Formation in his description of the Mascall fauna. The base of the Simtustus Formation is dated at 15.5 mya and the overlying Pelton Basalt is dated at 7.6 mya, with an unconformity between the two (Smith, 1986). The Simtustus Formation is dominantly fluvial and mixed pyroclastic and epiclastic sediments in contrast to the Mascall Formation that is dominantly lacustrine and pycroclastic sediments (Smith, 1986). Besides the Gateway Locality, Barstovian mammalian fossils have also been recovered from the Coburn Wells sites near Madras (JODA 248 and 249). Satellite imagery has revealed additional outcrop areas with potential for more fossil material. For the purposes of this faunal review, specimens from the Simtustus Formation (Coburn Wells and Gateway Localities) are not included; however, see the discussion below on regional faunal differences between all Mascall equivalent deposits.

Mascall-equivalent deposits located by the Crooked River, approximately 50 km south of the John Day Basin, also contain a Barstovian fauna. Downs (1956) considered these deposits as part of the Mascall fauna, but he listed the Mascall Type locality and Crooked River faunal lists separately. I do not include specimens from the Crooked River area in the type Mascall faunal list reported here because their geologic context and complex tectonic activity has not been determined. Localities that Downs (1956) considered as yielding components of the type Mascall fauna, but which I exclude here, are: Beaver Creek localities: V4949 (old -895), V4950 (old -897 and Osmont 7), Osmont 6(-896); Camp Creek locality V4951 (possibly old -900 and Paulina; Grindstone Creek (-901); Crooked River locality V4948. In addition, there is a more recently discovered locality in the Crooked River area, Cave Basin. The fauna recovered from this locality so far demonstrates similarities to the Mascall fauna *sensu stricto* (see below).

Farther away, in southern Oregon, the Butte Creek Volcanic Sandstone (in which the Beatty Buttes, Corral Butte and Fish Fin localities are found) contains an early Barstovian fauna. The Butte Creek Volcanic Sandstone also includes a late Barstovian fauna at the Red Basin localities in southeastern Oregon (Shotwell, 1968). Shotwell (1968) also collected late Barstovian fossils from the Quartz Basin localities in the Deer Butte Formation near Owhyee Reservoir, and from nearby localities that yielded the Skull Springs fauna from the Battle Creek Formation. To the east, across the Owhyee Reservoir, close to the Idaho border, is the Sucker Creek Formation, which contains an early Barstovian fauna. Numerous other Barstovian deposits are found throughout the western United States as described in Tedford et al. (2004) and include the faunas of the Virgin Valley Formation, Barstow Formation, Pawnee Creek Formation, Valentine Formation, and Olcott Formation.

MATERIALS AND METHODS

Institutional Abbreviations – **AMNH**, American Museum of Natural History; **CIT**, California Institute of Technology; **JDNM**, John Day Fossil Beds National Monument Locality; **JODA**, John Day Fossil Beds National Monument Specimen; **LACM**, Los Angeles County Museum; **RV**, University of California at Riverside Locality; **UCMP**, University of California Museum of Paleontology specimen; **UO**, University of Oregon Condon Museum; **YPM**, Yale Peabody Museum.
Measurement Abbreviations – **ap**, anteroposterior length; **t**, transverse length.

Specimen Collection

Over the 100+ years of collecting in the Mascall Formation the majority of specimens have been found as float material; however, some specimens are found *in situ*, particularly those from the Mascall Tuff (Unit 5 of Downs (1956). Screen washing has proven inefficient, because fossil material is not significantly abundant in any given horizon. Screen wash testing was performed on paleosol and channel deposits to recover microfossils. The paleosol deposits do not contain enough abundant material to make this approach beneficial and the channel deposits, which are in the upper member of the formation, do not contain fossil material.

Collection in the Mascall Formation occurred more or less continuously from the 1870s to the present. With the establishment of JODA, field crews have collected in the type area every year; however, not all sites in the type area are visited annually. In 1988, John Day Fossil Beds National Monument acquired an extensive collection of Mascall and Rattlesnake Formation specimens from the Grant County Chamber of Commerce. The specimens were originally collected by the Weatherfords, a local ranching family. Their property was on and surrounded by Mascall and Rattlesnake deposits. The two sons, Frank and Walter, collected fossils from these deposits, sometimes selling them to interested paleontologists such as to E.L. Furlong and C. Stock of UC Berkeley. Their collection contains some of the best representations of certain taxa in both the Mascall and Rattlesnake faunas. However, there is no locality information for any of the specimens and both brothers passed away before any of this data was relayed to JODA. In 1999, Elise Schloeder collected in the Mascall Formation, collecting valuable specimens that confirm species on the faunal list. During the summers of 2010 and 2011, I collected extensively in the Mascall Formation, adding new localities and placing specimens within the stratigraphic framework.

Taxonomic identification

Specimens collected from the Mascall Formation and curated at the UCMP, JODA, and LACM were identified by direct examination of comparable museum material and published descriptions. Taxonomy follows Janis and others (1998) and Janis and others (2008) unless otherwise noted. Measurements were taken with Folwer Sylvac digital calipers.

Localities and Biostratigraphy

Over many decades of collecting in the type Mascall area, several localities from multiple stratigraphic levels have been identified (Fig. 2). Early collections from the AMNH and the YPM have only descriptive names for specimen locations. Starting with collections made by J.C. Merriam of the UCMP, localities were numbered; however, exact location and stratigraphic level was not recorded. T. Downs (1956) established well georeferenced localities and tried to match old UCMP localities to his when possible. For example UCMP -903 (Old Sneider Ranch) encompasses UCMP V4831 through V4835 from Downs (1956). In addition, because local ranch ownership has changed, locality names have also changed. For example, Old Sneider Ranch is now referred to as the Clausen Ranch or Ferris Creek. And lastly, several institutions have collected in the type Mascall area. Each institution has used a different locality number or name for Mascall deposits. This is especially true when considering locality numbers given to general collections that are recorded from the Mascall type area (see Table 1.1). I have attempted to clarify and synonymize locality data in Table 1.1.

Localities were relocated using published records and field notes, indicated in Figure 1. These sites and specimens from the sites were assigned to one of the three Mascall Formation units. Also, extensive field surveys during the summers of 2010 and 2011 yielded additional fossil specimens that were placed in the stratigraphic framework. The stratigraphic range of each locality is presented in Figure 2. Because the Hemphillian age Rattlesnake Formation deposits are in close proximity and directly overlay parts of the Mascall Formation in the type area, there has been confusion regarding the provenance of some specimens. This is particularly true with earlier collections and those made by local ranchers. In addition, there is one locality (UCMP V4825) where the two formations outcrop and it is unclear which specimens originate from each deposit. Specimens from this locality can only be placed in a formation through taxonomic identification. Therefore specimens that represent species that range through the Barstovian (Mascall Formation) to Hemphillian (Rattlesnake Formation) have unknown formation origin. For the purposes of this study, specimens that fall into this situation are not included unless they are the only occurrence of the taxon in the Mascall, in which case it is noted and only tentatively assigned to the fauna. The same problem of provenence is true for specimens collected by the Weatherfords. Therefore, any specimen belonging to this collection is noted with an asterisk.

Radioisotopic Age Determinations

Samples of the four prominent tuffaceous layers (Mascall, Dreamtime, Kangaroo and Koala) in the Mascall Formation were collected for radioisotopic age determination. Of the four, two (Mascall and Kangaroo) contained a homogeneous population of zircons for analysis. U-Pb dates were obtained by laser ablation inductively coupled plasma-source mass spectrometry (LA-ICPMS) from spots placed on the zircons. Nine zircons were analyzed from the Kangaroo sample and 38 from the Mascall sample. Sample preparation and analyses were conducted by Elizabeth Lovelock, James Crowley, and Mark Schmitz in the Isotope Geology Laboratory at Boise State University using a ThermoElectron X-Series II quadrupole ICPMS and New Wave Research UP-213 Nd:YAG UV (213 nm) laser ablation system. Zircons were also analyzed by isotope dilution thermal ionization mass spectrometry (ID-TIMS) following previously published methods by Davydov and others (2010) and Mattinson (2005), and algorithms by Schmitz and Schoene (2007) and Jaffey and others (1971). 8 of the 10 original zircons from the Kangaroo sample were analyzed and 7 of the original 38 zircons from the Mascall sample were analyzed.

Faunal Comparisons

The Mascall faunal list was compared to compiled faunal lists for the following: early Barstovian Sucker Creek Formation fauna, early Barstovian Beatty Buttes fauna of the Butte

Creek Volcanic Sandstone Formation, early Barstovian Virgin Valley Formation fauna, early Barstovian Second Division fauna of the Barstow Formation, early Barstovian Green Hills fauna of the Barstow Formation, early Barstovian Lower Snake Creek fauna of the Olcott Formation, late Barstovian Red Basin fauna of the Butte Creek Volcanic Sandstone Formation, late Barstovian Quartz Baasin fauna of the Deer Butte Formation, late Barstovian Skull Springs fauna of the Battle Creek Formation, late Barstovian Pawnee Creek Formation fauna, late Barstovian Barstow fauna of the Barstow Formation, and late Barstovian Valentine Formation fauna. Faunal lists were compiled from the MIOMAP database (Carrasco et al., 2005) and Pagnac (2005).

These faunas are compared using the Jaccard, Bray and Raup-Crick similarity metrics (Hammer and Harper, 2006). The Jaccard index measures the similarity between two faunas and is defined as:

$$Jaccard\ Index = \frac{a}{a+b+c}$$

where a is the number of taxa in common between the two faunas, b is the number of taxa occurring in the first fauna but not the second fauna and c is the number of taxa in the second fauna but not the first fauna. For this analysis, a value closer to 1 indicates high similarity and a value closer to 0 indicates low similarity. The Bray Curtis metric is less sensitive to the size of the fauna and is defined as:

$$Bray\ Curtis\ Index = \frac{2a}{2a+b+c}$$

where the number of mutual presences is divided by the average number of taxa in the two faunas. As with the Jaccard index, a value closer to 1 indicates high similarity and a value closer to 0 indicates low similarity. Lastly, the Raup-Crick metric is the probability that two faunas will share the observed shared taxa compared to 200 randomly simulated faunas from the observed faunal lists using a Monte Carlo simulation; two identical communities will have an RC near 1 and those with no shared species near 0.

All faunas were also compared using the Ward's hierarchical cluster analysis on the similarity metrics described above as well as the following Euclidean similarity metrics: Euclidian, Canberra, Manhattan and Minkowski. Lastly, the faunal presence/absence matrix was analyzed using correspondence analysis to reduce all 13 faunas into two dimensions for comparison. All analyses were performed in R 3.0.2 for Mac OS X (R Core Team 2013).

RESULTS

Faunal List and Biostratigraphy

A revised faunal list for the Mascall fauna is presented in Table 1.2 along with biostratigraphic assignments to the lower, middle and upper sections of the formation. The majority of fossil specimens originated from the Mascall Tuff (Unit 5 of Downs (1956)) and in paleosols just below and above the tuff. Specimens in the upper member of the formation are rare and well-worn, indicating a high amount of transport. The scarcity of material in the upper member is peculiar given the similarity of the deposits to the lower and middle members of the formation (Bestland et al., 2008).

Patterns of faunal turnover are difficult to assess due to the unknown provenance of many specimens, specifically those collected by the Weatherfords, and low specimen counts for small-bodied taxa. However, some general trends for specific taxa can be discerned. Within Equidae, the low crowned genera, *Archaeohippus*, *Desmatippus* and *Parahippus* are only present in the lower and middle members of the formation while the high crowned *Merychippus* persists

Table 1.2 Vertebrate taxa from the type Mascall Formation and their stratigraphic range. Asterisks signify either collected by Weatherfords and/ or unknown stratigraphic provenance resulting in tentative placement on the faunal list.

Taxon	Stratigraphic Unit		
	Lower	Middle	Upper
Lipotyphla			
Soricidae			
Pseudotrimylus mawbyi	X	-	-
Talpidae	-	X	-
Carnivora			
Canidae			
Tephrocyon rurestris	X	X	-
Leptocyon cf. leidyi	X*	X*	-
Canidae indet.	X*	X	-
Amphicyonidae			
Cynelos sinapius	X*	X	-
Felidae			
*Pseudaelurus sp.**	n/a	n/a	n/a
Mustelidae			
Leptarctus oregonensis	X	X	-
Mustelidae indet.*	n/a	n/a	n/a
Procyonidae			
*Bassariscus lycopotamicus**	n/a	n/a	n/a
Lagamorpha			
Leporidae	X	X	X
Hypolagus fontinalus	-	X	-
Hypolagus parviplicatus	X*	X*	
Rodentia			
Castoridae			
Monosaulax indet.	-	X	-
Heteromyidae			
Balantiomys oregonensis	X*	X	-
Prodipodomys mascallensis	-	X	-
Geomyidae	-	X	-
Mylagaulidae			
Hesperogaulus gazini	X	X*	-
Mylagaulidae indet.	X*	X*	-
Sciuridae			
Nototamias	X*	X*	
Protospermophilus malheurensis	-	X	-
Protospermophilus oregonensis	X	-	-
Sciuridae indet.	X	X	X
Cricitidae	-	X	-

Table 1.2 Continued.

Taxon	Stratigraphic Unit		
	Lower	Middle	Upper
Rodentia indet.	-	X	-
Perissodactyla			
Equidae			
Cf. *Kalobatippus**	n/a	n/a	n/a
Desmatippus avus	X*	X	-
Parahippus indet.	X*	X	-
Archaeohippus ultimus	X	X	-
Merychippus species A	X	X	X
Merychippus species B	X	X	-
Rhinocerotidae	X	X	X
Artiodactyla			
Tyassuidae			
"Cynorca" hesperia	X*	X	
"Cynorca" sp.	X*	X	
Tayassuidea indet.	X	X	
Palaeomerycidae			
Dromomeryx borealis	X	X	
Rakomeryx sinclairi	X*	X	
Merycoidodontidae			
Ticholeptus zygomaticus	X	X	
Merycoidodontidae indet.			
Camelidae			
Miolabis transmontanus	-	X	-
Cf. *Procamelus*	-	X	-
Camelidae	X	X	-
Moschidae			
Blastomeryx gemmifer	X(?)	X	X(?)
Parablastomeryx	X*	X*	-
Proboscidea			
Zygolophodon proavus	X*	X*	
Proboscidea indet.	X	X	X(?)

throughout. This shift from an equid fauna that includes both low- and high-crowned equids initially to exclusively high-crowned equids in the time represented by the upper member is seen throughout North American faunas, most likely a results of high-crowned equids evolving at the same time grassland environments spread (Janis et al., 2002). Leporidae are present in all units of the formation and represented by multiple species. Sciurids also span all three units of the formation. Lastly, rhinoceroses span the entire formation. However the presence of only durable specimens from equids and rhinocerids in the upper unit is most likely a taphonomic artifact. All species but two (*Pseudotrimylus mawbyi* and *Protospermophilus oregonensis*) are found in the middle unit because the Mascall Tuff is in the middle unit, therefore high diversity of the middle unit probably simply reflects that the tuff yields the most fossils. The majority of species are also present in the lower unit; and absences may well be due to taphonomic or sampling issues, especially for small bodied mammals.

The fossiliferous horizons of the Mascall Formation (the lower unit and lower sections of the middle unit) are assigned to the early Barstovian (Ba1) based on: 1) the presence of *Zygolophodon*, *Hesperogaulus*, and *Monosaulax*, which have first occurrences during the early Barstovian; 2) that they contain *Desmatippus*, *Parahippus*, *Cynorca*, and *Rakomeryx*, which have their last occurrence during the early Barstovian; and 3) the presence *Tephrocyon*, which had a limited temporal occurrence during this time period (Tedford et al. 2004). Although the Mascall Formation deposits extend into the late Bastovian (upper deposits of the middle unit and the upper unit) as inferred by U/Pb dates reported here there are no defining taxa found in these horizons. Without accurately located diagnostic taxa or a better independent chronology, i.e., more dated tuffs or magnetostratigraphy in the middle and upper units, it is difficult to precisely place the boundary between the early and late Barstovian in the type Mascall area.

Systematic Paleontology

Reported here are the specimens that warrant description, either because they record a new occurrence of a taxon to the Mascall Formation or because they were synonymized with taxa thought previously to be taxonomically distinct. The remainder of the fauna is presented in the Supplementary Data. The faunal list (Table 1.2) is a compilation of the specimens discussed here and in Supplementary Data File S1.3. Localities with an asterisk indicate the specimen was collected by the Weatherfords.

Class MAMMALIA Linnaeus, 1758
Order SORICOMORPHA Gregory, 1910
Family SORICIDAE Fischer von Waldheim, 1817
Genus PSEUDOTRIMYLUS Gureev, 1971
Pseudotrimylus mawbyi Repenning, 1967
Fig. 1.3

Occurrence – JDNM-71.
Referred Material – Left dentary fragment with m1-m3, JODA 13865.
Description – Referral to this taxon was based on the following diagnostic characters: m1 is low crowned with inflated cingulum; entoconid is a blunt cuspid detached from metaconid and thoroughly merged with the hypolophid; metalophid joins protolophid more labially than in other species of the genus; talonid of the m3 has cresentic loph, is not distinctly bicuspid and is very small compared to the m1; the stout molars are far to the rear relative to the anterior edge of the ascending ramus; mental foramen is below the talonid of the m1 and placed in a depression on the labial side of the dentary that leads to the premolar region anterodorsally (Repenning 1967).
Comments – Repenning (1967) described the new species *Trimylus mawbyi* from UO 19486, found five miles southwest of the south end of Guano Lake in Lake County, Oregon. He placed it within the Barstovian and noted that the associated fauna is "virtually identical to that from the Mascall Formation". OU 19486 was originally described and assigned to *Heterosorex* by Mawby (1960) who also noted the specimen was from a Mascall Formation equivalent. Additional referred specimens for the species are from the Beatty Buttes fauna, age equivalent to

the Mascall Formation (Repenning, 1967; Gunnell et al. 2008). The species was reassigned to *Pseudotrimylus* by Gunnell and others (2008).

Family TALPIDAE Fischer von Waldheim, 1817
(Fig. 1.4)

Occurrence – JDNM-226.
Referred Material – Radius, JODA 15537.
Description and Comments – This is the only known specimen of Talpidae from the Mascall Type deposits. It was collected *in situ* from the Mascall Tuff. Its length is 6.88 mm. While not reported previously from the Mascall Formation, talpids are common from other mid Miocene sites in Oregon (Hutchison, 1968).

Order CARNIVORA Bowdich, 1821
Family CANIDAE Fischer, 1817
Subfamily CANINAE Gill, 1872
Genus LEPTOCYON Matthew, 1918
Leptocyon cf. leidyi Tedford, Wang, Taylor, 2009
(Fig. 1.5)

Occurrence – JDNM-4*.
Referred Material – Right dentary fragment with lower p3 and p4, JODA 2312; right dentary fragment with lower p4, JODA 2313.
Description – Referral to *Leptocyon* is based on the fact that both specimens display diastemata separating the premolars (characteristic of *Leptocyon* and *Vulpes*) and the presence of weak premolar cusplets (Tedford et al., 2009). As described by Tedford and others (2009), the lower premolars are lower crowned (note the p3 of JODA 2312) than the late Barstovian and Clarendonian *L. vafer*. Dimensions of the premolars fall within the range of *L. leidyi*; however, definitive diagnostic elements are not preserved. Measurements for each are JODA 2312: p3 ap=5.38 mm, p4 ap=6.82 mm, t=3.03 mm; JODA 2313: p4 ap=7.48 mm, t=3.01mm.
Comments – Specimens were collected by the Weatherfords without records of provenance, making it difficult to place them into a stratigraphic framework. A lower m2 (field # JDBLM13-24C) of *Leptocyon leidyi* was recovered by JODA staff from Cave Basin in 2013; diagnosis is based on absence of the m2 paraconid and overall tooth dimensions. Occurrence of *L. leidyi* in the Mascall Formation is not surprising given its wide distribution in the early Barstovian, including records from California, Colorado, Montana, Nebraska, and New Mexico (Tedford et al., 2009).

Canidae indet.

Occurrence – JDNM-4, JDNM-4*.
Referred Material – From JDNM-4: left calcaneum, JODA 4282; upper P2, JODA 6413. From JDNM-4*: left calcaneum, JODA 15283; lower premolar, JODA 2393.
Description – The two calcanea, JODA 4282 (ap=33.91 mm, t=14.18 mm) and JODA 15283 (ap=36.8 mm, t=17.55 mm), are similar in size especially when you take into account that JODA 4282 is significantly worn, which accounts for its smaller size. JODA 6413 is a large P2 with an

anteroposterior length of 8.13 mm and a transverse width of 3.95 mm. It may represent a larger canid or belong to *Tephrocyon*. JODA 2393 has an anteroposterior length of 9.27 mm and a transverse width of 5.821 mm.

Family AMPHICYONIDAE Haeckel, 1886
Genus CYNELOS Jourdan, 1862
Cynelos sinapius Matthew, 1902

Occurrence – CIT 113, UCMP V4835, JDNM-4*.
Referred material – From CIT 113: right dentary with lower third incisor through m2, CIT 207. From UCMP V4835: left calcaneum, UCMP 39304. From JDNM-4*: right M3, JODA 2315.
Description and Comments –The fourth premolar through second molar of CIT 207 have broken crowns; p1-p3 are worn and the canine is heavily worn on the medial side. Stock (1930) assigned CIT 207 to *Amphicyon sinapius* based on comparisons with specimens from the lower Snake Creek and Pawnee Creek beds. *A. sinapius* was recombined as *Cynelos sinapius* by Hunt (1998). Confirmation of identification is based on the size of m1 (ap=38 mm) which falls within the range reported in Hunt (1998). In addition, the lower third premolar is the same size as p2 and neither have accessory cusps. p1 is lost and p4 does not have posterior accessory cusps. Overall the premolars are slender and laterally compressed and m2 is rectangular. The locality description is listed as Dayville, Oregon so exact location in unknown, however Stock (1930) mentions that the specimen was found in Mascall deposits and he was aware of issues associated with Rattlesnake and Mascall faunas mixing in the area. UCMP 39304 has a maximum anteroposterior length of 85.07 mm and transverse width at the sustentaculum of 42.6 mm. It is assigned to *C. sinapius* based on size, however, this is a tentative identification. JODA 2315 is also tentatively assigned to *Cynelos sinapius*. It has an anteroposterior length of 10.23 mm and a transverse width of 15.48 which is small for the species. However, it was collected by the Weatherfords; if it came from the Rattlesnake it would mean either that *Cynelos sinapius* ranges higher than the Mascall, or that there is a Hemphillian amphicyonid with very similar morphology.

Family FELIDAE Gray, 1821
Genus PSEUDAELURUS Gervais, 1850
Pseudaelurus sp.
(Fig. 1.6)

Occurrence – JDNM – 4*.
Referred material – Right complete astragulus, JODA 15306.
Description and Comments – The size of this astragulus (length = 35.88 mm, width at trochlea facet = 20.08 mm, width at head = 19.46 mm) is the same as *Puma concolor* (length = 36.60 mm, width at trochlea facet = 20.86 mm, width at head = 20.28 mm) however the neck is longer and the head is oriented more perpendicular to the trochlea facet. Shotwell (1986) found an upper canine, lower m1 and a fragment of a P4 (UO 23469) of a similarly large felid from Red Basin locality 2495. The m1 measures 16.1 mm, close in size to a specimen assigned to *Puma concolor*, which measured is 15.6 mm (Rothwell, 2003). Three species of *Pseudaelurus* exhibit similar m1 lengths whose range overelaps the aforementioned specimens (*P. validus*, *P. intrepidus*, *P. marshi*) (Rothwell 2003) and therefore I cannot identify this specimen to species.

JODA 15306 was collected by the Weatherfords, therefore exact provenance is unknown; however, the last appearance of *Pseudaelurus* in North America is during the late Barstovian (Rothwell, 2003), which would be consistent with the occurrence in the Mascall, although it is impossible to say whether or not the specimen was actually recovered from the Mascall or Rattlesnake.

Family MUSTELIDAE Fischer, 1817
Genus MARTES Frisch, 1775
Mustelidae indet.

Occurrence – UCMP V67153.
Referred Material – Left dentary fragment with p4-m1 and alveoli for m2, UCMP 39958.
Description and Comments – UCMP 39958 is described in Downs (1951). The talonid and tragonid are about equal in length. The talonid is slightly basined with an internal cingulum that merges with the metaconid. The hypoconid is separated from the protoconid by a deep, worn groove. The tragonid is open with a medium sized metaconid, posterior to protoconid. The p4 has a posterior notch. It is unlike the Barstovian mustelid *Plionictis* in that the trigonid of m1 is not much longer than the talonid and the talonid is not narrow. It is too small to be *Sthenictis*, another Barstovian mustelid. The talonid is basined as in *Martes*. It was originally identified as *Martes* (Downs, 1951); however, Sato et al. (2003) suggested the oldest true *Martes* is from the Pliocene of Poland, and Anderson (1994) suggested the extant *Martes americanum* is a late Pleistocene immigrant to North America. Locality is unknown (V67153 is assigned to specimens with no locality information for the Mascall Formation). Specimen tag says Mascall or Rattlesnake Formation. Downs (1951) mentions UCMP 39958 and states “it cannot be considered a valid Mascall allocation” (pg. 102). Given the material, more precise taxonomic identification is not possible and it remains unknown if this specimen belongs to the Mascall or Rattlesnake Formation.

Family PROCYONIDAE Gray, 1825
Subfamily PROCYONINI Gray, 1825
Genus BASSARISCUS Coues, 1887
? Bassariscus lycopotamicus Cope, 1879

Occurrence – “Loup Fork of Cottonwood Creek” (Cope 1879, p.67).
Referred Material – No specimen number available.
Description – The type specimen, a lower jaw described by Cope (1879), has been lost but is figured in Cope and Matthew (1915). Gregory and Downs (1951) provide the taxonomic history of this specimen. They also provide a thorough description of the specimen and assign it to ? *B. lycopotamicus*.
Comments – Cope (1879) only mentions “Loup Fork of Cottonwood Creek” for locality information therefore making it impossible to assign this specimen to either the Mascall or the Rattlesnake Formation. Gregory and Downs (1951) mention a second specimen attributable to this species from Paulina Creek (YPM 14313) but state their uncertainty of whether it came from Miocene or Pliocene deposits.

Order LAGOMORPHA Brandt, 1885
Family LEPORIDAE Fischer von Waldheim, 1817
Genus HYPOLAGUS Dice, 1917
Hypolagus fontinalis Dawson, 1958
(Fig. 1.7)

Occurrence – UCMP V4833.
Referred Material – From UCMP V4830: left lower p3, UCMP 41205; left lower p3, JODA 4283.
Description – UCMP 41205 has a posteriorly inflected posteroexternal reentrant (PER) and a well-incised anteroexternal reentrant (AER). PER is larger than in *H. parviplicatus*. The third premolar has an anteroposterior length of 3.04 mm and transverse width of 2.42 mm. This falls between the average measurements for *H. fontinalis* and *H. parviplicatus* in Voorhies and Timperley (1997), but within the range of variation of the former. Based on the posteriorly inflected PER and smaller size than *H. parviplicatus* this specimen is assigned to *H. fontinalis*. The PER on JODA 4283 is not inflected posteriorly and there are no crenulations on the thin enamel of the PER (TN). The anteroposterior length is 2.86 mm and the transverse width is 2.1 mm falling within the size rang for *H. fontinalus* (Voorhies and Timperley, 1997). This specimen is placed in this taxon based on the uncrenulated TN and size.
Comments –This is the first record of this species in the Barstovian of Oregon. It differs from other Barstovian species (*H. tedfordi*, *H. parviplacatus*, *H.* cf. *voorhiesi*) (White, 1988) in the following ways: it differs from *H. tedfordi* in the posterior deflection of the PER and its larger ap length; it differs from *H. parviplicatus* in its smaller size, more well-incised AER, and an uncrenulated TN on the PER, and from all other species of *Hypolagus* in having a shallower incision of the PER.

Hypolagus parviplicatus Dawson, 1958
(Fig. 1.7)

Occurrence –JDNM-4*, CIT 183*.
Referred Material – From JDNM-4*: left lower p3, JODA 2326; left lower jaw with p3 through m2, JODA 2328. FROM CIT 183: lower right p3, CIT 4002.
Description – JODA 2326 does not have an inflected PER, AER is very shallow, thick enamel in PER (TH) is crenulated, ap=3.07 mm and t=3.15. The transverse width places this specimen within the size range of *H. parviplicatus* ((Voorhies and Timperley, 1997)Voorhies and Timperley, 1997). The p3 of JODA 2328 has a shallow AER, the PER is straight with no crenulations on the TN, ap=3.04 mm and t=3.26 mm also consistent with placing the specimen in *H. parviplicatus* as well. CIT 4002 has a shallow AER and the PER does not inflect posteriorly. Unfortunately, the PER is not well-preserved enough to make out whether the TN is crenulated, characteristic of *H. parviplicatus*. The specimen has an anteroposterior length of 2.96 mm and a transverse width of 3.01 mm which is on the smaller end of the size range of the species, closer to *H. fontinalus*.
Comments – CIT 4002 also contains three lower molars and one upper molar. All of these specimens were found in isolation by Weatherfords; therefore, I am hesitant to attribute them to the same species as CIT 4002, given that they cannot be distinguished morphologically and such assignment would be based on presumed age, thus introducing circularity. Instead, the

Weatherford specimens are referred to Leporidae indet. and discussed below. This is the first record of this species in Oregon. The specimens differ from other Barstovian species of *Hypolagus* in the following ways: it is larger and has a less well incised AER than *H. fontinalis* and *H. tedfordi* and from all other species in its less incised PER.

Leporidae indet.

Occurrence – UCMP V4830, UCMP V4832, UCMP V4834, JDNM-4*, CIT 183*, JDNM-266 JDNM-71, JDNM-270.
Referred Material – From UCMP V4830: ilium and ischium, UCMP 41204; proximal left third metatarsal, JODA 15318. From UCMP V4832: proximal end of tibia, UCMP 41211; left upper and lower molars, UCMP 39299; left jaw fragment with lower m1 and incisor, UCMP 39294. From UCMP V4834: upper molars, JODA 4253 and JODA 4256; two lower molars, one upper molar, and 1 incisor, JODA 15294; proximal second metatarsal, JODA 15291, right partial calcaneum, JODA 15742. From JDNM-4*: upper molars, JODA 2325 and JODA 2327. From CIT 183*: 3 lower molars and 1 upper molar, CIT 4002; 5 premolars, CIT 4002A. From JDNM-266: 3 podial phalanges and distal phalanx, JODA 15517. From JDNM-71: upper molar, JODA 3330. From JDNM-270: left calcaneum, JODA 15633.
Description – UCMP 41211, a proximal tibia, measures 13.75 mm anteroposteriorly and 13.75 mm transversly. Some of the molars listed above are within the size range of and could be attributed to *H. fontinalus* and others are larger and could represent *H. parviplacticus* but because they are not diagnostic they are not assigned to either species. Measurements for each are JODA 4253: ap=2.21 mm, t=4.06 mm; JODA 4256 ap=2.37 mm, t=3.61 mm; JODA 2325: ap=2.69 mm, t=4.76 mm; JODA 2327: ap=2.11 mm, t=3.68 mm; UCMP 39299: lower molar ap=2.67 mm, t= 2.51 mm and upper molar ap=2.13 mm, t=3.68 mm; UCMP 39294: ap=2.56 mm, t=2.94 mm; JODA 15294: lower molars ap=2.8 mm, t=3.33 mm and ap=2.38 mm, t=2.5 mm, upper molar ap=1.91 mm, t=2.95 mm, and incisor t=2.35 mm. JODA 15633, a complete left calcaneum, has a length of 25.37 mm and width at the proximal end of 6 mm. JODA 15742, an incomplete right calcaneum, has a width of 4.52 mm at the proximal end.
Comments – Downs (1956) identified CIT 4002 (right lower p3, 4 right lower molars and one upper molar) as cf. *H. vetus*. The lower p3 is reidentified as *H. parviplacitus* and the remaining specimens are not identified further than Leporidae because they do not contain diagnostic features. JODA 15633 confirms the presence of leporids in the upper member of the Mascall Formation making this taxon one of only four that spans the entire formation. JODA 15742, also a calcaneum, is smaller than 15633, suggesting more than one species of leporids in the Mascall fauna.

Order RODENTIA Bowditch, 1821
Family HETEROMYIDAE Gray, 1868
Genus BALANTIOMYS Korth, 1997
Balantiomys oregonensis Gazin, 1932
(Fig. 1.8)

Occurrence – CIT 1869*, UCMP -3043, UCMP V4823.

Referred Material – From CIT 1869: left dentary with p4-m3, CIT 4001; isolated P4, M1, M2 and M3, CIT 3999. From UCMP -3043: left dentary with dp4 and partial m1, JODA 3767. From UCMP V4823: upper right M3, JODA 15648.

Description – CIT 4001 is tentatively placed in this genus on the following characteristics of the p4: metalophid cusps large and subequal in size, no anterioposterior valley between the metconid and protstylid, anterostylid on anterior slope of protostylid. Korth (1997) has *B. oregonensis* as the only species belonging to the genus outside of the Great Plains. CIT 3999 is also tentatively placed in this genus following Downs (1956). JODA 3767 is the first occurrence of a dp4 for the species (Fig. 8). The posterior cingulum is broad anteroposteriorly connecting centrally to the hypoconid and entoconid. The hypoconid and entoconid are equal in size. The central enamel ridge connects to the protosylid. The protoconid/metaconid complex is crescent shaped.

Comments – Full descriptions and a thorough discussion of CIT 3999 and 4001 are in Downs (1956). Overall, the specimens are fragmentary and well worn, therefore, making identification difficult. Both specimens are from the Bode collection of 1929 and assigned to CIT location 1869. CIT 4001 is labeled from "West of Dayville Highway" and was purchased by the Weathfords. CIT 3999 is labeled from "North of Dayville". Downs (1956) identified UCMP 442, a partial skull with P4 through M3, as *Peridiomys* cf. *oregonensis* and claims it is from the Mascall based on this identification even though it was originally assigned to the Hemingfordian of the John Day Formation. It is not an entoptychine based on the protoloph shape of the P4, however, the amount of wear makes it impossible to assign this specimen to *B. oregonensis* rather than to another primitive heteromyid. An additional specimen from CIT 1869, CIT 4000, is a dentary with heavily worn p4-m2 making identification beyond Heteromyidae difficult, however it does fall within the size range of *B. oregonensis.*

Family GEOMYIDAE Bonaparte, 1845

Occurrence – UCMP -3043.

Referred Material – Dentary fragment with p4-m2, JODA 3770.

Description – The m1 and m2 of this specimen are broken down the middle but remain largely intact. All three teeth are heavily worn. The metalophid on the p4 is wide, flattened anteriorly and has broad connection with the hypolophid. The hypolophid has three cusps. This specimen is placed in Geomyidae based on the premolar's larger size than the molars.

Comments – This specimen is similar to the entoptychine, *Gregorymys,* by having p4 longer than the m1 and a hypolophid with three cusps (Flynn et al., 2008). It is unlike the Barstovian Geomyinae, *Parapliosaccomys,* because the metalophid is wide and it is too small to be *Geomys*. It may be *Gregorymys*, however; there is no anterior cingulum on the p4, but this character is known to be variable in the genus (Flynn et al., 2008).

Family MYLAGAULIDAE Cope, 1881
Genus HESPEROGAULUS Korth, 1999
Hesperogaulus gazini Korth, 1999

Occurrence – UCMP V4827, JDNM-4*.

Referred Material – From UCMP V4827: Almost complete skull with partial P4 and complete M3, JODA 3308; From JDNM-4*: M2, JODA 2330.

Description – Specimens are described in Calede and Hopkins (2012).

Comments – A third specimen of this species (JODA 8678) is from Coburn Wells in the Simtustus Formation, a Mascall equivalent approximately 70 miles west of the type locality for the formation.

Mylagaulidae indet.

Occurrence – JDNM-4*, UCMP -3059*.
Referred Material – From JDNM-4*: Partial left dentary with dp4-m2 and erupting p4, JODA 2329. From UCMP -3059: right partial dentary with m1-m2 and erupting m3, UCMP 39292.
Description – JODA 2329 is described in Calede and Hopkins (2012). UCMP 39292 has quadrate m1 with 5 fossettes and two roots, more ovoid m2 with 5 fossettes and an unworn m3 with pronounced metaconid.
Comments – Because JODA 2329 is a juvenile specimen, Calede and Hopkins (2012) did not assign it to a species but suggested it is either *Alphalagus vetus* or *Hesperogaulus gazini*. *A. vetus* has been recovered from Mascall age equivalent deposits in the Crooked River region to the south, but has not been identified from the type Mascall area to-date. It was found by the Weatherfords and therefore the exact locality is unknown. UCMP 39292 may also belong to *A. vetus* or *H. gazini* based on size but without the p4 it is impossible to identify further.

Family SCIURIDAE Gray, 1821
Genus PROTOSPERMOPHILUS Gazin, 1930
Protospermophilus oregonensis Downs, 1956

Occurrence – UCMP V4828.
Holotype – Left dentary with i1, p4-m3 and without coronoid and condylar processes, UCMP 39093.
Referred Material – left p4, UCMP 40241 (paratype).
Description – The type and paratype are described in Downs (1956) and Black (1963).
Comments – Downs (1956) assigned the species to *Arctomyoides* and Black (1963) reassigned it to *Protospermophilus*. The locality, UCMP V4828, is in deposits typical of a marginal lacustrine environment and possibly from the earliest sections of the formation (Downs, 1956). I did not visit this site because it is on inaccessible private land; however, the other Mascall sites in the area (which I did visit) are in the Lower Mascall, consistent with the interpretation in Downs (1956).

Protospermophilus malheurensis Gazin, 1932

(Fig. 1.9)

Occurrence –JDNM-4.
Referred Material – Left M1, JODA 6416.
Description – The M1 is quadrate with four transverse lophs. It is assigned to this taxon based on the following: all of the lophs unite at the protocone; the first loph is convex forward and attaches to the protocone lingually; the second loph is straight and has a small protoconule; the third loph is convex posteriorly, has a metaconule and unites with the metacone; the fourth loph is convex posteriorly and outward from the protocone and unites with the metacone labially. There is a small cuspule between the paracone and metacone.

Comments – This is the first occurrence of this species in the Mascall Formation. It was recovered as float 2 m below the Mascall Tuff in the type area. The species was originally described at *Sciurus tephrus* by Gazin (1932) from the laterally equivalent Skull Springs locality (Butte Creek Volcanis Sandstone Formation) in southeastern Oregon.

Genus NOTOTAMIAS Pratt and Morgan, 1989

Nototamias indet.

(Fig. 1.10)

Occurrence – JDNM-4*
Referred Material – Left dentary with incisor, p4-m3, JODA 2331.
Description – Lower molars lack mesoconid and mesostylid. It is difficult to see if the metalopohid is complete enough to enclose the trigonid valley. In addition, the poor quality of the specimen makes it difficult to assess the presence of a proximobuccal groove at the junction of the protolophid and protoconid. Anteroposterior length of the m2=1.4mm.
Comments – The lack of a mesoconid on the lower molars places this specimen in *Nototamias* and not *Tamias*. Other characters are difficult to assess due to the poor quality of the specimen, making it impossible to assign it to a species. Although similar in size and morphology to *Nototamias ateles*, it cannot be assigned to that species because the enclosure of the talonid is not confirmed. Whether that species belongs to *Nototamias* or *Tamias* is debated (Sutton and Korth, 1995; Wilson and Reeder, 1993; Pratt and Morgan, 1989), because of the mixture of characteristics of both genera and confusion about the fusion of the lower molar roots. I follow Goodwin (2008) in placing this specimen in *Nototamias* and suggesting affinity to *N. ateles* recognizing that future revision may place it in *Tamias.* The higher taxonomic consequence of assigning it to *Nototamias* rather than *Tamias* would be to place the species outside the true chipmunck group, Tamini.

Sciuridae indet.

Occurrence – UCMP V4823, JDNM-4, JDNM-70, JDNM-71.
Referred Material – From UCMP V4823: right calcaneus, JODA 15794. From JDNM-4: distal ulna, JODA 15750. From JDNM-70: right distal tibia, JODA 4278. From JDNM-71: incisor fragment, JODA 15769.
Description – Length of JODA 15694, right calcaneus, is 7.7 mm. The right distal tibia, JODA 4278, is similar in shape and size to *Sciurus niger.* The incisor is oval in cross section with a larger anteroposterior length than transverse width, therefore, belonging to Sciuridae.
Comments – This fragmentary postcranial material and incisor demonstrate the persistence of squirrels through the lower, middle and upper units of the Mascall Formation. JODA 15750 was collected from the Mascall Tuff in the type area. JODA 15794 was most likely collected from the upper unit deposits close to V4823.

Family CRICETIDAE Fischer von Waldheim, 1817

Occurrence – UCMP V4834.
Referred Material – Incisor, JODA 4957.

Description – The incisor is a long oval shape (deeper than wide) in cross section with a curved face, bearing no ornamentation. The incisor has a length of 11.92 mm.
Comments – *Copemys* (known from the Barstovian Sucker Creek, Quartz Basin and Skull Springs locality) has an incisor size and shape consistent with this specimen and similarly lacks ornamentation (Lindsay, 2008). The eomyids *Pseudadjidaumo* (known from the Barstovian Quartz Basin locality) and *Leptodontomys* (known from Clarendonian and Hemphillian localities in Oregon) are far smaller than *Copemys* and JODA 4957. In addition, *Pseudadjidaumo* has rounded enamel and smooth incisors (Flynn, 2008). The eomyid *Pseudotheridomys* (known from the Barstovian Skull Springs and Quartz Basin localities) is similar in size to *Copemys,* but it bears a medially flattened incisor (Shotwell, 1967). This specimen marks the only identifiable occurrence of cricetids in the Mascall Formation, collected from the Mascall Tuff. The lack of cricetid material, however, is most likely due to preservational issues. Fossil material from the Mascall Formation is typically large and from large-bodied taxa.

Family CASTORIDAE Gray, 1821
(Fig. 1.11)

Occurrence – JDNM-4.
Referred Material – Upper left fourth premolar, JODA 4682.
Description – The premolar is mesodont and measures ap=3.6 mm and t=3.7 mm. There are two small fossettes comprising the metafossette; the paraflexus is almost closed creating a parafossette; the mesoflexis is long and curves posterioraly; the hypoflexus is also long and bypasses the paraflexus; the parastria are persistent; and the parasagittal crests do not meet at the midline.
Comments – This specimen may belong to *Monosaulax* based on the parasagittal crests not meeting at the midline, long hypostria and it is mesodont. Shotwell (1968) described two species of *Monosaulax* from the early Barstovian Quartz Basin localities (*M. typicus* and *M. progresus*). It may also belong to *Euroxenomys* based on the persistence of the parastria (Sutton and Korth, 1995). This specimen is not assigned to a genus because there are not enough defining dental characteristics. In addition, stages of wear and how it affects dental morphology have not been determined for these genera (Stirton, 1935). It has been shown with *Monosaulax* that stages of wear change morphology (Stefen, 2001). A specimen of *Monosaulax* has been recovered from Cave Basin (JODA JZ8123).

Rodentia indet.

Occurrence - JDNM-4.
Referred Material – Right astragulus, JODA 15793.
Description – The astragulus is 6.5 mm in length.
Comments – There are about a dozen other rodent post-cranial elements found in the Mascall Formation. JODA 15793 is presented here to demonstrate the presence of rodent postcranial material within the Mascall Formation, however; it is impossible to identify this material past Rodentia.

Order PERRISODACTYLA Owen, 1848
Family EQUIDAE Gray, 1821

Genus KALOBATTIPUS Osborn, 1915
cf. *Kalobatippus*
(Fig. 1.12)

Occurrence – RV6855.
Referred Material – Left lower dp2, UCMP 312849.
Description – UCMP 312849 is a well worn, low crowned, lower deciduous second premolar in the size range of *Kalobatippus* (ap=19.8, t=14 mm).
Comments – There is no locality data for RV6855; only that it is an old CIT location, labeled from the Mascall Formation, Oregon. Therefore this specimen is tentatively placed on the faunal list. Another specimen of *Kalobattipus* (UCMP 1702) was collected from the Crooked River locality UCMP V4949. UCMP 1702 is a partial molar or premolar with a part of the base of the protocone, one half of the metaloph, a small internal section of the metacone and all of the hypostyle is present. It is too small to be *Hypohippus* (approximate molar length: M1/M2 = 27.5 mm; m1/m2 = 26.0 mm) and is closer in size to *Kalobattipus* (approximate molar length: M1/M2 = 17.0 mm; m1/m2 = 19.0 mm) (McFadden, 1998). Downs (1956) assigned this specimen to cf. *Hypohippus* based on size, however he could not rule out *Kalobatippus*. Comparison of these specimens to *Hypohippus* specimens from the Virgin Valley fauna indicate that it is too small to fall within this genus and most likely belongs to *Kalobatippus*.

Genus DESMATIPPUS Scott, 1893
Desmatippus avus Marsh, 1874

Occurrence – UCMP V65400, JDNM-4, JDNM-4*, UCMP V4830-4835, UCMP V4834, CIT 113, JDNM-4.
Holotype – From UCMP V65400: lower right p3-m2, left p2, p3, p4 and m1, upper left P2-M1 and M3 right P2, M2, a canine and fragments, YPM 11281.
Referred Material –From JDNM-4: three upper molars (former type of *Parahippus brevidens*), YPM 11274. From JDNM-4*: right upper molar or premolar, JODA 1983; upper right M3, JODA 1992; right upper molar, JODA 2050; upper right and left P1 through M3, 2435; upper molar, JODA 2428. From UCMP V4830-4835: left upper molar, UCMP 1701. From UCMP V4834: upper partial left premolar or molar, UCMP 40240. From CIT 113: upper molars or premolars, CIT 406 and CIT 407.
Description – All YPM and CIT material is described in Downs (1956). JODA specimens are new occurrences. JODA 1983 is a well-worn, low crowned cheek tooth. It does not contain a crochet; however, there is cement present. It measures ap=17.42 mm and t=19.72 mm. JODA 1992 is also a well-worn, low crowned specimen with no crochet (ap=16.87, t=18.65 mm). JODA 2050 has the following measurements: ap= 17.25, t=15.29 mm. None of the molars nor premolars of JODA 2435 contain a crochet, and all are low crowned and have minimal cement. They are similar in size and wear stage as YPM 11281. JODA 2428 also lacks a crochet, is low crowned and has no cement. Placement of these specimens in this taxon is based on the absence of crochet and no connection between the protoloph and protocone on upper cheek teeth, minimal cement in cheek teeth and bunodont dentition.
Comments – MacFadden (1998) places primitive parahippines into *Desmatippus*. This includes subsuming *Parahippus avus* into *Desmatippus* based on low crowned molar teeth, lack of a

crochet and lack of cement. Downs (1956) synonymized *P. brevidens and P. avus*. YPM 11281 was originally reported by Downs (1956) as YMP 1128.

Genus PARAHIPPUS Leidy, 1858

There are several equid premolars and molars in the JODA collection that are similar to *Desmatippus avus* except they contain a fair amount of cement and some have a crochet. Therefore, they most likely fall further along on the morphocline between *Desmatippus* and *Parahippus* (Stirton, 1940; MacFadden, 1998). Here they are placed within *Parahippus* but a taxonomic revision of both genera may shed more light on the identification of these specimens.

Occurrence – JDNM-4*, UCMP V4941.
Referred Material – From JDNM-4*: left upper P2, JODA 2401; left upper P3, JODA 2402; left upper P4 or M1, JODA 2403; left upper M2 or M3, JODA 2404; left upper P4, JODA 2405; left upper P4, JODA 2406; right upper M1, JODA 2407; right upper P2, JODA 2408; right upper P4, JODA 2409; right upper M3, JODA 2411; left upper M3, JODA 2412; lower left p2, JODA 2413; lower left molar or premolar, JODA 2415, lower right molar or premolar, JODA 2417; upper right M1 through M3?. From UCMP V4941: upper right molar, UCMP 40314.
Description – The protoloph does not connect to the protocone on upper cheek teeth. Some have complex crenulation patterns and/or crochets while others lack them. The majority of specimens have at least some cement; in some cases the amount of cement is considerable (pre- and postfossettes are filled and protocone is surrounded), especially in teeth that are unworn or slightly worn. All specimens are all low crowned with height ranging from 9.25-16.4 mm and an average of 12.5 mm. These characteristics place these specimens within parahippines and align them more closely to *Parahippus* than *Desmatippus*.
Comments – Downs (1956) reported a small deciduous tooth (UCMP 31987) from UCMP - 3059 as *P. sp.*, however, this specimen is a lower molar or premolar and belongs to *Archaeohippus ultimus*.

Genus MERYCHIPPUS Leidy, 1857

There are two distinct morphotypes of merychippines in the type Mascall Formation (Woodburne, pers. communication). A thorough revision of merychippine taxonomy, which is beyond the scope of this paper, is needed before formal naming of these specimens is possible. Therefore, for the purposes of this analysis, they will be referred to as ‘species A’ and ‘species B’.

Merychippine Species A
aff. *Acritohippus isonesus* Kelly, 1995
(Fig. 1.13)

Occurrence – CIT 183, UCMP V67153, JDNM-4*.
Referred Material – From CIT 183: skull with P2 through M3, LACM (CIT) 532. From UCMP V67153: skull with left I1-3, C, P2-M3 and left P2-M3, AMNH 8175. From JDNM-4: skull with P2 through M3, left I1 and right I1-2, JODA 1316; skull with P2, dP3 through erupting M3 with

broken rostrum and right zygomatic arch, JODA 1317; poorly preserved partial skull with P3 through M3, JODA 1318.

Description – Narrow preorbital bar, moderately deep lacrimal fossa, infraorbital foramen on floor of lacrimal fossa, shallow malar fossa with no foramen, malar fossa separated from lacrimal fossa by low, indistinct ridge. Cheek teeth have protoloph connected to protocone, no crochets, one medium pli caballin, simple fossette borders with occasional pli protoconule and pli postfossettes, open hypoconal groove, simple hypocone, considerable cement and hypsodont.

Comments – This is the larger of the two species present in the type Mascall Formation, identified by Downs (1956) as *Merychippus seversus*, in part. AMNH 8175 from AMNH Mascall locality (=UCMP V67153) is the type specimen for *Acritohippus isonesus* (Kelly, 1995) and the original type specimen for *Merychippus isonesus* (referred to as *Stylonus isonesus* by Kelly and Lander, 1988, as *Hippotherium isonesum* by Cope, 1889 and as *H. seversum* by Cope, 1886) which Downs (1956) synonomized with *Merychippus seversus*. Kelly (1995) distinguishes *Acritohippus* based on a shallow malar fossa only separated from the dorsal preorbital fossa (DPOF) by a low, indistinct ridge. All of the skulls referred here have this feature but a formal comparison, currently being undertaken by M.O. Woodburne (pers. communication), needs to be completed to confirm assignment to this taxa. There are hundreds of (>300) dental specimens collected from this taxon in the AMNH, JODA, UCMP and YPM collections, many of which Downs (1956) assigned to *Merychippus seversus*, which are being re-evaluated. Fragmentary enamel and postcranial material of a larger merychippine was recovered from upper Mascall deposits (KCM810-102, KCM810-104 and KCM810-105) demonstrating this species' persistence into the later part of the formation and Late Barstovian.

Merychippine Species B

Occurrence – "Lake deposits of eastern Oregon", UCMP V4942, UCMP V4827, V4825(?), V4824 UCMP V67153, CIT 113.

Referred Material – From "Lake deposits of eastern Oregon": Left upper M1 and right upper unworn M2(?), AMNH 8673. From UCMP V4942: upper molar, UCMP 23090. From UCMP V4827: upper molar, UCMP 23096. From UCMP V4825(?): lower molar, UCMP 499. From UCMP V4824: lower molar, UCMP 39101. From UCMP V67153: upper molar, UCMP 27237; upper molar, UCMP 27238. From CIT 113: upper right deciduous fourth premolar, CIT 4004.

Description – This species is represented only by cheek teeth, which, are smaller than the merychippine species A, and have a rounded protocone that is isolated and does not have a spur. The hypocone is simple and relatively long, and the hypoconal groove is open and narrow. The teeth typically have one medium pli caballine, one pli protoconule and one to two pli foessettes, hyposodont.

Comments – This material was identified by Downs (1956) as *Merychippus relictus*. This species is smaller and more rare than species A. Two lower teeth of this taxon have also been recovered from Mascall deposits. UCMP 499 was recovered from old UCMP locality -884 which Downs (1956) suggests is the same as UCMP V4825. These are also smaller than lower cheek teeth of species A. M.O. Woodburne is currently revising this taxon and determining its classification. An additional third species of a merychippine is present from the Mascall equivalent Gateway locality (LACM (CIT) 2929), not included in this study. This species has a wider post orbital bar, a deeper lacrimal fossa, no malar fossa, and the infraorbital foramen is outside of the lacrimal fossa.

Family RHINOCEROTIDAE Gray, 1821

Occurrence – UCMP -884, UCMP -903, JDNM-4, JDNM-70, JDNM-71A, JDNM-71B, JDNM-71D.
Referred Material – From -884: podial, UCMP 475; cuneiform(?), UCMP 35669. From -903: pisiform, UCMP 2176. From JDNM-70: partial tooth, JODA 4275; enamel fragments, JODA 15303. From JDNM-71A,B,D: enamel fragments, JODA 10314 and JODA 15766; molar fragment, JODA 15555 and 15644. From JDNM-4: teeth fragments; JODA 15326, JODA 15341, JODA 15612, JODA 15613, JODA 15615, JODA 15631, JODA 15678, JODA 15720, JODA 15690, JODA 15792, JODA 16124.
Description and Comments – Specimens of Rhinocerotidae are very rare in the Mascall type area; fragmentary postcranial elements and pieces of enamel have been found in all units of the Mascall Formation. Tooth material is fragmentary but contains the characteristic Hunter-Schreger bands characteristic of Rhinocerotidae (Rensberger and von Koenigswald, 1980). To the south, by the Crooked River, rhinocerotid material is more abundant, but still only represented by fragmentary postcranial material. A calcaneum (UCMP 1682) from the Beaver Creek locality (UCMP -895) is assigned to *Teloceras medicornutum* (Prothero, 2005). A partial maxilla with P2 and P3 most likely belongs to *Aphelops* because the teeth are brachyodont and lack an antecrochet; however, they have a well developed crochet. Although fragmentary and rare, the rhinocerotid material from the type Mascall demonstrate the persistence of this family throughout the Mascall Formation.

Order ARTIODACTYLA Owen, 1848
Family TAYASSUIDAE Palmer, 1897
Genus CYNORCA Cope, 1868
"Cynora" hesperia Woodburne, 1969
(Fig. 1.14-1.16)

Occurrence – UCMP V67153, CIT 1869, UCMP V4945, JDNM-4*.
Holotype – From UCMP V67153: right maxilla with P4-M3, YPM 11899.
Referred Material –From CIT 1869: upper fourth premolar, LACM 5964. From JDNM-4*: cranium with snout missing but containing right and left P4 through M3, JODA 1320; partial maxilla with M2 and M3, JODA 2229; upper right M1 or M2 in maxillary fragment, JODA 2241. From UCMP V4945: partial cranium with incomplete palate containing left P2 through P4, M1, M3, partial left M2 and partial left and right canines, mandible with left i1-2, canine, alveoli of p2-p3, p4-m3 and right i1-3, canine, alveoli of p2-p3, p4-partial m2, m3, distal right humerus, and right proximal ulna and radius, JODA 3773.
Description – YPM 11899, JODA 1320, and JODA 3773 all have upper fourth premolars with a "deep trenchant groove that passes lingually between protocone and metaconule" (Woodburne, 1969 p.304) and unreduced M3 placing them in *Cynorca hesperia* (Fig. 16, 17). JODA 2229 also has an unreduced M3. JODA 1320 is the most complete specimen of *C. hesperia* containing the palate and most of the braincase with well-preserved auditory bullae; however most of the snout is missing (Fig. 16). The zygomatic arch of JODA 1320 does not flare resulting in a narrow cranium shape. JODA 3773 contains most of the rostrum, part of the frontals, anterior portion of the left zygomatic arch and palate with left dentition (Fig. 17, 18). The zygomatic arch of JODA

3773 flares laterally causing a wing like projection and a more broad cranium shape than JODA 1320.

Comments – YPM 11899 is the type specimen of *C. hesperia* (Woodburne, 1969). It was collected by Thomas Condon, from the upper John Day River, Oregon. Marsh (1871) reported it from "the Pliocene beds of Oregon"; however Woodburne (1969) interpreted the locality as probably the Mascall. Wright (1998) only recognizes two species of "*Cynorca*" ("*C.*" *sociale* and "*C.*" *occidentale*) which are paraphyletic. "*C.*" *sociale* falls outside of Tayassuinae, while *"C."* *occidentale* falls within. A character that is shared between *"C." occidentale* and YPM 11899 is the presence of a metaconule on the P4 and the trenchant groove that passes lingually between the protocone and metaconule of P4. However, the two differ in that the M3 of YPM 11899 is not significantly smaller than the M1 or M2. The presence of the metaconule of the P4 places YPM 11899 within Tayassuinae, however, this specimen does not belong to *"C." occidentale*. This specimen is similar to *"C." sociale* in having an unreduced M3, length of m2 is 10.87 mm (near the average of 11.2 mm reported in Wright (1998)); however, it does not belong to this species because of morphology of the P4 discussed above. Given this, I retain YPM 11899 as *C. hesperia*. Because all of the other specimens listed above share the same P4 and M3 morphology as well as size range (Table 1.3), they are also assigned to *C. hesperia.* The difference in zygomatic arch shape of JODA 1320 and 3773 may be due to sexual dimorphism; however, their tooth morphology and size are identical. Wright (1993) demonstrated that zygomatic arches are a sexually dimorphic character in Tayassuidae and that some Miocene and Pliocene female peccaries have smaller zygomatic arches.

Table 1.3 Specimen measurements of *"Cynorca" hesperia*.

Specimen	**P2**	**P3**	**P4**	**M1**	**M2**	**M3**
YPM 11899						
ap						
t						
JODA 2229						
ap					R12.57	R11.2
t					R10.68	R9.62
JODA 2241						
ap				R11.08'		
t				R9.95'		
JODA 1320						
ap			R8.44	R10.45	R12.05	R11.53
			L8.42	L10.43	L12.37	L11.97
t			R9.18	R9.72	R10.68	R9.5
			L9.33	L10.28	L10.58	L10.11
JODA 3773						
ap	L7.22	L7.8	L7.6	L.9.9		L11.71
t	L5.02	L7.2	L8.69	L10.27		L10.43

' M1 or M2.

"Cynora" sp. Woodburne, 1969

Occurrence – UCMP V4834, CIT 1869.

Referred Material – UCMP V4834: partial mandible with complete left canine, left i1-2, right i1 and partial right canine, JODA 4250; right partial dentary with m1 and m2, JODA 4258. From CIT 1869: upper fourth premolar, LACM 5964.

Description – JODA 4258 is a right dentary with m1 and m2. The m1 of JODA 4258 measures 11.02 mm anteroposteriorally and 7.78 mm transversally. The m2 of JODA 4258 measure 11.75 mm anteroposteriorally and 10.03 transversally. The simple morphology of the m1 and m2 is similar to "*C." occidentale* and *"C." sociale.* JODA 4250 belongs to *"Cynorca"* based on i2 lying posterolateral to i1, i1 and i2 being subconical and the canine having lateral ridges and a lingual groove developed half way up the tooth from the jaw.

Comments – These specimens are attributed to *"Cynorca"* but not assigned to a species due to limited material that is not diagnostic. The type specimen for *C. hesperia* is a partial maxilla and does not contain comparable lower dentition. JODA 3773, assigned above to *C. hesperia,* has a comparable lower jaw, however the m1 and m2 are too worn for morphological comparison. The m1 and m2 of JODA 4258 are the same size as the m1 and m2 of JODA 3773 suggesting they belong to the same taxon. No other small tyassuid has been recovered from the Mascall Formation. JODA 4250 and 4258 may belong to the same individual. They have similar preservation and were found at the same site. LACM 5964 was collected by Bode in 1929. It is highly worn so it is impossible to determine if there is a metaconule present or not and therefore unidentifiable to the species level.

Tayassuidae indet.

Occurrence – JDNM-4*, JDNM-71, UCMP -884.

Referred Material – Partial dentary with m1-m2, JODA 301; partial molar, JODA 302; partial dentary with p2 and p3(?), JODA 2230; molar, JODA 2238; molar, JODA 2239; molar, JODA 2240; premolar, JODA 2241; premolar, JODA 2242; deciduous premolar, JODA 2244; partial molar, JODA 2245; partial molar, JODA 2246; p2, JODA 2324; premolar, JODA 2341; M3, JODA 2342; premolar, JODA 2349; premolar, JODA 2391. From JDNM-71: molar fragment, JODA 12946. From UCMP -884: m3, UCMP 1682.

Comments – These specimens can be attributed to Tayassuidae; however, there is no locality information because they were collected by the Weatherfords or park rangers during the first years of the National Monument or are assigned to a general locality number. Therefore it is unclear which formation they are from. The specimens are all too big to belong to "*Cynorca*" but lack the diagnostic characters that would be required to assign them to another genus. They fall within the size range of *Dyseohyus fricki* and *"Prosthennops" xiphidonticus*, two Barstovian species (Wright, 1998); however, they also fall within the size range of Hemphillian peccaries such as *Platygonus oregonensis*, which is known from the Rattlesnake Formation (Merriam et al., 1925). A lower right m3, UCMP 1628, was collected from locality -884 (Mascall Misc. 2). It has an anteroposterior length of 16.48 mm and a transverse width of 10.87 mm, the same size as *D. fricki*, the locality information is minimal and it is unclear if the specimen was found in the Mascall Formation or the Rattlesnake Formation.

A small Tayassuidae molar fragment (JODA 12946) was collected at JDNM-71 Rock Creek locality from the lower Mascall unit, demonstrating the stratigraphic persistence of peccaries throughout the lower and middle units of the formation.

Family PALEOMERYCIDAE Lydekker, 1883

Genus RAKOMERYX Frick, 1937
Rakomeryx sinclairi Matthew, 1918
(Fig. 1.17)

Occurrence –UCMP V4831, JDNM-4*.
Referred Material – From UCMP V4831: left p3, p4 and m1 or m2, and right p4, JODA 7195; right lower p3; JODA 3682. From JDNM-4*: left p4-m3, JODA 2362.
Description – Anterior fossette on the p4 of JODA 7195 is not closed by the anterior extension of the metaconid. Measurement for JODA 7195 are: left p3 ap=12.93, t=6.28 mm; left p4 ap=16.49, t=8.55 mm; left m1 or m2 ap=18.99, t=11.5 mm, right p4 ap=16.73, t=8.7 mm. The anterior fossette on the p4 of JODA 2362 is closed by the anterior extension of the metaconid but not more so than FAM 31782 of which Frick identified as *R. raki* (Frick, 1937). Prothero and Liter (2008) and Janis and Manning (1998) mentioned that the p4 may lack closure of anterior fossette for this taxon. Measurements for JODA 2362 are: p4 ap=15.26, t=8.79 mm; m1 ap=17.17, t=12.35 mm, m2 ap=19.68, t=12.72 mm; m3 ap=27.64, t=12.97 mm; m1-m3 length=63.79mm. JODA 3682 measurements are: p3 ap=12.94, t=6.53 mm. This specimen is the same size and has the same preservation as the p3 of JODA 7195 and because they were collected in the same area, they probably belong to the same individual. These specimens are assigned to this taxon based on reduced premolars compared to *Dromomeryx* and morphology of the p4 (Janis and Manning, 1998)
Comments – Prothero (2008) places all species of the genus into *R. sinclairi*. There is another specimen at LACM (no specimen number) that may be attributed to this species; however, additional preparation is needed for identification. JODA 7195 and 2362 further confirm the presence of *Rakomeryx* in the early Barstovian as argued in Janis and Manning (1998).

Family MERYCOIDODONTIDAE Thorpe, 1923
Genus TICHOLEPTUS Cope, 1878
Ticholeptus zygomatics Cope, 1878

Occurrence – UCMP V67153, JDNM-4*, UCMP V4834, UCMP V4835, CIT 113, JDNM-71D, JDNM-179.
Referred Material – From UCMP V67153: lower right third incisor, UCMP 35670; lower left molar, lower p2 and p3, deciduous p4, UCMP 95757; upper M1 and partial P4 in maxilla fragment, JODA 3776; right upper M1 and M2, JODA 6604. From JDNM-4*: upper dentition including right P1 through M3 and left I1 though m3, JODA 1327; lower dentition including right p2-m3 and left i3-m3, JODA 1328; dentary with erupting i3-p3, dp4, m1-m2 and erupting m3, JODA 1329. From UCMP V4834: left upper P4, UCMP 39298. From UCMP V4835: left upper P4, UCMP 39301; right upper P1 and tooth fragment, UCMP 39302. From CIT 113: lower p4 and m1, CIT 1730. From JDMN-71D: lower right c1 through p3 in dentary fragment, JODA 295. From: JDNM-179: right partial lower canine, JODA 6509.
Description and Comments – Cope (1886) described *Ticholeptus* from Cottonwood Creek beds (FM 8192) and named a new species (*T. obliquidens*) from a mandibular ramus with an entire tooth series. Lander (1998) synonymized all species in the genus to one species, *T. zygomaticus* but based on the description in Cope (1886), it is unclear whether FM 8192 belongs to *T. zygomaticus*. Scharf (1935) identified *Ticholeptus* from the Mascall deposits (CIT 113, specimen CIT 1730). More recent collections confirm this genus occurrence, as well as identification of the

the species *T. zygomaticus* in the Mascall Formation based on the following: P1-P3 are elongate, rectangular and the anterior intermediate crest does not form cusp (unlike in *Merychyus*); larger in size than *Merychyus* (average P1-M3 length 59-152 mm); smaller in size than other contemporaneous ticholeptines; p2-p4 complexly crested (Lander, 1998). All new material assigned to this taxon is dental material. JODA 1327 and 1328 were collected by the Weatherfords as individual teeth and then plastered together into a tooth row. Therefore, toothrow measurements are unreliable, but the individual tooth measurements are given in Table 1.4. JODA 1329 is a dentary also collected by the Weatherfords with all teeth *in situ*. The remaining material consists of isolated teeth referred to this species based on size. The lower premolars of UCMP 95857, JODA 1328 and JODA 295 are complexly crested, even more complex than the lower premolars of *T. zygomaticus* from Massacre Lake (UCMP V6160 and V6161). JODA 6509, a partial canine, and the canine of JODA 1328 are similar in size, have a worn surface on the anterior portion of the tooth and are flat posteriorly. Two additional specimens are tentatively placed in the genus, JODA 3776, an upper left M1 and partial P4 in a maxilla fragment, and JODA 6604, an upper M1 and M2. The first molar of JODA 3776 is larger (ap=13.96) than JODA 1327 (M1 is broken down the midline and split, therefore a transverse

Table 1.4 Specimen measurements of *Ticholeptus zygomaticus*.

Specimen	**C**	**P1**	**P2**	**P3**	**P4**	**M1**	**M2**	**M3**
JODA 1327								
ap	9.18	10.48	10.97	11.61	10.07	12.42	17.16	20.2
t		5.51	6.97	8.84	11.03	13.29	14.84	15.89
UCMP 39298								
ap					10.4			
t					12.85			
UCMP 39301								
ap					9.51			
t					12.88			
UCMP 39302								
ap		9.85						
t		5.36						
Specimen	**c**	**p1**	**p2**	**p3**	**p4**	**m1**	**m2**	**m3**
JODA 1328								
ap	12.58	--	10.83	12.94	12.38	12.41	14.51	23.52
t		--	5.07	8.08	9.25	9.96	11.29	10.19
UCMP 95857								
ap			9.64	11.79	17.19*	17.74’		
t			4.56	5.78	7.27*	9.35’		
CIT 1730								
ap					12.92	13.37		
t					10.06	9.29		
JODA 6509								
ap	12.06							

‘ M1 or M2.; * deciduous.

width could not be measure). JODA 6604 is an unworn smaller individual (M1: ap=n/a, t=11.07 mm; M2: ap=12.32 mm, t=10.49 mm).

Family CAMELIDAE Gray, 1821
Genus PROCAMELUS Leidy, 1858
cf. *Procamelus*
(Fig. 1.18)

Occurrence – UCMP V67153.
Referred Material – Left dentary with anterior portion of p2 and p3, alveoli of p4, complete m2 and partial m3, right m1, CIT 4003.
Description – The m2 of CIT 4003 has an anteroexternal stylid and measures 24 mm in anteroposterior length and 13.5 mm in transverse width. Cheek teeth are more hypsodont than in protolabines.
Comments - The size, presence of the anteroexternal stylid and presence of the second premolar place this specimen within *Procamelus* (Honey et al., 1998), but because the posterior portions of the p2 and p3 are missing as well as the p4, the specimen is only tentatively placed in this genus. This represents the earliest occurrence of *Procamelus* in Oregon and one of the earliest records of Camelini (Honey et al., 1998). *Procamelus* cf. *grandis* is also known from the Clarendonian aged Black Butte Local Fauna (Shotwell and Russell, 1963).

Camelidae indet.
(Fig. 1.19)

Occurrence – UCMP -3043, UCMP -3059, UCMP V4827.
Referred Material – From UCMP -3043: right external acoustic meatus, JODA 15592. From UCMP -3059: right partial dentary with p3(?) and m1(?) alveoli, JODA 15560. From UCMP V4827: molar enamel fragment, JODA 4685.
Description and Comments – JODA 15560 is a small camel, the dentary is gracile and the premolar has an anteroposterior length of 9.85 mm and a transverse width of 4.49 mm. JODA 4685 is high crowned (height = 25.12 mm) and from the lower unit of the Mascall Formation. This specimen demonstrates not only the presence of camels in the lower unit of the Mascall formation but also demonstrates hypsodonty in the family in the earliest deposits of the Mascall fauna. There are several postcranial elements assigned to Camelidae indet. (e.g. UCMP 472, 503, 553, 1604, 723, 1719).

Family MOSCHIDAE Gray, 1821
Genus BLASTOMERYX Cope, 1877
Blastomeryx gemmifer Cope, 1874
(Fig. 1.20)

Occurrence – JDNM-4*, UCMP -3043, UCMP V4823, UCMP V4835.
Referred Material – From UCMP -3043: right dentary fragment with m2-m3, UCMP 39309. From JDNM-4*: lower left premolar, JODA 2256; m2, JODA 2257; left dentary with p3-m3, JODA 2359; right M3, 2376; right upper M1, JODA 2377; left dentary fragment with m2-m3,

LACM 5934. From UCMP V4823: left p2, JODA 6623. From UCMP V4835: right maxilla fragment with P4-M1, UCMP 39310.

Description – Specimens are attributed to this taxon based on slightly reduced premolars, brachyodont molars, and size (Prothero, 2008). Referred specimens with m2 have anteroposterior length of 8.5-9.4 mm. JODA 2359 has an m1-m3 length of 30.32 mm. Specimens from the Mascall Formation are on the larger spectrum of specimens assigned to this species; however, they are smaller than *Parablastomeryx* specimens from Virgin Valley.

Comments – Prothero (2008) placed all species of *Blastomeryx* into a single species, *B. gemmifer*, based on size comparisons. The size of postcranial material such as astragali and podials (i.e. UCMP 496, 1730, 1746) indicates they are referable to *Blastomeryx* (Prothero, 2008). One fragmentary tooth specimen, JODA 6503, collected at JDNM-71 in the lower unit of the Mascall Formation is most likely *Blastomeryx* but because of its fragmentary nature, it is only assigned to Blastomerycinae here. Its presence, however, does suggest the clade was present in the lower unit of the Mascall Formation. Downs (1956) mentions YPM 14314, a partial maxilla with P4-M2 attributed to Blastomerycini and as possibly belonging to the Mascall; however, original locality description says “down river from the cove”, meaning down river from Turtle Cove in the John Day Formation, yet there are no Mascall deposits down river from Turtle Cove. Downs (1956) also mentions USNM 7720, a lower molar, which is now attributed to the Arikareean of the John Day Formation.

Genus PARABLASTOMERYX Frick, 1937
Parablastomeryx gregorii Frick, 1937
(Fig. 1.21)

Occurrence – JDNM – 4*.

Referred Material – Left m1; JODA 2255.

Description – Brachyodont molar with *Palaeomeryx* fold, anteroposterior length of 10.27 mm and transverse width of 5.81 mm (falls within the size range of *Parablastomeryx*).

Comments - Prothero (2008) placed all species of the genus into a single species *P. gregorii*. JODA 2255 falls within the size range of *Parablastomeryx* from Virgin Valley (UCMP 10661, 11564-11567) and presence of the *Palaeomeryx* fold and brachyodont molars places it within this taxon (Prothero, 2008).

Order PROBOSCIDEA Illiger, 1811
Family Mammutidae Hay, 1922
Genus ZYGOLOPHODON Vacek, 1877
Zygolophodon proavus Cope, 1873

Occurrence – JDNM-4*.

Referred Material –Lower right m2 and m3, JODA 1321; upper left M3 and third loph of upper M2, JODA 1322.

Description – Assignment of JODA 1321 to this taxon is based on the following: a trilophodont m2 and tetralophodont m3 (anterior loph broken) with true zygodonty, cingulum not well developed, medial sulcus between lophs is present however it does not separate the lophs with a valley in between. Measurements are: m2 ap=103.84 mm, t=72.83 mm; m3 ap=163.06 mm,

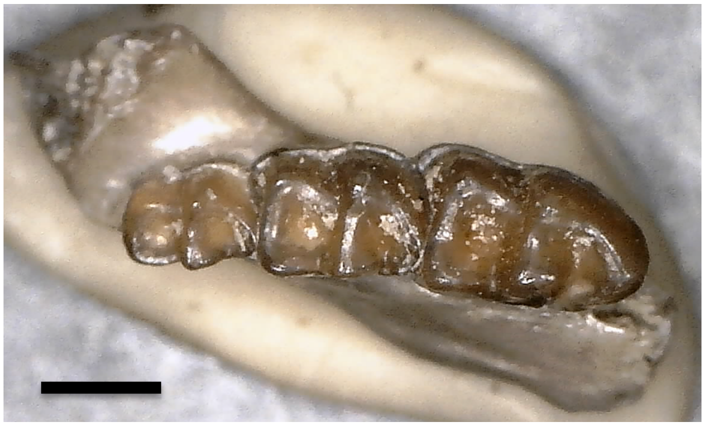

Figure 1.3 *Pseudotrimylus mawbyi*, JODA 13865 dentary with m1-m3 in occlusal view. Scale bar = 1mm.

Figure 1.4 Talpidae, JODA 15537, radius. Scale bar = 1 mm.

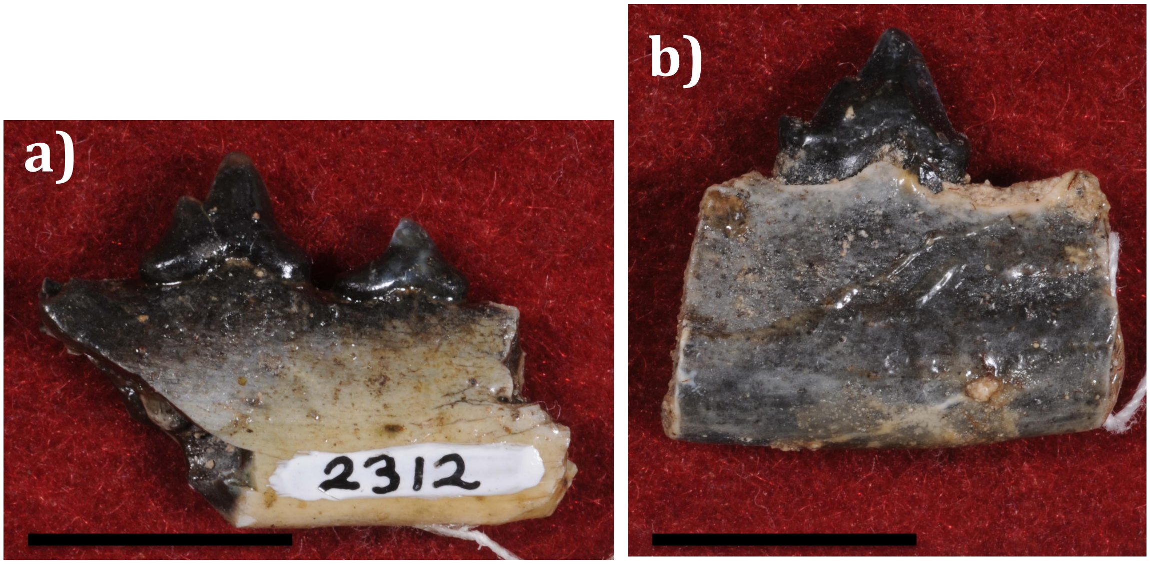

Figure 1.5 *Leptocyon cf. leidyi,* a) JODA 2312 dentary fragment with p3-p4 in lateral view, b) JODA 2313 dentary fragment with p4 in lateral view. Scale bar = 1cm

Figure 1.6 *Pseudaelurus sp.* JODA 15306, astragulus in dorsal view. Scale bar = 1cm.

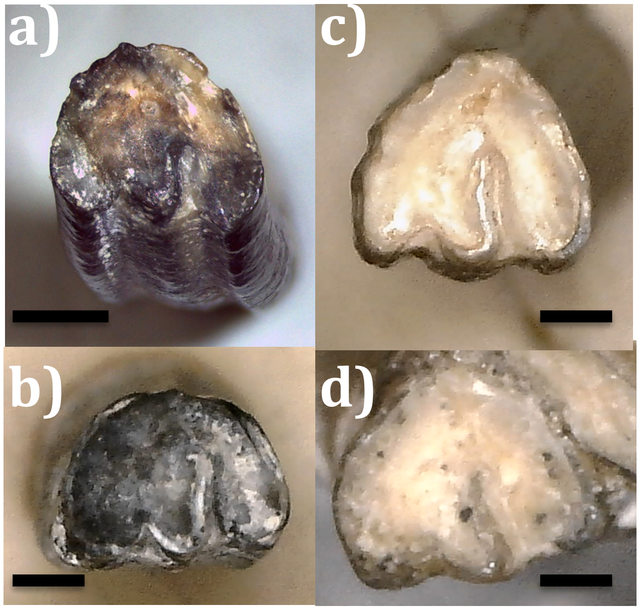

Figure 1.7 *Hypolagus fontinalis* left p3 a) UCMP 41205, b) JODA 4283; *H. parviplicatus* left p3 c) JODA 2328, d) JODA 2326. All in occlusal view. Scale bar = 1mm

Figure 1.8 *Balantiomys oregonensis* JODA 3767, right dp4 in occlusal view. Scale bar = 1mm.

Figure 1.9 *Protospermophilus malheurensis*, JODA 6416, left M1 in occlusal view. Scale bar = 1mm.

Figure 1.10 *Nototamias sp*., JODA 2331, left dentary with I, p4-m3 in occlusal view. Scale bar = 1 mm.

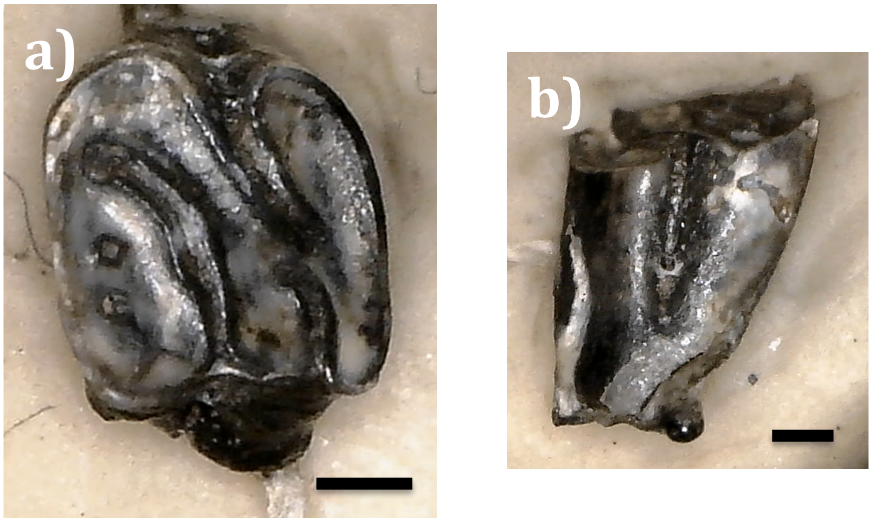

Figure 1.11 Castoridae, JODA 4682, left P4 a) occlusal view, b) medial view. Scale bar = 1mm.

Figure 1.12 Cf. *Kalobatippus*, UCR 12849, left dp2 in occlusal view. Scale bar = 1 mm.

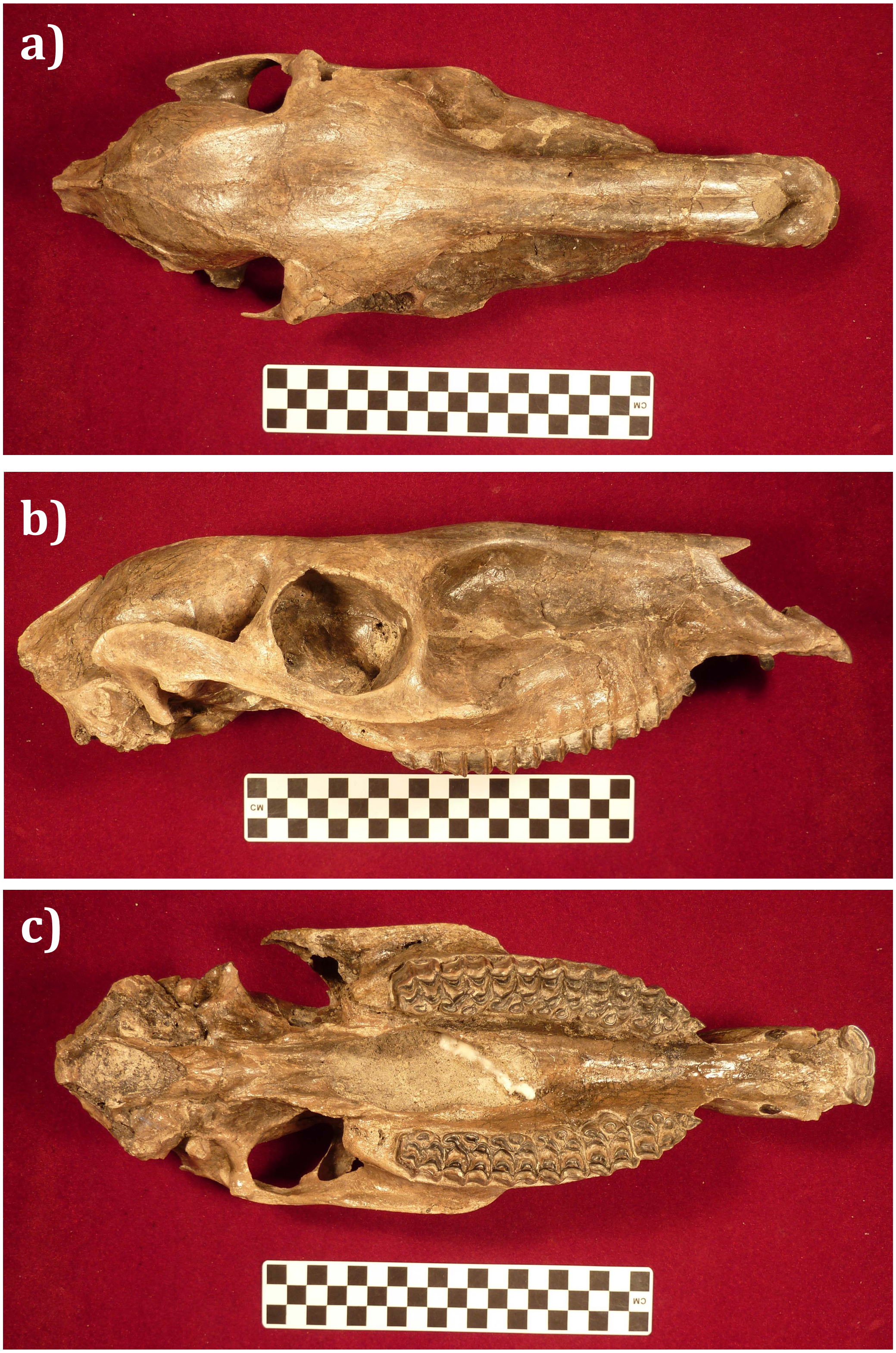

Figure 1.13 aff. *Acritohippus* JODA 1316, skull, a) dorsal view, b) lateral view, c) ventral view. Scale bar is in centimeters.

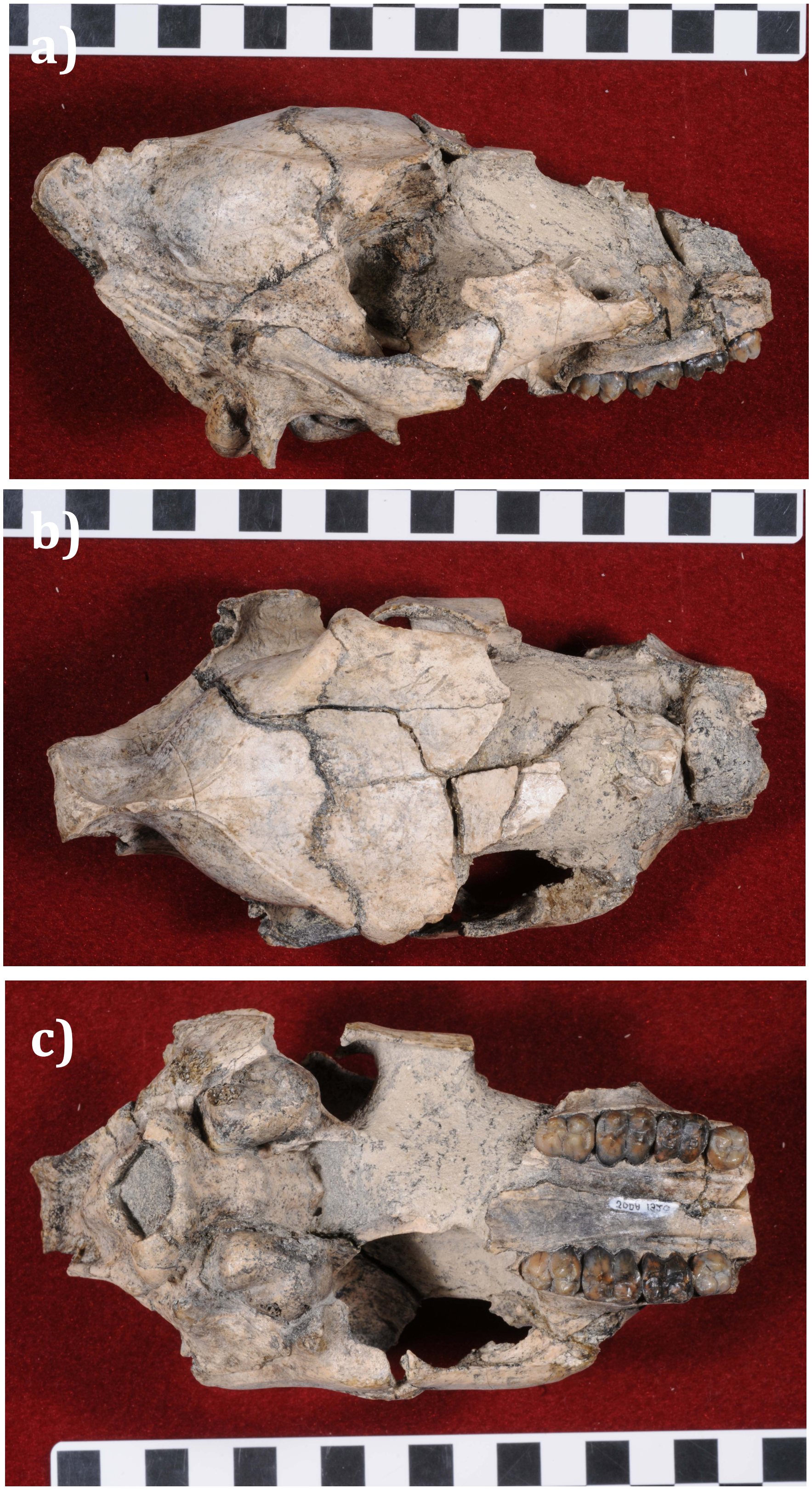

Figure 1.14 *Cynorca hesperia,* JODA 1320, skull, a) lateral view, b) dorsal view, c) ventral view. Scale bar = 1cm.

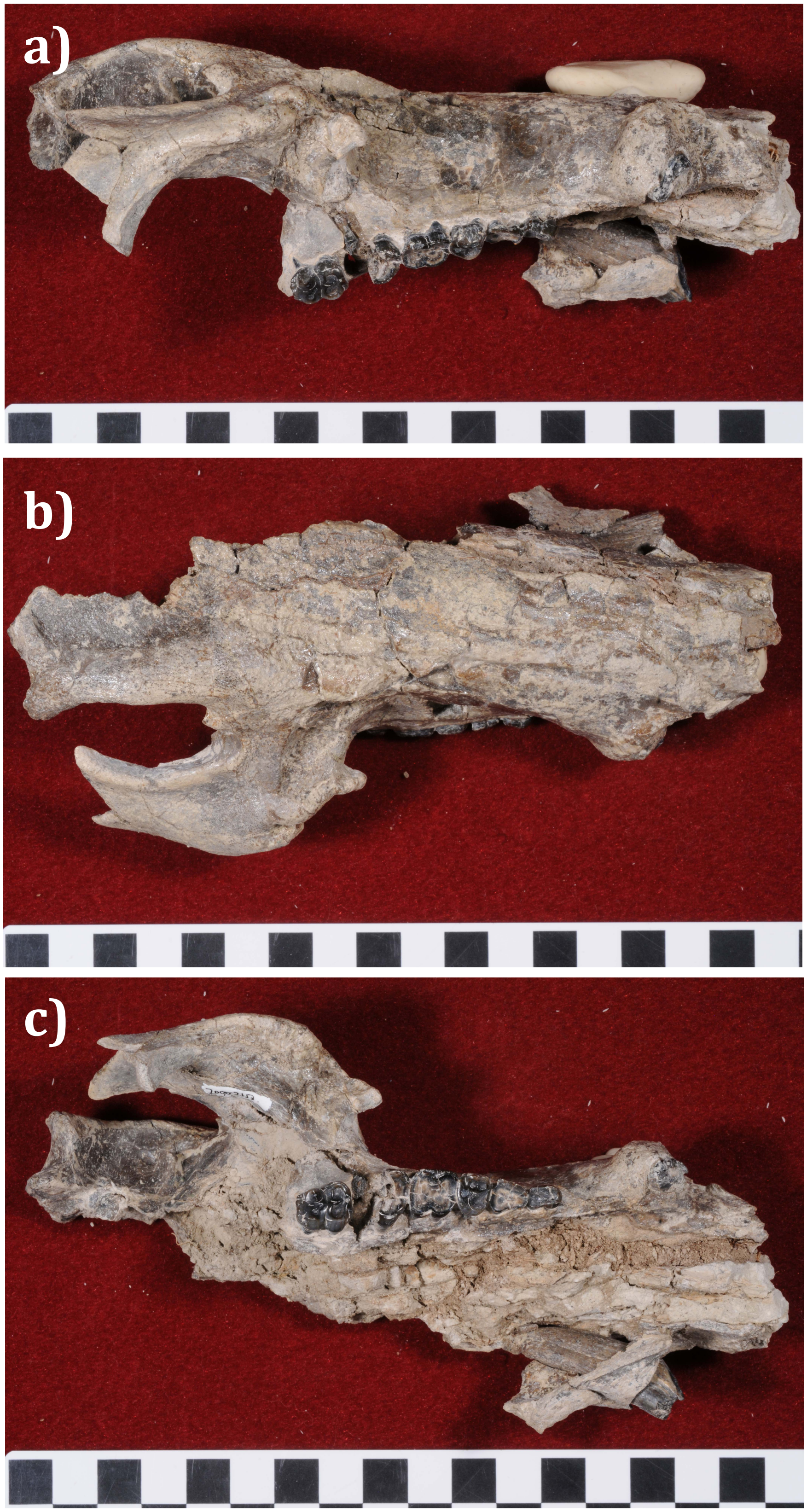

Figure 1.15 *Cynora hesperia,* JODA 3773 skull, a) lateral view, b) dorsal view, c) ventral view. Scale bar = 1cm.

Figure 1.16 *Cynorca hesperia*, JODA 3773, mandible, a) occlusal view, b) lateral view. Scale bar = 1cm.

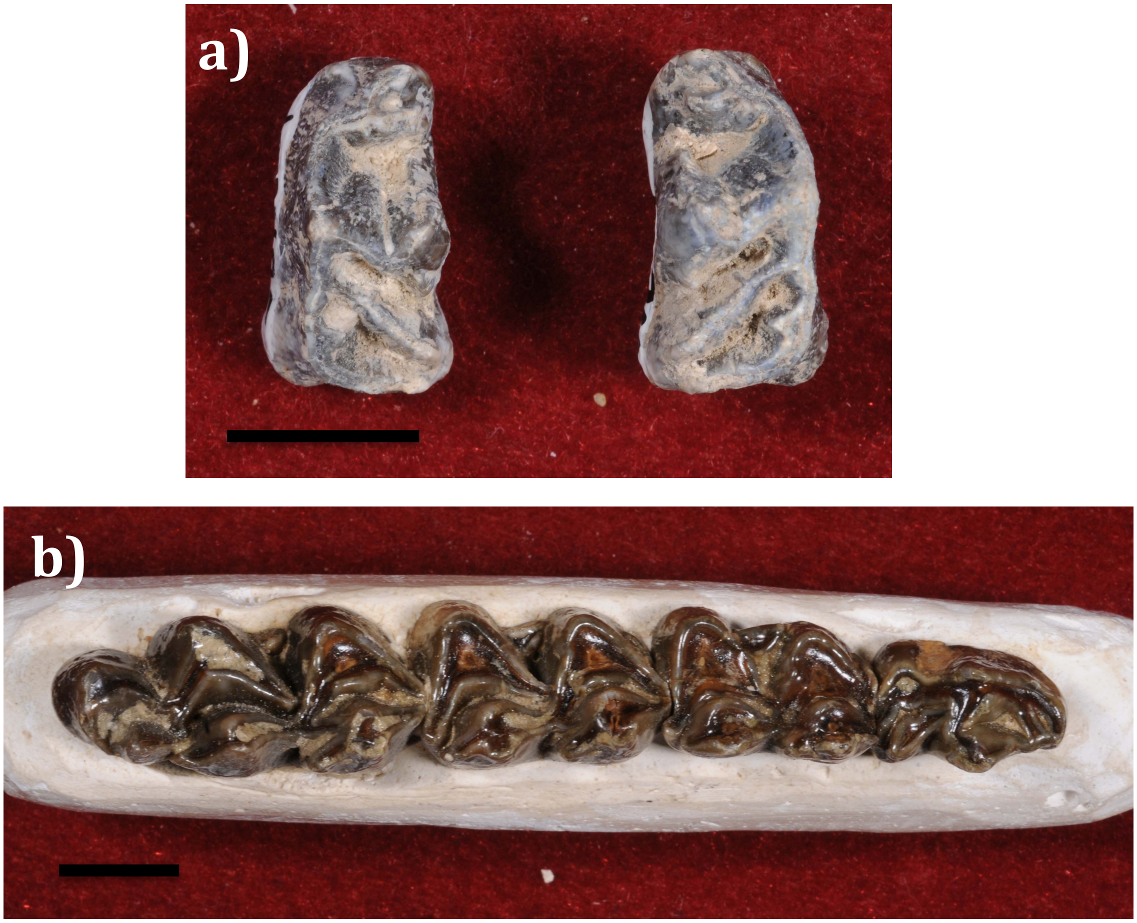

Figure 1.17 *Rakomeryx sinclairi* a) left and right p4, JODA 7195, b) left p4-m3, JODA 2362. Scale bars = 1cm.

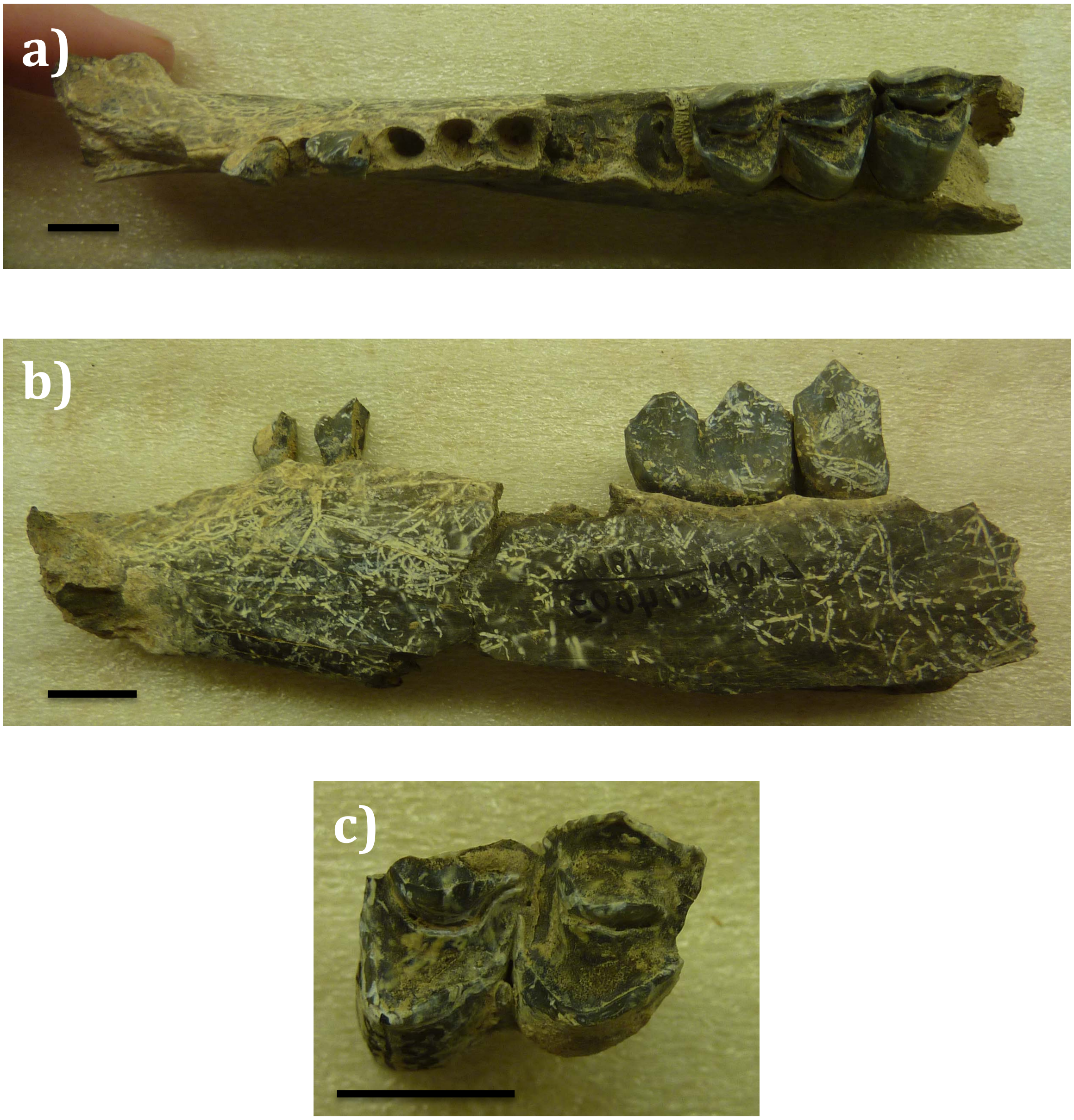

Figure 1.18 cf. *Procamelus,* CIT 4003, left dentary with partial p2 and p3, alveoli of p4 and m1, complete m2 and partial m3, a) occlusal view, b) lateral view, c) right m1 in occlusal view. Scale bars = 1cm.

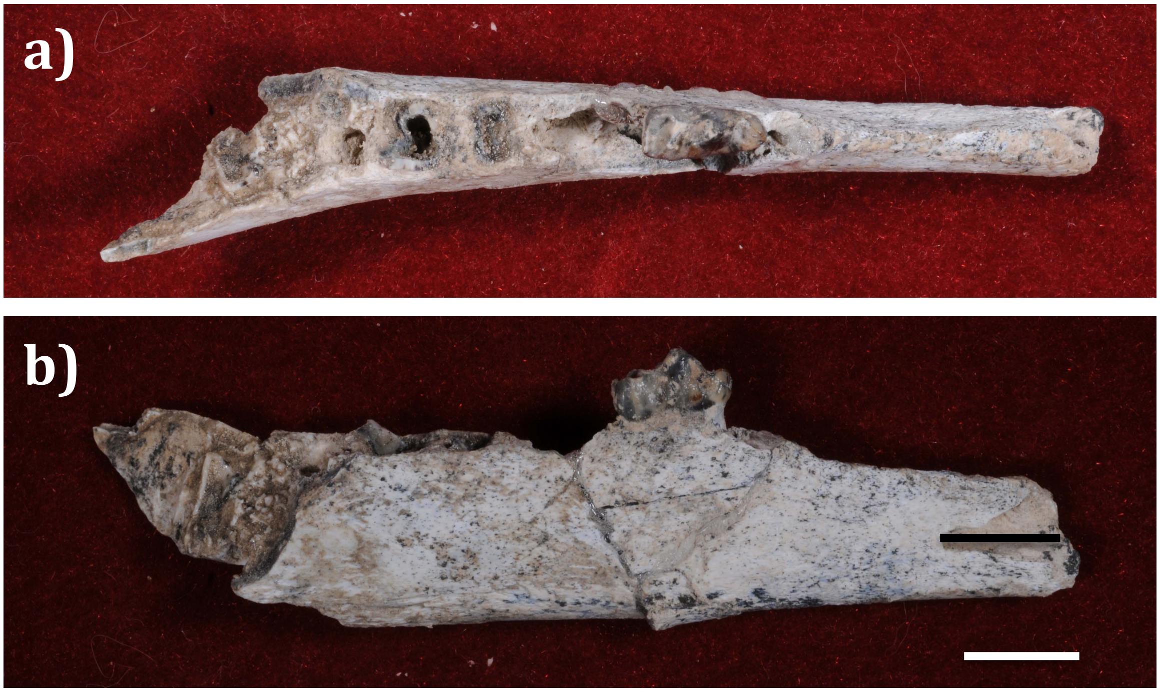

Figure 1.19 Camelidae JODA 15560, right dentary fragment with p3, a) occlusal view, b) lateral view. Scale bar = 1cm.

Figure 1.20 *Blastomeryx gemmifer,* JODA 2359, left dentary fragment with p3-m3 in occlusal view. Scale bar = 1cm.

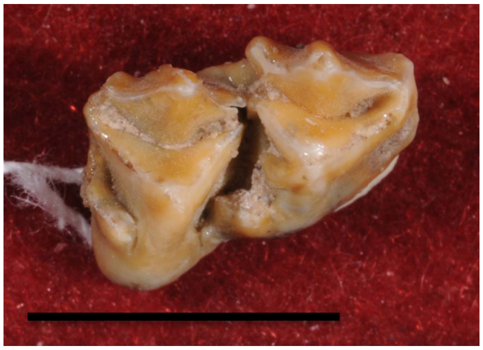

Figure 1.21 *Parablastomeryx gregorii,* JODA 2255, left m1 in occlusal view. Scale bar = 1cm.

t=80.83 mm. The m3 of JODA 1322 is also tetralophodont with a very weakly developed fourth loph, minimal cementum, medium sulcus present and forms V-shaped trough between conules, no center conules and accessory conules on the labial side of the lingual lophs. Measurements are: M3 ap=147.7 mm, t=83.54 mm; M2 third loph t=70.57 mm.

Comments – A third specimen, JODA 1323, is a partial tusk, but because it was collected by the Weatherfords, it is unclear if it is from Mascall deposits. *Zygolophodon* is one of the taxa Tedford et al. (2004) list as characterizing the early Barstovian fauna, however it is present in the Hemingfordian age Massacre Lake Fauna in Nevada (Lambert and Shoshani, 1998). *Zygolophodon* has also been recovered from the early Barstovian Sucker Creek and Skull Springs Faunas of Oregon, and the Virgin Valley and High Rock Canyon Faunas of Nevada (Tedford et al., 2004). Its presence in the Mascall Formation further demonstrates the age of these deposits.

Prodoscidea indet.

Very fragmentary tooth material has been collected in the lower and middle units of the Mascall Formation (JODA 2475, JODA 3754, JODA 3756, JODA 7192, JODA 12898, JODA 15346, JODA 15554, JODA 15628, JODA 15795, JODA 15797, JODA 15328). JODA 7192 is the anterior portion of a molar with one full loph and half of the second loph. It is smaller than the m3 of JODA 1321, has a medial sulcus, and lacks central conules; those features suggest it may be atrributable to *Zygolophodon.* Estimated transverse width of the first loph is 44.39 mm and estimated width of second loph is 53.06 mm. JODA 15554 and JODA 15328 are from the lower Mascall unit deposits at Rock Creek Southeast (JDNM-71D) and Rock Creek Southwest (JDNM-71B). JODA 15268 was collected from middle Mascall unit deposits at UCMP V4834. The remaining specimens listed above are from the middle Mascall unit around JDNM- 266. These specimens are float material and may have weathered from the upper Mascall units above JDNM-266. Earlier work on the Mascall deposits has reported the presence of *Gomphotherium* in the formation (e.g. Prothero et al., 2006), but this study cannot find evidence for this genus in the type Mascall area.

Radioisotopic Age Determinations

Zircon crystals from the Kangaroo Tuff are prismatic grains with oscillatory zoning from one homogeneous population (NPS Report J8R07110010). Coupled with LA-ICPMS U-Pb data, this suggests a single population of primary volcanic crystals. LA_ICPMS U-pb and CA-TIMS analyses yielded concordant and equivalent U-Pb dates with a weighted mean ^{206}Pb/^{238}U age of 13.564 ± 0.009 (0.016) [0.022] Ma (n = 8; MSWD = 2.78; probability of fit = 0.0068) (Fig. 22, Supplementary Data File S.1.1). This age is interpreted to estimate the eruption and depositional age of the volcanic deposit.

The Mascall Tuff sample contained equant to elongate prismatic grains from a heterogeneous population. Of the selected zircons for analysis, ten were Cretaceous, ten Oligocene and eighteen Miocene. Seven of the Miocene zircons were targeted for CA-TIMS. Of these, four produced older ages ranging from 17.62 to 15.40 Ma. The remaining three grains produced a weighted mean ^{206}Pb/^{238}U age of 15.297 ± 0.009 (0.012)[0.020] Ma (n=3; MSWD=1.12; probability of fit=0.325) (Fig. 3; Supplementary Data File S1.1), representing the last eruption event and time of deposition of the Mascall Tuff.

The Koala Tuff sample contained few (<20) zircon crystals from a heterogenous population. LA-ICPMS spot ages of 15 crystals range from 211 to 13 Ma, with only three crystals producing Miocene ages. Results indicate the detrital nature of the Koala Tuff and demonstrate that it is a reworked deposit. The Dreamtime Tuff sample did not contain zircons and therefore was no analyzed further.

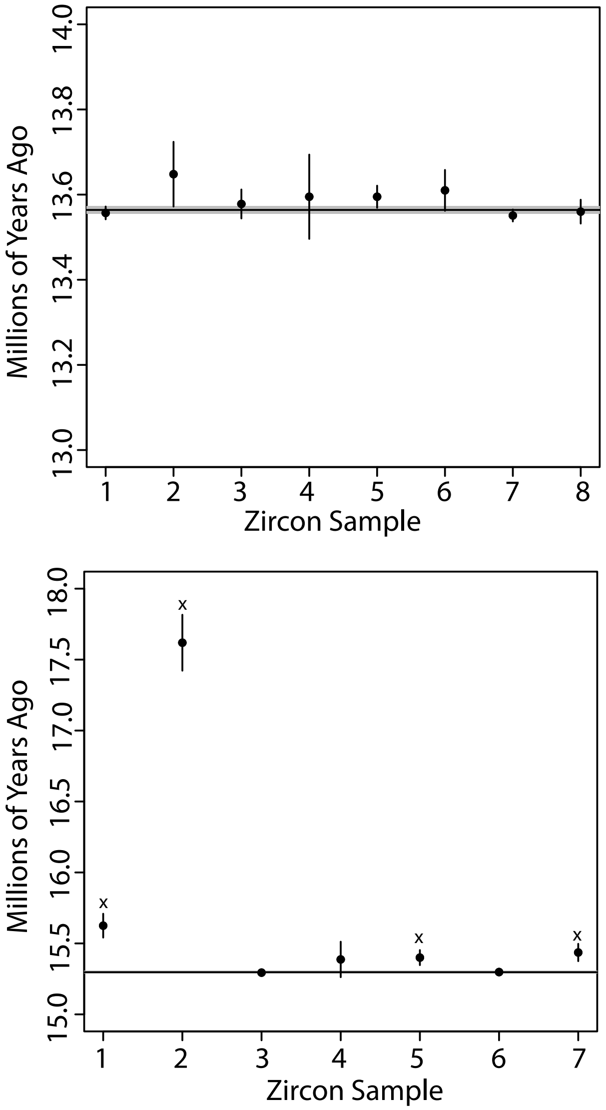

Figure 1.22 Chemical abrasion isotope dilution thermal ionization mass spectrometry (CA-TIMS) zircon age results for the Kangaroo Tuff (above) and Mascall Tuff (below). All error bars are plotted as 2 standard deviations. Horizontal line indicates calculated age. (NPS Report #J8R07110010).

Previously reported dates of 16.0 ± 0.2 Ma for a tuffaceous paleosol within the Dayville Basalts (Sheldon, 2006), 16.2 Ma for the top of the Dayville Basalts (Feilbenbork, 1983), and 15.77 for unit 2 of Downs (1956) dated by Swisher (1992) in concordance with the current report of the Mascall Tuff at 15.29 Ma indicates the lower unit of the Mascall Formation is about one million years in duration. Because the Dreamtime Tuff was not datable, the length of the Middle Mascall is unclear. The upper date of 13.56 Ma provided by the Kangaroo Tuff indicates the Upper Mascall extends through the Late Barstovian. Therefore, the Mascall Formation as a whole spans almost the entire Barstovian, from 16.2 to 13.56 Ma (Woodburne, 2004). However, as mentioned above, the majority of the fossils are collected in the lower and middle units of the formation, which correlate with the Early Barstovian.

Bestland et al. (2008) hypothesized that all of the paleosols of the Mascall formation represented the mid-Miocene Climatic Optimum because they all have the same degree of weathering. However the dates presented here demonstrate that the deposits span through the end of the warming event. Therefore, this suggests that the precipitation did not change after the mid-Miocene Cliamtic Optimum in the Pacific Northwest. And it further demonstrates that the Pacific Northwest had more mesic conditions than the Great Plains during the middle Miocene and after the mid-Miocene Climatic Optimum (Bestland et al. 2008).

Local and Regional Faunal Comparisons

Overall, the fauna from the Mascall type area is similar to other early and late Barstovian sites in Oregon. The Mascall equivalent beds to the south in the Crooked River area (UCMP V4948-V4951) differs only in the presence of *Hypohippus* and *Teleoceras medicornutum*. The limited material from the Mascall-equivalent beds to the west of the John Day Basin in the Simtustus Formation Gateway localities (UCMP V3427) likewise resembles the type Mascall fauna with the only exception being the addition of the distinctive "*Merychippus*" [LACM (CIT) 2929] skull discussed previously.

The several Barstovian faunas in southern and southeastern Oregon (Early Barstovian: Sucker Creek, Beatty Buttes; Late Barstovian; Red Basin, Quartz Basin, Skull Springs) in general are all similar to the Mascall Type fauna, as indicated by high similarity values (Tables 1.5-1.7). In Oregon, the Jaccard and Bray-Curtis similarity indices indicate the Mascall fauna is quite similar to the Skull Springs and Red Basin faunas, while the Raup-Crick index also reveals strong similarity between the Mascall fauna and Early Barstovian Beatty Buttes. The differences between these other Oregon Barstovian faunas and the Mascall fauna is that they contain more species of talpids and soricids (most likely due to preservational reasons as discussed earlier); have *Hypohippus* instead of *Kalobatippus*; have aplodontids (e.g. *Liodontia alexandrae*) and antilocaprids (e.g. *Merycodus* and *Paracosoryx*); have fewer or no moschids; have fewer camels; and lack mastodons. Other fauna-specific differences in comparision to the Mascall are as follows: Early Barstovian Sucker Creek has a chalicothere; early Barstovian Beatty Buttes has *Amphicyon frendens*, *Oreolagus wallacei* and *Pliohippus mirabilis*; Late Barstovian Quartz Basin has a greater diversity of cricetids and mustelids but fewer canids, contains Eomyids (*Pseudadjidaumo quartzi* and *Pseudotheridomys pagei*) and an erinaceid; the Late Barstovian Skull Springs fauna has two additional amphicyonids (*Amphicyon* and *Pliocyon*), two different canids (*Euoplocyon brachygnathus* and *Paratomarctus temerarius*), a mustelid (*Plionictis gazini*) and a chalicothere; the Late Barstovian Red Basin has *Amphicyon*, an eomyid (*Pseudothidomys pagei*), an erinaceid, *Copemys pagei,* rhinocerotids *Aphelops* and *Teleoceras*, and higher squirrel diversity.

Table 1.5 Jaccard similarity matrix.

	Sucker Creek (EBAR)	Beatty Buttes (EBAR)	Red Basin (LBAR)	Quartz Basin (LBAR)	Skull Springs (LBAR)	Virgin Valley (EBAR)	Second Division (EBAR)	Green Hills (EBAR)	L. Snake Creek (EBAR)	Pawnee Creek (LBAR)	Barstow (LBAR)	Valentine (LBAR)
Mascall	0.209	0.195	0.226	0.149	0.209	0.228	0.117	0.095	0.175	0.224	0.086	0.157
Sucker Creek (EBAR)		0.286	0.556	0.311	0.267	0.283	0.125	0.121	0.112	0.100	0.157	0.221
Beattys Butte (EBAR)			0.35	0.132	0.367	0.344	0.120	0.115	0.107	0.154	0.083	0.070
Red Basin (LBAR)				0.372	0.326	0.255	0.161	0.194	0.164	0.187	0.209	0.179
Quartz Basin (LBAR)					0.122	0.143	0.130	0.145	0.114	0.102	0.148	0.155
Skull Springs (LBAR)						0.278	0.135	0.196	0.194	0.145	0.133	0.078
Virgin Valley (EBAR)							0.109	0.125	0.189	0.182	0.129	0.095
Second Division (EBAR)								0.617	0.232	0.219	0.566	0.186
Green Hills (EBAR)									0.338	0.212	0.44	0.154
L. Snake Creek (EBAR)										0.329	0.196	0.256
Pawnee Creek (LBAR)											0.225	0.263
Barstow (LBAR)												0.252

Table 1.6 Bray-Curtis similarity matrix.

	Sucker Creek (EBAR)	Beatty Buttes (EBAR)	Red Basin (LBAR)	Quartz Basin (LBAR)	Skull Springs (LBAR)	Virgin Valley (EBAR)	Second Division (EBAR)	Green Hills (EBAR)	L. Snake Creek (EBAR)	Pawnee Creek (LBAR)	Barstow (LBAR)	Valentine (LBAR)
Mascall	0.338	0.327	0.369	0.259	0.347	0.37	0.209	0.174	0.298	0.366	0.158	0.27
Sucker Creek (EBAR)		0.444	0.714	0.475	0.421	0.441	0.222	0.216	0.202	0.184	0.272	0.362
Beattys Butte (EBAR)			0.519	0.233	0.537	0.512	0.214	0.207	0.193	0.267	0.154	0.131
Red Basin (LBAR)				0.542	0.491	0.407	0.278	0.324	0.283	0.316	0.346	0.304
Quartz Basin (LBAR)					0.217	0.25	0.771	0.254	0.205	0.185	0.257	0.268
Skull Springs (LBAR)						0.435	0.237	0.328	0.326	0.254	0.235	0.144
Virgin Valley (EBAR)							0.197	0.222	0.318	0.308	0.229	0.173
Second Division (EBAR)								0.763	0.376	0.359	0.723	0.314
Green Hills (EBAR)									0.505	0.35	0.612	0.268
L. Snake Creek (EBAR)										0.495	0.327	0.407
Pawnee Creek (LBAR)											0.368	0.417
Barstow (LBAR)												0.403

Table 1.7 Raup-Crick similarity matrix.

	Sucker Creek (EBAR)	Beatty Buttes (EBAR)	Red Basin (LBAR)	Quartz Basin (LBAR)	Skull Springs (LBAR)	Virgin Valley (EBAR)	Second Division (EBAR)	Green Hills (EBAR)	L. Snake Creek (EBAR)	Pawnee Creek (LBAR)	Barstow (LBAR)	Valentine (LBAR)
Mascall	0.733	0.934	0.875	0.576	0.921	0.951	0.097	0.020	0.208	0.839	0.007	0.010
Sucker Creek (EBAR)		0.999	0.999	0.997	0.993	0.998	0.065	0.05	0	0.008	0.124	0.192
Beattys Butte (EBAR)			0.999	0.620	0.999	0.999	0.390	0.324	0.122	0.653	0.061	0
Red Basin (LBAR)				0.999	0.999	0.978	0.280	0.515	0.038	0.399	0.520	0.008
Quartz Basin (LBAR)					0.489	0.597	0.302	0.419	0.038	0.074	0.380	0.171
Skull Springs (LBAR)						0.997	0.423	0.873	0.811	0.467	0.311	0
Virgin Valley (EBAR)							0.144	0.238	0.672	0.702	0.182	0
Second Division (EBAR)								0.999	0.455	0.670	0.999	0.006
Green Hills (EBAR)									0.980	0.519	0.999	0
L. Snake Creek (EBAR)										0.951	0.018	0
Pawnee Creek (LBAR)											0.501	0.286
Valentine (LBAR)												

A comparison to Barstovian localities farther away in the western United States demonstrates the similarity between the Mascall fauna and the early Barstovian Virgin Valley fauna of Nevada (Tables 1.5-1.7). In fact, the Virgin Valley fauna is the most similar fauna to the Mascall fauna according to the Jaccard, Bray-Curtis and Raup-Crick indices. The Virgin Valley fauna, like other Barstovian sites in Oregon, differs from the Mascall fauna in containing the aplodontid *Liodontia*, different canids (*Paracynarctus* and *Protomarctus*), *Oreolagus*, the chalicothere *Moropus*, *Hypohippus*, and a more diverse rhinocerotid fauna (*Aphelops, Peraceras* and *Teleoceras*).

The similarity indices also indicate affinity between the Mascall fauna and the late Barstovian Pawnee Creek fauna of Colorado. Although the Pawnee Creek fauna is more diverse than the type Mascall fauna and only contains large mammals, all indices place it as the second most similar to the Mascall fauna outside of Oregon. While the large mammal taxa are largely similar in both faunas, the Pawnee Creek has significantly more equid taxa. In addition, there are different peccaries in the Pawnee Creek fauna and no *Tephrocyon*, *Rakomeryx, Parablastomeryx* or *Paratylopus.*

All cluster analyses resulted in the same relative relationships between faunas (except for the Raup-Crick method) (Figs. 23). Faunas cluster based on geography rather than by time period

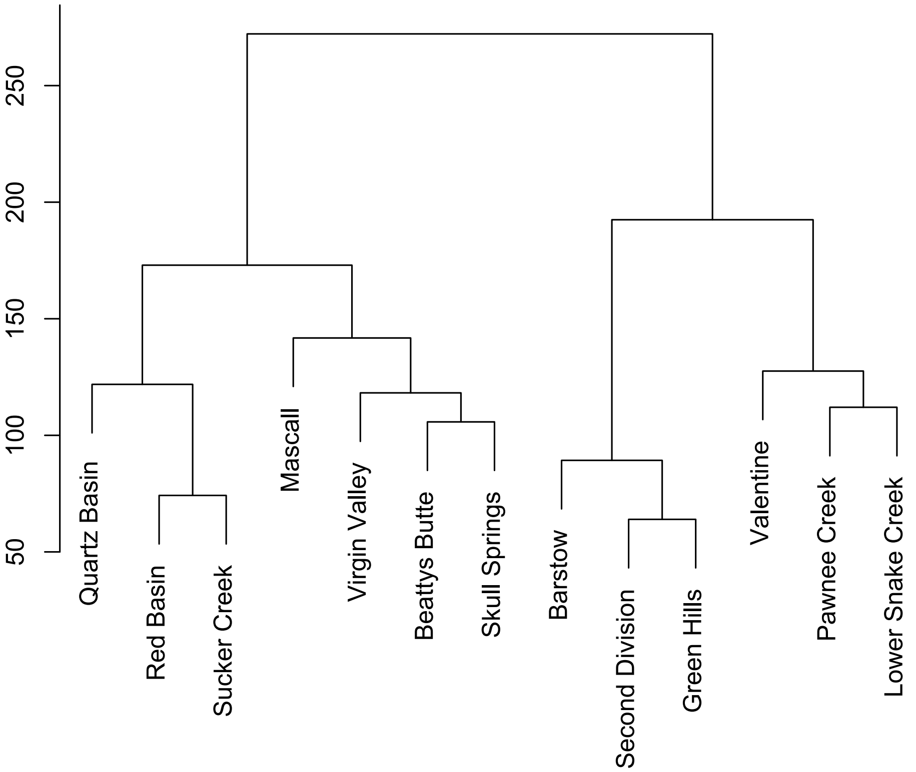

Figure 1.23 Example community cluster dendogram using Jaccard dissimilarity metric and the Ward cluster method.

(Early vs. Late Barstovian). All of the Pacific Northwest localities clump together, including the Virgin Valley Fauna. The Barstow Formation faunas of the Great Basin group together as well as the Great Plains faunas (Pawnee Creek, Valentine and Lower Snake Creek). This provinciality demonstrates an endemic character to all of the faunas that may reflect important environmental gradients across the continent (Barnosky and Carrasco, 2002; Tedford et al. 2004). During the Barstovian the climatic changes associated with the the mid-Miocene Climatic Optimum, of the migration of the Yellowstone hotspot (Kent-Corson et al., 2013) may well have increased regional provinciality. Within the Pacific Northwest, the Mascall fauna groups more closely with the Early Barstovian Virgin Valley fauna and secondarily with the Early Barstovian Beatty Buttes and Late Barstovian Skull Springs faunas. These two later faunas have the lowest diversity of all the sites analyzed and therefore the similarity may be skewed due to smaller sample sizes. The southeastern Oregon sites group together in the dendogram (Fig. 24), again regardless of age. The correspondence analysis groups faunas similarly to the cluster analyses however, there is less of a provinciality signal (Fig. 24). The Lower Snake Creek and Pawnee Creek faunas group closely with the Barstow, Green Hills and Second Division faunas. The

Figure 1.24 Correspondence analysis plot of Barstovian faunas. The inertia percentages are reported on each axis.

Valentine fauna does not group with any other faunas suggesting it contains a unique faunal composition. The Oregon faunas are dispersed but maintain the same groupings observed in the cluster dendogram with the Mascall fauna plotting closest to Skull Springs, Virgin Valley and Beatty Buttes faunas, and the Red Basin, Quartz Basin and Sucker Creek faunas plotting together. These groupings emphasize provinciality rather than groupings driven by faunal turnover from the Early Barstovian to the Late Barstovian.

CONCLUSION

The Mascall type area contains an early Barstovian fauna with a diverse assemblage. The following taxa are added to the faunal list: *Pseudotrimylus mawbyi, Leptocyon* cf. *leidyi, Pseudaelurus, Hypolagus fontinalus, Hypolagus parviplicatus, Monosaulax, Hesperogaulus gazini, Protospermophilus malheurensis, Nototamias,* cf. *Kalobatippus, "Cynorca" hesperia, "Cynorca" sp., Rakomeryx sinclairi,* cf. *Protocamelus, Blastomeryx gemnifer, Parablastomeryx, Zygolophodon proavus.* In addition, three families are added to the list: Talpidae, Cricetidae and Rhinocerotidae. A preliminary reevaluation of the merychippine horses concludes that there are at least two species; however, a more thorough analysis is needed to assign the two morphotypes to species. The following synonymies are updated for the Mascall fauna: *Tephrocyon rurestris* (*=Tomarctus rurestris*)*, Cynelos sinapius* (*=Amphicyon sinapius*)*, Balantiomys oregonensis* (*=Peridiomys oregonensis*)*, Desmatippus avus* (*=Parahippus avus*)*, Protospermophilus oregonensis* (*=Arctomyiodes oregonensis*)*, Ticholeptus zygomaticus* (*=Ticholeptus obliquidens*).

The deposits range from approximately 16 Ma to 13 Ma, although the majority of the fossils are recovered from or stratigraphically close to the Mascall Tuff, dated here at 15.3 Ma. Assigning the fossiliferous part of the Mascall Formation to the Early Barstovian North American Land Mammal age is supported by the presence of *Tephrocyon* and *Zygolophodon*, *Hesperogaulus*, and *Monosaulax* which have first occurrences during the Early Barstovian, and *Desmatippus*, *Parahippus*, *Cynorca*, and *Rakomeryx* which have their last occurrence during the Early Barstovian. The Kangaroo Tuff in the upper unit of the Mascall Formation is dated here at 13.6 Ma. There are 90 m of unfossiliferous Mascall deposits undated above the Kangaroo Tuff, leaving the upper age of the formation unknown. The date on the Kangaroo Tuff indicates that the Mascall Formation extends into the Late Barstovian; however, the majority of fossils are recovered from the Early Barstovian horizons.

This updated faunal list placed into a stratigraphic framework with new ages for tuff deposits allows for more direct comparisons of the Mascall fauna with other Barstovian sites that have also been recently updated and placed in a stratigraphic framework (e.g. Pagnac, 2005). The Mascall fauna is similar to other Barstovian faunas of Oregon and is most similar to the Virgin Valley fauna of Nevada. The fauna also shows strong similarities with the Pawnee Creek fauna of Colorado. The Mascall fauna is least similar to the Barstow Formation faunas of the Great Basin province. Barstovian faunas from the Great Plains, Great Basin and Pacific Northwest group by region rather than by time period indicating provinciality during the Barstovian, possibly as a result of distinctive landscapes separated by geographic barriers that resulted from the relatively pronounced climate change and tectonic activity that characterizes the mid-Miocene.

REFERENCES

Anderson, E., 1994. Evolution, prehistoric distribution, and systematics of *Martes* in Buskirk, S.W., Harestad, A.S., Raphael, M.G., Powell, R.A. (eds.) *Martens, Sables, and Fishers Biology and Conservation*. Cornell University Press, Ithaca, NY, p. 13-25.

Badgley, C., Finarelli, J.A., 2013. Diversity dynamics of mammals in relation to tectonic and climatic history: comparison of three Neogene records from North America. Paleobiology 39, 373–399.

Barnosky, A.D., Carrasco, M.A., 2002. Effects of Oligo-Miocene global climate changes on mammalian species richness in the northwestern quarter of the USA. Evolutionary Ecology Research 4, 811-841.

Bestland, E.A., Krull, E.S., 1997. Mid-Miocene climatic optimum recorded in paleosols from the Mascall Formation (Oregon). Geological Society of America Abstracts with Programs 29, 67.

Bestland, E.A., Forbes, M.S., Krull, E.S., Retallack, G.J., Fremd, T., 2008. Stratigraphy, paleopedology and geochemistry of the middle Miocene Mascall Formation (type area, central Oregon, USA). Paleobios 28, 41–61.

Black, C.C., 1963. A review of the North American Tertiary Sciuridae. Bulletin of the Museum of Comparative Zoology 130(3), 109-248.

Bonaparte, C.-L.J.L., 1845. Catalogo methodico dei mammiferi Europei. L. Di Giacomo Pirola, Milan, Italy, 36 pp.

Bowdich, T.E., 1821. An Analysis of the Natural Classification of Mammalia for the Use of Students and Travelers. J. Smith, Paris, France, 115 pp.

Brandt, J.F., 1855. Beiträge zur nähern Kenntniss der Säugethiere Russlands. Mémoires de l'Académie Impériale des Sciences de Saint-Pétersbourg, Sixtéme Série, Mathématiques, Physiques et Naturelles 9, 1-365.

Calede, J.J.M., Hopkins, S.S.B., 2012. Intraspecific versus interspecific variation in Miocene Great Basin mylagaulids: implications for systematics and evolutionary history. Zoological Journal of the Linnean Society 164, 427–450.

Carrasco, M.A., Kraatz, B.P., Davis, E.B., Barnosky, A.D., 2005. Miocene Mammal Mapping Project (MIOMAP). University of California Museum of Paleontology, http://www.ucmp.berkeley.edu/miomap/

Chaney, R.W., 1925. The Mascall flora; its distribution and climatic relation. Carnegie Institute Washington Publication 349, 23-48.

Chaney, R.W., 1956. The ancient forests of Oregon. Condon Lectures, Oregon State System of Higher Education, University of Oregon, Eugene, Oregon.

Condon, T., 1896. Scientific description of two new fossil dogs. Bulletin of the University of Oregon 2, 11 pp.

Cope, E.D., 1868. Second contribution to the history of the Vertebrata of the Miocene period of the United States. Ibid, 184-194.

Cope, E.D., 1873. Synopsis of new Vertebrata from the Tertiary of Colorado obtained during the summer of 1873. Government Printing Office, Washington, DC, 19 pp.

Cope, E.D., 1874. Notes on the Santa Fe marls and some of the contained vertebrate fossils. Proceedings of the Philadelphia Academy of Natural Sciences 1984, 147-152.

Cope, E.D., 1877. Report upon the extinct Vertebrata obtained in New Mexico by parties of the expedition of 1874. Wheeler Survey 4, 1-370.

Cope, E.D., 1878. Descriptions of new extinct Vertebrata from the Upper Tertiary and Dakota Formations. Bulletin of the United States Geological and Geographic Survey of the Territories, 4(2), 379-396.

Cope, E.D., 1879. Observations on the Faunae of the Miocene Tertiaries of Oregon. Bulletin of the United States Geological and Geographic Survey of the Territories 5(1), 55-70.

Cope, E.D., 1881. Review of the Rodentia of the Miocene period of North America. Bulletin of the United States Geological and Geographic Survey of the Territories 6, 361-386.

Cope, E.D., 1886. On two new species of three-toed horses from the Upper Miocene, with notes on the fauna of the *Ticholeptus* Beds. Proceedings of the American Philosophical Society 23 (123), 357-361.

Coues, E., 1887. *Bassariscus*, a new generic name in Mammalogy. Science 9(225), 516.

Davydov, V.I., Crowley, J.L., Schmitz, M.D., Poletaev, V.I., 2010. High-precision U-Pb zircon age calibration of the global Carboniferous time scale and Milankovitch band cyclicity in the Donets Basin, eastern Ukraine. Geochem. Geophys. Geosyst. 11.

Dawson, M.R., 1958. Later Tertiary Leporidae of North America. University of Kansas Paleontological Contributions Vertebrata 6, 1-75.

Dice, L.R., 1917. Systematic position of several American Tertiary lagomorphs. University of California Publication, Bulletin of the Department of Geology, 10(12), 179-183.

Downs, T., 1951. A review of the Mascall Miocene fauna and related assemblages. Ph.D. thesis, Department of Paleontology, University of California, Berkeley, 386 pp.

Downs, T., 1956. The Mascall fauna from the Miocene of Oregon. University of California Publications in Geological Sciences 31, 199-354.

Fiebelkorn, R.B., Walker, G.W., MacLeod, N.S., McKee, E.H. and Smith, J.G., 1983. Isochron/West Index to K-Ar determinations for the State of Oregon. Isochron/West, 37.

Fischer von Waldheim, G., 1817. Adversaria zoologica. Mémoires de la Société Impériale des Naturalistes de Moscou 5, 357-446.

Flower, B.P., Kennett, J.P., 1993. Relations between Monterey Formation deposition and middle Miocene global cooling: Naples Beach section, California. Geology 21, 877.

Flynn, L.J., 2008. Eomyidae in Janis, C.M., Gunnell, G.F., Uhen, M.D. (eds.) *Evolution of Tertiary Mammals of North America Volume 2: Small Mammals, Xenarthrans, and Marine Mammals.* Cambridge University Press, p. 415-427.

Flynn, L.J., Lindsay, E.H., Martin, R.A., 2008. Geomorpha in Janis, C.M., Gunnell, G.F., Uhen, M.D. (eds.) *Evolution of Tertiary Mammals of North America Volume 2: Small Mammals, Xenarthrans, and Marine Mammals.* Cambridge University Press, p. 428-455.

Frick, C., 1937. Horned ruminants of North America. Bulletin of the AMNH; v. 69.

Frisch, J.L., 1775. Das Natur-system der vierfuszigen Thiere, in Tabellen, darinnen alle Ordnungen, Geschlechte un Arten, nicht nur mit bestimmenden Benennungen, sondern beygeseszten unter-scheidenden Kennzeichen angezeigt werden, zum Nutzen der erwachsenen Schuljugend, Glogan, Gunther, 35 pp.

Gazin, C.L., 1930. A Tertiary Vertebrate fauna from the upper Cuyama drainage basin, California. Carneige Institute of Washington Publications 404, 55-76.

Gazin, C.L., 1932. A Miocene mammalian fauna from south-eastern Oregon. Contributions to Paleontology from Carnegie Institution of Washington 418, 37-86.

Gervais, P., 1850. Zoologie et paléontologie français. Nouvelles recherches sur les animaux vertébrés dont on trouve les ossements enfouis dans le sol de la France et sur leur comparaison avec les espèces propres aux autres regions du globe. Zoologie et Paléontologie Française 8, 1-271.

Gidley, J.W., 1906. A new genus of horse from the Mascall beds, with notes on the small collection of equine teeth in the University of California. American Museum of Natural History Bulletin 22, 385-388.

Gill, T., 1872. Arrangement of the families of mammals with analytical tables. Smithsonian Miscellaneous Collections 11, 1-98.

Goodwin, H.T., 2008. Sciuridae in Janis, C.M., Gunnell, G.F., Uhen, M.D. (eds.) *Evolution of Tertiary Mammals of North America Volume 2: Small Mammals, Xenarthrans, and Marine Mammals.* Cambridge University Press, p. 355-376.

Gunnell, G.F., Bown, T.M., Hutchison, J.H., Bloch, J.I., 2008. Lipotyphla in Janis, C.M., Gunnell, G.F., Uhen, M.D. (eds.) *Evolution of Tertiary Mammals of North America Volume 2: Small Mammals, Xenarthrans, and Marine Mammals.* Cambridge University Press, p. 89-125.

Gureev, A.A., 1971. Shrew (Socricidae) fauna of the World. Akademiâ Nauk, Saint Petersburg, Russia, 253 pp.

Gray, J.E., 1821. On the natural arrangement of vertebrose animals. London Medical Repository 15, 296-310.

Gray, J.E., 1825. Outline of an attempt at the disposition of the Mammalia into tribes and families, with a list of genera apparently appertaining to each tribe. Annals of Philosophy 26, 337-344.

Gray, J.E., 1868. Synopsis of the species of Saccomyidae, or pouched mice, in the collection of the British Museum. Proceedings of the Zoological Society of London 1868, 199-206.

Gregory, W.K., 1910. The orders of mammals. Bulletin of the American Museum of Natural History 37, 1-524.

Gregory, J.T., Downs, T., 1951. *Bassariscus* in Miocene faunas and *Potamotherium lycopotamicum* Cope. Postilla 8, 1-10.

Haeckel, E., 1866. Generelle Morphologie der Organismen. Allgemeine Grudziige der Organischen Formenwissenschaft, Mechanisch Begriindet Durch die von Charles Darwin Reformierte Deszendenz-Theorie. Band I: Allgemeine Anatomie der Organismen. Georg Reimer, Berlin, 574 pp.

Hammer, O., Harper, D.A.T., 2006. Paleontological Data Analysis. Blackwell Publishing, 351 pp.

Hay, O.O., 1899. On the names of certain North American fossil vertebrates. Sciences, Series 2, 9, 593-594.

Hay, O.P., 1922. Further observations on some extinct elephants. Proceedings of the Biological Society of Washington 35, 97-102.

Hibbard, C.W., 1939. Notes on additional fauna of Edson Quarry of the middle Pliocene of Kansas. Transactions of the Kansas Academy of Science 42, 457-462.

Honey, J.G., Harrison, J.A., Prothero, D.R., Stevens, M.S., 1998. Camelidae in Janis, C.M., Scott, K.M., and Jacobs, L.L. (eds.) *Evolution of Tertiary Mammals of North America Volume 1: Terrestrial Carnivores, Ungulates, and Ungulatelike Mammals*. Cambridge University Press, p. 439-462.

Hooper, P. R., and Swanson, D.A., 1990. The Columbia River Basalt group and associated volcanic rocks of the Blue Mountains Province. U.S. Geological Survey Professional Paper 1437, 63-99.

Hunt, R.M., Jr., 1998. Amphicyonidae in Janis, C.M., Scott, K.M., and Jacobs, L.L. in (eds.) *Evolution of Tertiary Mammals of North America Volume 1: Terrestrial Carnivores, Ungulates, and Ungulatelike Mammals*. Cambridge University Press, p. 196-227.

Hutchison, H.J., 1968. Fossil Talpidae (Insectivor, Mammalia) from the later Tertiary of Oregon. Bulletin of the Museum of Natural History, University of Oregon 11, 1-117.

Illiger, C., 1811. Prodromus Systematis Mammalium et Avium Additis Terminis Zoographicis Utriusque Classis. Salfeld, Berlin, Germany, 301 pp.

Jaffey, A.H., Flynn, K.F., Glendenin, L.E., Bentley, W.T., Essling, A.M., 1971. Precision Measurement of Half-Lives and Specific Activities of U^{235} and U^{238}. Physical Review C 4, 1889.

Janis, C.M., Manning, E., 1998. Dromomerycidae in (eds.) *Evolution of Tertiary Mammals of North America Volume 1: Terrestrial Carnivores, Ungulates, and Ungulatelike Mammals*. Cambridge University Press, p. 477-490.

Janis, C.M., Scott, K.M., and Jacobs, L.L., 1998. Evolution of Tertiary Mammals of North America Volume 1: Terrestrial Carnivores, Ungulates, and Ungulatelike Mammals. Cambridge University Press, 691 pp.

Janis, C.M., Damuth, J., Theodor, J.M., 2002. The origins and evolution of the North American grassland biome: the story from the hoofed mammals. Palaeogeography, Palaeoclimatology, Palaeoecology 177, 183–198.

Janis, C.M., Gunnell, G.F., Uhen, M.D., 2008. Evolution of Tertiary Mammals of North America Volume 2: Small Mammals, Xenarthrans, and Marine Mammals. Cambridge University Press, 795 pp.

Jourdan, M., 1862. La déscription de restes fossiles de grands Mammiferes. Part 2. Les terrains sidérolithiques. Rev. Soc. Sav., Publ. Min. Instr. Publ. Desc. 1, 126-130.

Kelly, T.S., 1995. New Miocene horses from the Caliente Formation, Cuyama Valley Badlands, California. Natural History Museum of Los Angeles Contribution in Science 455, 1-33.

Kelly, T.S., Lander, E.B., 1988. Biostratigraphy and correlation of Hemingfordian and Barstovian land mammal assemblages, Caliente Formation, Cuyama Valley area, California.

In W.J.M. Bazeley (ed.) *Tertiary tectonics and sedimentation in the Cuyama Basin, San Luis Obispo, Santa Barbara, and Ventura Counties, California*. Pacific Section, Society of Economic Paleontologists and Mineralogists, Papers and Field Guide from the Cuyama Symposium and Field Trip, 1-19.

Kent-Corson, M., Barnosky, A.D., Mulch, A., Carrasco, M.A., Chamberlain. C.P., 2013. Possible regional tectonic controls on mammalian evolution in western North America. Palaeogeography, Palaeoclimatology, Palaeoecology 387, 17-26.

Korth, W.W., 1997. A new subfamily of primitive pocket mice (Rodentia, Heteromyidae) from the middle Tertiary of North America. Paludicola 1(2), 33-66.

Korth, W.W., 1999. *Hesperogaulus*, a new genus of mylagaulid rodent (Mammalia) from the Miocene (Barstovian to Hemphillian) of the Great Basin. Journal of Paleontology 73, 945-951.

Krull, E.S., 1998. Stratigraphy and collection of leaf-bearing units in the Miocene Mascall Formation, central Oregon. Unpublished report for John Day Fossil Beds National Monument, 24 pp.

Lambert, W.D., Shoshani, J., 1998. Probocidea in (eds.) *Evolution of Tertiary Mammals of North America Volume 1: Terrestrial Carnivores, Ungulates, and Ungulatelike Mammals*. Cambridge University Press, p. 606-622.

Lander, B., 1998. Oreodontoidea in (eds.) *Evolution of Tertiary Mammals of North America Volume 1: Terrestrial Carnivores, Ungulates, and Ungulatelike Mammals*. Cambridge University Press, p. 402-425.

Leidy, J., 1857. Notices of extinct Vertebrata discovered by F.V. Hayden, during the expedition to the Sioux Country under the command of Lieut. G.K. Warren. Proceedings of the Academy of Natural Sciences, Philadelphia 8, 311-312.

Leidy, J., 1858. Notice of remains of extinct Vertebrata, from the Valley of the Niobrara River, collected during the exploring expedition of 1857, in Nebraska, under the command of Lieut. G.K. Warren, U.S. Top. Eng, by Dr. F.V. Hayden, Geologist to the Expedition. Proceedings of the Academy of Natural Sciences, Philadelphia 10, 20-29.

Lindsay, E.H., 2008. Cricetidae in Janis, C.M., Gunnell, G.F., Uhen, M.D. (eds.) *Evolution of Tertiary Mammals of North America Volume 2: Small Mammals, Xenarthrans, and Marine Mammals.* Cambridge University Press, p. 456-479.

Linnaeus, C., 1758. Systema Naturae per Regna Tria Naturae, Secundum Classis, Ordines, Genera, Species cum Characteribus, Differentiis, Synonymis, Locis, [Tenth Edition, Volume I]. Laurentii Salvii, Stockholm, Sweden, 824 pp.

Long, P.E., Duncan, R.A., 1982. ^{40}Ar/^{39}Ar ages of Columbia River Basalt from deep boreholes in south-central Washington. Rockwell Hanford Operations Report RHO-BW-SA-233p, 11 pp.

Lydekker, R., 1883. Selenodont Siwalik Suina. Pal. Indica, 10, 142-177.

MacFadden, B.J., 1998. Equidae in Janis, C.M., Scott, K.M., and Jacobs, L.L. (eds.) *Evolution of Tertiary Mammals of North America Volume 1: Terrestrial Carnivores, Ungulates, and Ungulatelike Mammals*. Cambridge University Press, p. 537-559.

Matthew, W.D., 1902. New Canidae from the Miocene of Colorado. Bulletin of the American Museum of Natural History 16, 281-290.

Matthew, W.D., 1918. Contributions to the Snake Creek Fauna. Bulletin of the American Museum of Natural History 38(7), 183-229.

Marsh, O.C., 1871. Notice of some new fossil mammals from the Tertiary formation. American Journal of Science Series 3 Vol. 2, 35-44.

Marsh, O.C., 1874. Notice of new equine mammals from the Tertiary formation. American Journal of Science 7, 247-258.

Mattinson, J.M., 2005. Zircon U–Pb chemical abrasion (“CA-TIMS”) method: Combined annealing and multi-step partial dissolution analysis for improved precision and accuracy of zircon ages. Chemical Geology 220, 47–66.

Mawby, J.E., 1960. A new occurrence of *Heterosorex* Gaillard. Journal of Paleontology 34(5), 950-956.

Merriam, J.C., 1901. A contribution to the geology of the John Day Basin. University of California Bulletin, Department of Geology 2(9), 269-314.

Merriam, J.C., 1906. Carnivora from the Tertiary formations of the John Day region. Ibid. 5, 1-64.

Merriam, J.C., Sinclair, W.J., 1907. Tertiary faunas of the John Day region. University of California Publications in Geological Sciences 5, 171-205.

Merriam, J.C., Stock, C., Moody, C.L., 1925. The Pliocene Rattlesnake formation and fauna of eastern Oregon, with notes on the geology of the Rattlesnake and Mascall deposits. Carnegie Institute of Washington Publication 347, 43-92.

Osborn, H.F., 1915. [No title: Description of *Kalobatippus*] in Cope, E.D, Matthew, W.D. (eds.) *Hitherto unpublished plates of Tertiary Mammalia and Permian Vertebrata.* U.S. Geological Survey and American Museum of Natural History, Monograph Series 2, Plate CVIII.

Owen, R., 1848. Description of teeth and portions of jaws of two extinct anthracotherioid quadrupeds (*Hyopotamus vectianus* and *Hyop. bovinus*) discovered by the Marchioness of Hastings in the Eocene deposits on the N.W. coast of the Isle of Wight: with an attempt to develop Cuvier's idea of the classification of pachyderms by the number of their toes. Quarterly Journal of the Geological Society of London 4, 103-141.

Pagnac, D.C., 2005. A systematic review of the mammalian megafaun of the Middle Miocene Barstow Formation, Mojave Desert, California. Ph.D. thesis, Department of Geology, University of California, Riverside, 384 pp.

Palmer, T.S., 1897. Notes on the nomenclature of four genera of Tropical American mammals. Proceedings of the Biological Society of Washington 11, 173-174.

Pratt, A.E., Morgan, G.S., 1989. New Sciuridae (Mammalia: Rodentia) from the early Miocene Thomas Farm local fauna, Florida. Journal of Vertebrate Paleontology 9, 89-100.

Prothero, D.R., 2005. The evolution of North American rhinoceroses. Cambridge University Press, 218 pp.

Prothero, D.R., 2008. Systematics of the musk deer (Artiodactyla: Moschidae: Blastomerycinae) from the Miocene of North America. New Mexico Museum of Natural History and Science Bulletin 44, 207-224.

Prothero, D.R., Draus, E., Foss, S.E., 2006. Magnetic stratigraphy of the lower portion of the middle Miocene Mascall Formation, central Oregon. PaleoBios 26(1), 37-42.

Prothero, D.R., Liter, M.R., 2008. Systematics of the dromomerycines and aletomerycines (Artiodactyla: Palaeomerycidae) from the Miocene and Pliocene of North America. New Mexico Museum of Natural History and Science Bulletin 44, 273-298.

R Core Team, 2013. R: A language and environment for statistical computing. R Foundation for Statistical Computing, Vienna, Austria. URL http://www.R-project.org/.

Rensberger, J.M., von Koenigswald, W., 1980. Functional and phylogenetic interpretation of enamel microstructure in rhinoceroses. Paleobiology 6(4), 477-495.

Repenning, C.A., 1967. Subfamilies and genera of the Soricidae. Geological Survey Professional paper 565, 69p.

Rothwell, T., 2003. Phylogenetic Systematics of North American *Pseudaelurus* (Carnivora: Felidae). American Museum of Novitates 3403, 1-64.

Sato, J.J., Hosoda, T., Wolsan, M., Tsuchiya, K., Yamamoto, M., Suzuki, H., 2003. Phylogenetic relationships and divergence times among mustelids (Mammalia: Carnivora) based on nucleotide sequences of the nuclear interphotoreceptor retinoid binding protein and mitochondrial cytochrome b genes. Zool. Sci. 20, 243–264.

Scharf, D.W., 1935. A Miocene mammalian fauna from Sucker Creek, Oregon. Carnegie Institute of Washington 453, 97-118.

Schmitz, M.D., Schoene, B., 2007. Derivation of isotope ratios, errors, and error correlations for U-Pb geochronology using 205Pb- 235U-(233U)-spiked isotope dilution thermal ionization mass spectrometric data. Geochem. Geophys. Geosyst. 8.

Schmitz, M.D., Lovelock, E.C., 2013. Radiometric Dating of Volcanic Rocks in the John Day Basin. National Park System Task Agreement Report J8R07110010 Phase 1, 5 pp.

Scott, W.B., 1893. The mammals of the Deep River beds. American Naturalists 27, 659-652.

Sheldon, N.D., 2006. Using paleosols of the Picture Gorge Basalt to reconstruct the Middle Miocene Climatic Optimum. PaleoBios 26, 27-36.

Shotwell, J.A., 1967. Late Tertiary Geomyoid rodents of Oregon. Bulletin of the Museum of Natural History, University of Oregon, v. 9, p. 1-51.

Shotwell, J. A., 1968. Miocene mammals of southeast Oregon: Bulletin of the Museum of Natural History, University of Oregon, v. 14, p. 1-67.

Shotwell, J.A., Russell, D.E., 1963. Mammalian fauna of the upper Juntura Formation, the Black Butte local fauna. Transactions of the American Philosophical Society 53, 42-69.

Smith, G. A., 1986. Simtustus Formation: Paleogeographic and stratigraphic significance of a newly defined Miocene unit in the Deschutes basin, central Oregon. Oreg. Geol. 48, 63–72.

Stefen, C., 2001. The Barstovian (Miocene) beavers of Stewart Valley, Nevada, and a preliminary discussion of the genus *Monosaulax* mainly on the basis of tooth morphology. PaleoBios 21, 1-15.

Stirton, R.A., 1935. A review of the Tertiary beavers. University of California Publications, Bulletin of the Department of Geological Sciences 23(13), 391-485.

Stirton, R.A., 1940. Phylogeny of North American Equidae. University of California Publications, Bulletin of the Department of Geological Sciences, 25, 165-198.

Stock, C., 1930. Carnivora new to the Mascall Miocene fauna of eastern Oregon. Carnegie Institute of Washington Publication 404, 43-48.

Streck, M.J., Grunder, A.L., 1995. Crystallization and welding variations in a widespread ignimbrite sheet; the Rattlesnake Tuff, eastern Oregon, USA. Bulletin of Volcanology 57, 151–169.

Streck, M.J., Johnson, J.A., and Grunder, A.L., 1999. Field guide to the Rattlesnake tuff and

High Lava Plains near Burns, Oregon. Oregon Geology 61, 64-76.

Sutton, J.F., Korth, W.W., 1995. Rodents (Mammalia) from the Barstovian (Miocene) Anceney local fauna, Montana. Annals of the Carnegie Museum 64, 267-314.

Swisher, C.C., 1992. ^{40}Ar/^{39}Ar Dating: Application to the Calibration of North American Land Mammal Ages. Ph.D. thesis, Department of Paleontology, University of California, Berkeley, 239 pp.

Tedford, R.H., Wang, X., Taylor, B.E., 2009. Phylogenetic systematics of the North American fossil Caninae (Carnivora: Canidae). Bulletin of the American Museum of Natural History 325, 218 pp.

Tedford, R.H., Albring, L.B., III, Barnosky, A.D., Ferrusquia-Villafranca, I., Hunt, R.M., Jr., Storer, J.E., Swisher, C.C., III, Voorhies, M.R., Webb, S.D., Whistler, D.P., 2004. Mammalian biochronology of the Arikareean through Hemphillian interval (late Oligocene through early Pliocene epochs) in M.O. Woodburne (ed.) *Late Cretaceous and Cenozoic Mammals of North America: Biostratigraphy and Geochronology*. Columbia University Press, p 169-231.

Thorpe, M.R., 1923. The primitive and carnivore-like characters of the Merycoidodontidae. American Journal of Science 5(6), 239-246.

Vincent, E., and Berger, W.H., 1985. Carbon dioxide and polar cooling in the Miocene: the Monterey hypothesis. In E.T. Sundquist and W.S. Broecker (eds.) *The Carbon Cycle and Atmospheric CO2: Natural Variations Archean to Present.* American Geophysical Union, Geophysical Monograph Series 32, 13–27.

Voorhies, M.R., Timperley, C.L., 1997. A new *Pronotolagus* (Lagomorpha: Leporidae) and other leporids from the Valentine Railway Quarries (Barstovian, Nebraska), and the archaeolagine-leporine transition. Journal of Vertebrate Paleontology 17, 725–737.

White, J.A., 1988. The Archaeolaginae (Mammalia, Lagomorpha) of North America, excluding *Archaeolagus* and *Panolax*. Journal of Vertebrate Paleontology 7(4), 425-450.

Wilson, D.E., Reeder, D.M. (eds), 1993. Mammal species of the world: a taxonomic and geographic reference. Smithsonian Institution Press, Washington, DC.

Wolfe, J.A., 1981. Paleoclimatic significance of the Oligocene and Neogene floras of the northwestern United States in Niklas, K.J. (ed.) *Paleobotany, Paleoecology, and Evolution*. Praeger Publishers, New York, p. 79-101.

Wood, A.E., 1935. Evolution and relationships of the heteromyid rodents with new forms from the Tertiary of western North America. Annals of the Carnegie Museum 24, 73-262.

Wood, A.E., 1936. Fossil heteromyid rodents in the collections of the University of California.

American Journal of Sciences 32, 112-119.

Wood, H.E., III, Chaney, R.W., Clark, J., Colbert, E.H., Jepsen, G.L., Reeside, J.B., Jr., Stock, C., 1941. Nomenclature and correlation of the North American continental Tertiary. Geological Society of American Bulletin 52, 1-48.

Woodburne, M.O., 1969. Systematics, biogeography, and evolution of Cynorca and Dyseohyus (Tayassuidae). Bulletin of the AMNH; v. 141, article 2.

Woodburne, M.O., 2004. Late Cretaceous and Cenozoic Mammals of North America: Biostratigraphy and Geochronology. Columbia University Press, 376 pp.

Wright, D.B., 1993. Evolution of sexually dimorphic characters in peccaries (Mammalia, Tayassuidae). Paleobiology 19, 52-70.

Wright, D.B., 1998. Tayassuidae in Janis, C.M., Scott, K.M., and Jacobs, L.L. (eds.) *Evolution of Tertiary Mammals of North America Volume 1: Terrestrial Carnivores, Ungulates, and Ungulatelike Mammals*. Cambridge University Press, p. 389-401.

Zachos, J., 2001. Trends, Rhythms, and Aberrations in Global Climate 65 Ma to Present. Science 292, 686–693.

CHAPTER 2: THE DIETS OF EQUIDS ACROSS THE MID-MIOCENE CLIMATIC OPTIMUM IN OREGON, USA

INTRODUCTION

The Late Early Miocene and Middle Miocene was a period of environmental and climatic change in North America associated with evolutionary changes and faunal turnover within mammals (Badgley and Finarelli, 2013; Barnosky, 2001; Janis, 1993; Janis et al., 2000, 2002, 2004; Kohn and Fremd, 2008; Webb, 1977). Several ungulate clades (eg. Camelidae, Dromomerycidae, Antilocapridae) diversified, morphological innovations (e.g. hypsodonty) emerged and average body size increased within many lineages (Davis, 2007; Honey et al. 1998; Janis, 1993; Prothero and Foss, 2007). In particular, equids within the subfamily Equinae underwent an adaptive radiation in which at least 19 new species originated (MacFadden and Hulbert, 1988). This diversification is associated with the emergence of characteristics associated with grazing such as hypsodonty, complex enamel patterns, increased body size, and postcranial adaptations for cursorial locomotion in open habitats (MacFadden 1992, 1997). And during this time period there is a decrease in browsing equids and an increase in grazing equids (Janis et al., 2000, 2004). Here I examine details of this trend at a local scale in Miocene deposits of central Oregon, where the equid fauna shifts from dominance of browsers to dominance of grazers. I use carbon stable isotope analyses to: 1) differentiate the diets of browsers and grazers, 2) examine changes in their diets through time, and 3) investigate if changes in their dietary niches were correlated with the success of grazing equids and the demise of browsing equids.

The morphological changes and diversification of equids in North America during the Miocene is associated with environmental and climatic changes, this is especially evident in the Pacific Northwest (Kohn and Fremd, 2008). The mid-Miocene Climatic Optimum (MMCO) occurred approximately 17-14 Ma during which global temperatures rose to a mean annual surface temperature of 18.4°C, approximately 3°C higher than today (You et al., 2009). There is dispute as to the cause of the warming and whether it was associated with increased atmospheric CO_2 (Berner, 1998; Cerling, 1991; Pagani et al., 1999a; Pagani et al., 1999b), but paleobotanical analyses, mammalian paleobiology data, and recent climate simulations suggest CO_2 levels were elevated compared to today at about 500 ppm (Janis et al., 2000; Kürschner et al., 2008; You et al., 2009). Shifts in local climate during the MMCO were not uniform across North America (Retallack, 2007). The Pacific Northwest experienced increased temperatures and humidity during the warming event (Retallack, 2007). Other regions also experienced increased temperatures and humidity but to a lesser extent, such as the Northern Rockies that had a subhumid climate during the Barstovian (Barnosky and Lebar, 1989; Barnosky, 2001; Retallack, 2007). Tectonic activity increased during the Miocene with the onset of the basin and range province in the Great Basin and uplift of the Rocky Mountains beginning by 17.5 Ma (McMillan et al., 2002; Wernicke and Snow, 1998). In Oregon, eruptions of the Columbia River Basalts intensified at 17.2 Ma associated with regional extension and eruption of the Steens Mountain in southeastern Oregon at 16.6 Ma (Camp and Ross, 2004; Hooper et al., 2002; Lui and Stegman, 2012). In addition, the Yellowstone Hotspot began erupting at about 16 Ma in southeastern Oregon, increasing topographic relief, diversifying the landscape and potentially stimulating mammalian faunal change in its wake (Kent-Corson et al., 2013). Patterns in mammalian faunas have been placed in the context of these regional and local changes in the environment. For example, increased diversification (Badgley and Finarelli, 2013; Barnosky and Carrasco, 2002;

Kent-Corson et al., 2013; Kohn and Fremd, 2008) and associated changes in the proportion of browsers to grazers (Janis et al., 2000, 2004) have been documented. The trend towards decreased browsers relative to grazers was originally hypothesized to be associated with the onset and spread of grasses that utilize the C4 photosynthetic pathway. However, later work demonstrated that a switch from a C3 to a C4 diet by equids and other ungulates occurred much later, at about 7-8 Ma (Wang et al., 1994), and although C4 grasses existed on the landscape as far back as the Early Oligocene, they did not become widespread until the Late Miocene (Edwards et al., 2010). The C4 photosynthetic pathway occurs in about 5% of plant species, typically in warm-growing-season grasses and sedges, and composing most of the diet of equids today. The C3 photosynthetic pathway is characteristic of the majority (85%) of plant species, typically in trees, shrubs, and cool-growing-season grasses (Ehleringer et al., 1991). A third photosynthetic pathway, Crassulacean acid metabolism (CAM) is utilized by 10% of plant species and is characteristic of succulent and epiphytic plants. During the early Miocene, more open habitats emerged in the Great Plains and Northern Rockies with the spread of C3 grasses (Retallack, 1997, 2001, 2004; Strömberg, 2005). Prior to this time, habitats were “closed” and consisted of forested vegetation such as woody or herbaceous angiosperms, conifers, and ferns (Strömberg, 2005). However, there is evidence of C3 grasses earlier in Oregon. During the Late Oligocene in Oregon, bunch grasses grew in wooded grassland and sagebrush habitats and in the Early Miocene, sod grasses were abundant in wooded grassland habitats (Retallack, 2004, 2007). This, along with paleosol evidence and diversification of burrowing mammals (Calede et al., 2011; Samuels and Van Valkenburgh, 2009) suggests woodlands were already present and more open habitats were spreading substantially earlier than the Early Miocene in Oregon.

In the Late Early Miocene and Middle Miocene deposits of central and eastern Oregon, there are three equid morphotypes belonging to four genera consistently recovered from fossil localities. *Archaeohippus* was a small-bodied equid (average M1=10-13 mm) with brachydont molars (MacFadden, 1998). The *Archaeohippus* lineage is a clear example of dwarfism within the seemingly ubiquitous trend of increased body size in Equidae through time (MacFadden, 1992). Although a small browser, it is adapted for cursorality with reduced lateral metapodials and an elongate proximal phalanx of the third digit (O'Sullivan, 2003). *Archaeohippus* is within the subfamily Anchitheriinae although its relationship to other members in this subfamily is currently unknown (MacFadden, 1998). In Oregon deposits, *Acrhaeohippus* specimens are recovered from Late Arikareean through Early Barstovian deposits (Fig. 2.1). Specimens from the Early Barstovian are assigned to *A. ultimus*. Specimens from Arikareean and Hemingfordian deposits are not assigned to a species (Dingus, 1990; Hunt and Stepleton, 2004). Those from the Hemingforidan Warm Springs locality are slightly smaller and lower crowned than *A. ultimus* (Dingus, 1990).

The second morphotype of equids in the Miocene of Oregon consists of the brachydont medium-sized (M1=15-16 mm) genera *Desmattipus* and *Parahippus*. These genera have similar tooth morphologies but represent opposite ends of the spectrum of Anchitheriinae equids leading up to the Equinae lineage. *Desmatippus* molars lack a crochet and have little to no cement. *Parahippus* molars are mesodont to almost hypsodont with “advanced” forms having a crochet and cement (MacFadden, 1998). They have reduced lateral metapodials and an elongate phalanx of the third digit. *Desmatippus* is found in the Early Barstovian of Oregon and assigned to the species *D. avus* while *Parahippus* is recovered from Late Arikareean to Early Barstovian deposits, with Hemingforidan specimens referred to *P. pawniensis* and *P.* aff. *leonensis* (Dingus, 1990; Hunt and Stepleton, 2004) and the Bastovian specmines not assigned to a species (Fig.

2.1). Because *Desmatippus* and *Parahippus* represent end points of a morphological grade, species assignment for specimens is difficult and not attempted here until a thorough reevaluation of the genera is conducted, which is outside the scope of this study. Confusion regarding identification may be influencing the stratigraphic ranges discussed here and until a thorough taxonomic analysis and reidentification of specimens is undertaken, the Oregon stratigraphic ranges reported here represent estimates.

The last morphotype examined in this study is a larger-bodied, hypsodont, tridactyl equid with reduced lateral metapodials, in the merychippine grade of equids. The paraphyletic merychippine grade is basal to the Equinae adaptive radiation and part of the Early Miocene diversification of the clade. It is an intermediate between the brachydont browsers and the very hypsodont, large bodied cursorial grazers. There are at least two species of merychippines recovered from Middle Miocene deposits in Oregon, a larger species and a smaller species (Woodburne, pers. communication). The type specimen of the larger species has been attributed to *Hippotherium seversum* (Cope, 1886) *H. isonesum* (Cope, 1889), *Stylonus isonesus* (Kelly and Lander, 1998), *Merychippus isonesus* (Gidley, 1906), *Merychippus seversus* (Downs, 1956) and most recently *Acritohippus isonesus* (Kelly, 1995). Assignment to *Acritohippus* is largely based on cranial features and not tooth morphology. Kelly (1995) places the genus within Equidae but does not assign it to a tribe. The specimens, all teeth, analyzed here belong to the larger species of the merychippines from the Mascall deposits; however, a more precise taxonomic assignment than aff. *Acritohippus* is not given to them because the teeth are not diagnostic and a more thorough analysis of all merychippine specimens from Oregon is needed (Woodburne, in prep.). In Oregon, merychippines are recovered from the latest Hemingfordian localities and Barstovian deposits (Fig.2.1). The specimens of aff. *Acritohippus* analyzed in this study are all from the Barstovian Mascall Formation.

Browsing ungulate diversity was greatest during the mid-Miocene, higher than any other period in the Cenozoic (Janis et al., 2004). Browsers began to decline by the Late Miocene and grazers became the dominant ungulates, as they are today. It was traditionally hypothesized that grazers out-competed browsers, leading to the extinction of many browsing species. However, in the mid-Miocene, browsing ungulates coexisted with grazing ungulates across the continent, suggesting that competition alone did not lead to their extinction (Janis et al., 2004). Instead, it is hypothesized that environmental changes such as spreading grasslands and decreased primary productivity associated with decreased atmospheric CO_2, increased selective pressures so that browsing ungulates became extinct and grazers survived and diversified (Janis et al., 2000; 2004). This hypothesis requires that the dietary niches of browsers were not broad enough to permit effective utilization of the new vegetation types that accompanied environmental change, nor were the dietary niches able to evolve to adapt to the changing environment. Research using stable carbon isotopes has shown that the dietary niche of genera can change and vary as the environment (and particularly the vegetation) changes (DeSantis et al., 2009). Given this, I test the hypothesis that dietary niches of browsers were narrow and did not evolve, leading to their extinction, by examining the dietary niches of the four genera of equids represented in the Late Early Miocene and Middle Miocene deposits of Oregon. Conducting the analysis at the genus level is appropriate given that *Archaeohippus* and aff. *Acritohippus* are most likely monospecific in Oregon. *Parahippus* and *Desmatippus* specimens may represent more than one species, however, the amount of variation within and among these genera is unknown. Characters separating these two taxa from one another are variable and due to uncertain taxonomic identification, analyzing their diets at the species level may results in erroneous conclusions.

Instead, specimens of *Parahippus* and *Desmatippus* are analyzed together (see Results) and interpretations made with the understanding that the observed diet may represent multiple species and genera.

CARBON ISOTOPES AND DIET

Tooth enamel is composed of the mineral hydroxylapatite ($Ca_{10}[PO_4]_6[OH]_2$) with some carbonate substituting in at the hydroxyl and phosphate lattice sites (Koch et al., 1997). Tooth enamel is the most resistant part of any vertebrate body, resulting in high fossilization potential as well as low susceptibility to diagenetic processes thus maintaining the original stable carbon isotope signature from when the mammal was developing its teeth (Koch et al., 1997; Wang and Cerling, 1994). Here, I analyze stable carbon isotope composition of the carbonate component of enamel to infer diet. Stable carbon isotope ratios are reported in standard δ-notation:

$$\delta^{13}\mathrm{C} = \left[\left(\frac{\mathrm{R_{sample}}}{\mathrm{R_{standard}}}\right) - 1\right] \times 100$$

where R is $^{13}C/^{12}C$. Units are per mil (‰) and results are reported as the per mil deviation from the internationally accepted standard for carbon, the Vienna PeeDee Beleminite (VPDB). The stable carbon isotope ratio in the bioapatite of mammalian teeth reflects the stable carbon isotope ratio of the vegetation in their diet (DeNiro and Epstein, 1978; Tieszen et al., 1979). This is useful, as plants utilizing the C3 photosynthetic pathway fractionate carbon differently than plants using the C4 photosynthetic pathway. C3 plants, which includes most trees, shrubs, and grasses that grow in cool seasons and/or climates, are enriched in the light carbon isotope (^{12}C) where as C4 plants, which includes most grasses of warm and dry climates, are enriched in the heavy carbon isotope (^{13}C). On modern landscapes C3 plants have an average δ of -28.5‰ and range from -20‰ to -37‰ (Kohn, 2010) while C4 plants have an average δ of -13‰ and range from -9‰ to -19‰ (Cerling et al., 1997). An isotopic signature between the range of C3 and C4 isotope values can indicate a mixed feeding diet (MacFadden, 1997). Within C3 plants, those that are in water stressed environments will have high $\delta^{13}C$ ratios. $\delta^{13}C$ values above -25.5‰ are from open and arid environments in which the mean annual precipitation is < 500 mm/yr (Kohn, 2010). Plants growing in more moist habitats that have canopy cover fall in the lower range of $\delta^{13}C$ values (Kohn, 2010). Other factors that can lead to enriched $\delta^{13}C$ values of plants are growth at high elevation (Tieszen et al., 1979). The third photosynthetic pathway, CAM, has $\delta^{13}C$ values between the range of C3 and C4 plants (Elheringer and Monsoon, 1993). The CAM pathway occurs in succulent plants and is assumed to not be part of the diet of large herbivores (Feranec and Pagnac, 2013). Enamel of medium to large-bodied mammal herbivores is consistently enriched by about +14.0‰ from their food (Cerling and Harris, 1999; Passey et al., 2005). In addition, fluctuating atmospheric CO_2 and its $\delta^{13}C_{CO2}$ influence the $\delta^{13}C$ ratios of plants through time. This is especially true today, where the Industrial Revolution and fossil fuel burning has caused the mean atmospheric $\delta^{13}C_{CO2}$ to become more negative by about -1.5‰ (Marino et al., 1992). Given this and the discrimination factor of +14.0‰ from the food source to the mammal's enamel, $\delta^{13}C$ ratios reported here are +15.5‰ above the vegetation source.

I examine the carbon isotope signature of the tooth enamel of each morphotype in order to determine if a C3 or C4 diet was consumed. If the genus is eating a C3 diet, I then examine the $\delta^{13}C$ values to determine if it was occupying an "open" or "closed" habitat. For the purposes of this analysis, a closed habitat is a densely forested environment with a closed canopy. Following

Strömberg (2005), a closed habitat consists of woody or herbaceous dicotyledons, conifers, ferns, palms, and spiral gingers. Vegetation in a closed environment will have lower $\delta^{13}C$ values because of low light and ^{13}C-depleted CO_2 near the forest floor (Quade et al., 1995; Cerling et al., 2004). A more open habitat for the purposes of this analysis is a woodland habitat with a mosaic of trees and open C3 grass patches. Vegetation from this habitat will be more enriched in ^{13}C encompassing normal $\delta^{13}C$ values due to exposure to more sunlight and normal concentrations of CO_2 (Cerling et al., 2004). These habitat types represent points in a spectrum of environmental gradients and therefore habitat diagnosis is a relative application.

I first establish the dietary niche of each morphotype and whether dietary niche partitioning occurred between the genera. Based on tooth morphology and body size, *Archaeohippus* is expected to emphasize a C3 diet and live in closed forested habitats. *Desmatippus* and *Parahippus* are also expected to eat primarily C3 vegetation; however they are expected to have a carbon isotope signature of more open habitats than *Archaeohippus*, as they may be incorporating C3 grasses into their diet because they are more hypsodont than *Archaeohippus*, have a larger body size, and are hypothesized to be an intermediate morphotype between the browsing and grazing equids (MacFadden, 1998). And aff. *Acritohippus* is expected to eat C3 vegetation in a more open grassland environment than the other taxa. I do not expect them to incorporate C4 grasses into their diet because C4 grasses never spread into Oregon (Cerling et al. 1997; Fox and Koch, 2003; Passey et al., 2002; Retallack, 2004). After determining the extent to which the three morphotypes partition their dietary niches, I track their dietary niches through the MMCO and then draw conclusions about how the capacity to change dietary niches and dietary niche breadth influenced the success of grazing equids and the extinction of browsing equids in Oregon.

OXYGEN ISOTOPES AND DIET

Stable oxygen isotope values of the carbonate in enamel are also reported here. The oxygen isotope signal of enamel is indicative of the meteoric water that the mammal consumed, the leaf water it consumed through its diet and its metabolic water (Cerling et al., 2004). Water in leaves is generally 10-30% enriched in ^{18}O compared to the water source. Therefore, obligate drinkers will have a depleted oxygen isotope signature than taxa that get the majority of their water from their diet. In addition, leaves that are higher in the canopy, exposed to more light, will have enriched oxygen isotope values than leaves towards the bottom of a plant or in the shaded understory (Quade et al., 1995). Stable oxygen isotope ratios are reported in standard δ-notation:

$$\delta^{18}O = \left[\left(\frac{R_{sample}}{R_{standard}}\right) - 1\right] \times 100$$

where R is $^{18}O/^{16}O$. Units are per mil (‰) and results are reported as the per mil deviation from the internationally accepted standard for oxygen, the Vienna PeeDee Beleminite (VPDB).

STUDY DESIGN AND METHODS

Institutional Abbreviations – **JDNM**, John Day Fossil Beds National Monument Locality; **JODA**, John Day Fossil Beds National Monument Specimen; **RV**, University of California at

Riverside locality; **UCMP**, University of California Museum of Paleontology specimen and/or locality.

Study Design – Isotope samples were taken from specimens collected in Late Arikareean to Barstovian deposits of Oregon. Samples for *Archaeohippus, Parahippus* and *Desmatippus* are divided into two groups: 1) an "early" group which consists of specimens from Late Arikareean deposits of the Campbell Ranch (JDNM-140 and Picture Gorge 36 localities (JDNM-49), and Hemingfordian deposits of the Warm Springs (RV7608, RV7711, RV7713), Rose Creek Member (Bridge Creek 6 = JDNM-160), and Hawk Rim localities; and 2) a "late" group which consists of specimens from the Barstovian Mascall type locality area (Table 2.1, Fig. 2.1). All *Archaeohippus, Parahippus* and *Desmatippus* specimens collected from the Mascall Formation are from the lower and middle units, which belong to the Early Barstovian. No specimens belonging to these genera are found in younger deposits in Oregon. Specimens of aff. *Acritohippus* all come from the Barstovian Mascall Formation. They are divided into three groups: 1) an "early" group from the lower unit of the Mascall Formation; 2) a "middle" group from the middle unit of the Mascall Formation; and 3) a "late" group from the upper unit of the Mascall Formaiton (Table 2.1, Fig. 2.1). Aff. *Acritohippus* specimens from the Arikareean or Hemingfordian are not included because this taxon was not present on the landscape during that time.

Isotope analysis – I analyzed the enamel of 72 equid teeth belonging to *Acrhaeohippus, Desmatippus, Parahippus*, and aff. *Acritohippus*. At least five specimens were selected from each time period for each taxon, the minimum number required to get an accurate estimate of the population's mean and standard deviation (Clementz and Koch, 2001). All selected specimens for analysis were mature and fully erupted to avoid a signal introduced from the pre-weaned period of tooth development. In addition, only specimens with no exterior signs of diagenesis were chosen, because diagenesis can lead to alterations of the original stable isotope signature. Between 10 and 30 mg of powdered enamel was sampled from each specimen using a multispeed Dremel Stylus V7.2 drill. Powered samples were treated with 30% hydrogen peroxide (approx. 1 mL per 25 mg of sample) for 18 hours, washed with distilled water 5 times, treated with 0.1 N acetic acid (approx. 1 mL per 25 mg of sample) for 18 hours and washed with distilled water 5 times. Samples were frozen overnight and then lyophilized overnight using a Labanco freeze-drier in the Center for Stable Isotope Biogeochemistry in the Department of Integrative Biology at UC Berkeley. Sample preparation methods follow Feranec and Pagnac (2013) in order to facilitate direct comparisons of results and are based on methods from MacFadden and Cerling (1996), Koch et al. (1997) and Clementz et al. (2012). Samples were analyzed using a GV IsoPrim mass spectrometer with Dual Inlet and MultiCarb systems in the Laboratory for Environmental and Sedimentary Isotope Geochemistry (LESIG) at the Department of Earth and Planetary Science at UC Berkeley. Several replicates of one international standard NBS19, and two lab standards CaCO3-I & II were measured along with samples for each run. The overall external analytical precision is ±0.04‰ for δ^{13}C and ±0.07‰ for δ^{18}O.

Twelve samples were removed from the dataset after isotope analysis, either due to insufficient material for analysis or evidence of diagenesis upon secondary examination of the specimen. To test for differences between mean carbon isotope ratios for species and stratigraphic subsamples, ANOVA, with Tukey's post hoc procedure, and two sample T-tests

Table 2.1 $\delta^{13}C$ and ratios $\delta^{18}O$ for each specimen, indicating locality and stratigraphic assignment. (d) indicates the sample was either lost in the preparation process or discarded from the analysis due to diagenesis. JODA = John Day Fossil Beds National Monument Specimen; JDNM=John Day Fossil Beds National Monument Locality; UCMP = University of California Museum of Paleontology Specimen and/or Locality; RV = University of California Riverside Locality.

Specimen #	**Genus**	**Locality**	**Strat. Assign.**	**$\delta^{13}C$ (‰)**	**$\delta^{18}O$ (‰)**
JODA 7010	*Archaeohippus*	JDNM-160	Early	-11.15(d)	-10.29
JODA 7368	*Archaeohippus*	JDNM-140	Early	n/a(d)	n/a(d)
JODA 14141	*Archaeohippus*	Hawk Rim	Early	-8.75	-6.73
JODA 14620	*Archaeohippus*	Hawk Rim	Early	-9.00	-6.58
UCMP 316832	*Archaeohippus*	RV7608	Early	-9.42	-2.37
UCMP 317306	*Archaeohippus*	RV7608	Early	-8.87	-4.21
JODA JXS610103	*Archaeohippus*	JDNM-202	Late	-8.85	-6.95
UCMP 26643	*Archaeohippus*	UCMP -3059	Late	-9.10	-7.45
UCMP1689A	*Archaeohippus*	UCMP -903	Late	-9.39	-6.5
UCMP1689B	*Archaeohippus*	UCMP -903	Late	-9.21	-7.02
UCMP 41203	*Archaeohippus*	UCMP V4829	Late	-8.52	-5.55
JODA 5763	*Desmatippus*	JDNM-160	Early	-9.72	-7.65
JODA 5795A	*Desmatippus*	JDNM-140	Early	-10.57	-7.76
JODA 5795B	*Desmatippus*	JDNM-140	Early	-11.12(d)	-6.84(d)
JODA 14137	*Desmatippus*	Hawk Rim	Early	-9.99	-7.42
UCMP 1701	*Desmatippus*	UCMP -903	Late	-10.56	-10.84
JODA 10037	*Parahippus*	JDNM-49	Early	-10.80	-7.55
UCMP 317738	*Parahippus*	RV7713	Early	-8.06	-7.68
UCMP 317739	*Parahippus*	RV7713	Early	-8.38	-5.58
UCMP 317302	*Parahippus*	RV7608	Early	-11.18	-5.97
UCMP 317346	*Parahippus*	RV7713	Early	-12.49	-8.16
UCMP 317330	*Parahippus*	RV7711	Early	-10.01	-5.56
JODA 4211	*Parahippus*	UCMP V4945	Late	-9.29	-8.38
JODA 2410	*Parahippus*	JDNM-4	Late	-11.74	-9/06
JODA 2416	*Parahippus*	JDNM-4	Late	-11.60	-8.32
UCMP 40240	*Parahippus*	UCMP V4834	Late	-10.32	-8.89
JODA 4269	*Merychippus*	JDNM-70	Lower	-9.90	-6.73
JODA 4276	*Merychippus*	JDNM-70	Lower	-12.12	-8.33
JODA 4277	*Merychippus*	JDNM-70	Lower	-10.99	-9.25
JODA 3334	*Merychippus*	JDNM-71	Lower	-10.11	-5.88
JODA 8894	*Merychippus*	JDNM-71	Lower	-9.61	-7.86
JODA KCM71128	*Merychippus*	JDNM-71	Lower	-10.45	-7.38
JODA KCM71131	*Merychippus*	JDNM-71	Lower	-12.97(d)	-7.88(d)
JODA 10309	*Merychippus*	JDNM-71	Lower	-10.48	-7.11
JODA 10310	*Merychippus*	JDNM-71	Lower	-9.94	-6.69
JODA 10311	*Merychippus*	JDNM-71	Lower	-13.01(d)	-9.15

Table 2.1 Continued.

Specimen #	**Genus**	**Locality**	**Strat. Assign.**	**δ^{13}C (‰)**	**δ^{18}O (‰)**
JODA 8570	*Merychippus*	JDNM-201	Lower	-9.64	-5.52
JODA 14943	*Merychippus*	JDNM-226	Lower	-11.47	-8.59
JODA 6696	*Merychippus*	JDNM-226	Lower	-13.45(d)	-9.86
UCMP 39110	*Merychippus*	UCMP V4827	Lower	-12.63(d)	-11.27
UCMP 39111	*Merychippus*	UCMP V4829	Lower	-9.60	-5.5
UCMP 41202	*Merychippus*	UCMP V4829	Lower	-11.07	-6.85
JODA 14950	*Merychippus*	JDNM-71B	Lower/ Middle	-11.07	-5.58
JODA 14951	*Merychippus*	JDNM-71C	Lower/ Middle	-10.38(d)	-7.85(d)
JODA 1113	*Merychippus*	JDNM-4	Middle	-11.34	-8.56
JODA 8010	*Merychippus*	JDNM-265?	Middle	-10.40(d)	-8.88(d)
JODA 6286	*Merychippus*	JDNM-226	Middle	-8.82	-6.05
JODA 6300	*Merychippus*	JDNM-226	Middle	-12.05	-8.15
JODA JXS610104	*Merychippus*	JDNM-259	Middle	-9.69	-7.66
JODA 14949	*Merychippus*	JDNM-261	Middle	n/a(d)	n/a(d)
JODA 6277	*Merychippus*	JDNM-262	Middle	-10.22	-6.82
JODA 4213	*Merychippus*	JDNM-264	Middle	-9.98	-4.66
JODA 6622	*Merychippus*	JDNM-266	Middle	-10.83	-6.82
JODA 7575	*Merychippus*	JDNM-266	Middle	-11.26	-8.39
JODA CJS81011	*Merychippus*	JDNM-266	Middle	-10.53	-8.97
JODA ECL081001B	*Merychippus*	JDNM-266	Middle	-11.50	-9.11
JODA ECL081005	*Merychippus*	JDNM-266	Middle	-10.67	-7.42
JODA JXS810138	*Merychippus*	JDNM-266	Middle	-11.24	-10.25
JODA 4294	*Merychippus*	UCMP -3059	Middle	-9.47	-6.92
JODA 4246	*Merychippus*	UCMP V4830	Middle	-9.86	-8.37
JODA 4252	*Merychippus*	UCMP V4834	Middle	-10.62	-6.37
JODA 12050	*Merychippus*	n/a	n/a	-9.69	-7.26
JODA 14942	*Merychippus*	UCMP V4834	Middle	-8.14(d)	-6.51(d)
JODA 14945	*Merychippus*	UCMP V4830	Middle	-10.68	-8.00
JODA 14948	*Merychippus*	UCMP V4944	Middle	-9.77	-6.44
UCMP 40322	*Merychippus*	UCMP V4834	Middle	-10.37	-8.99
UCMP 40322	*Merychippus*	UCMP V4834	Middle	-10.16	-8.22
UCMP 39114	*Merychippus*	UCMP V4834	Middle	-8.15(d)	-6.46
UCMP 39296	*Merychippus*	UCMP V4834	Middle	-10.67	-6.31
UCMP 39296	*Merychippus*	UCMP 4834	Middle	-10.07	-5.67
JODA 10026	*Merychippus*	JDNM-4	Upper	-12.26	-11.35
JODA 6350	*Merychippus*	JDNM-4	Upper	-10.59	-6.45
JODA 3333	*Merychippus*	JDNM-4	Upper	-10.81	-7.87

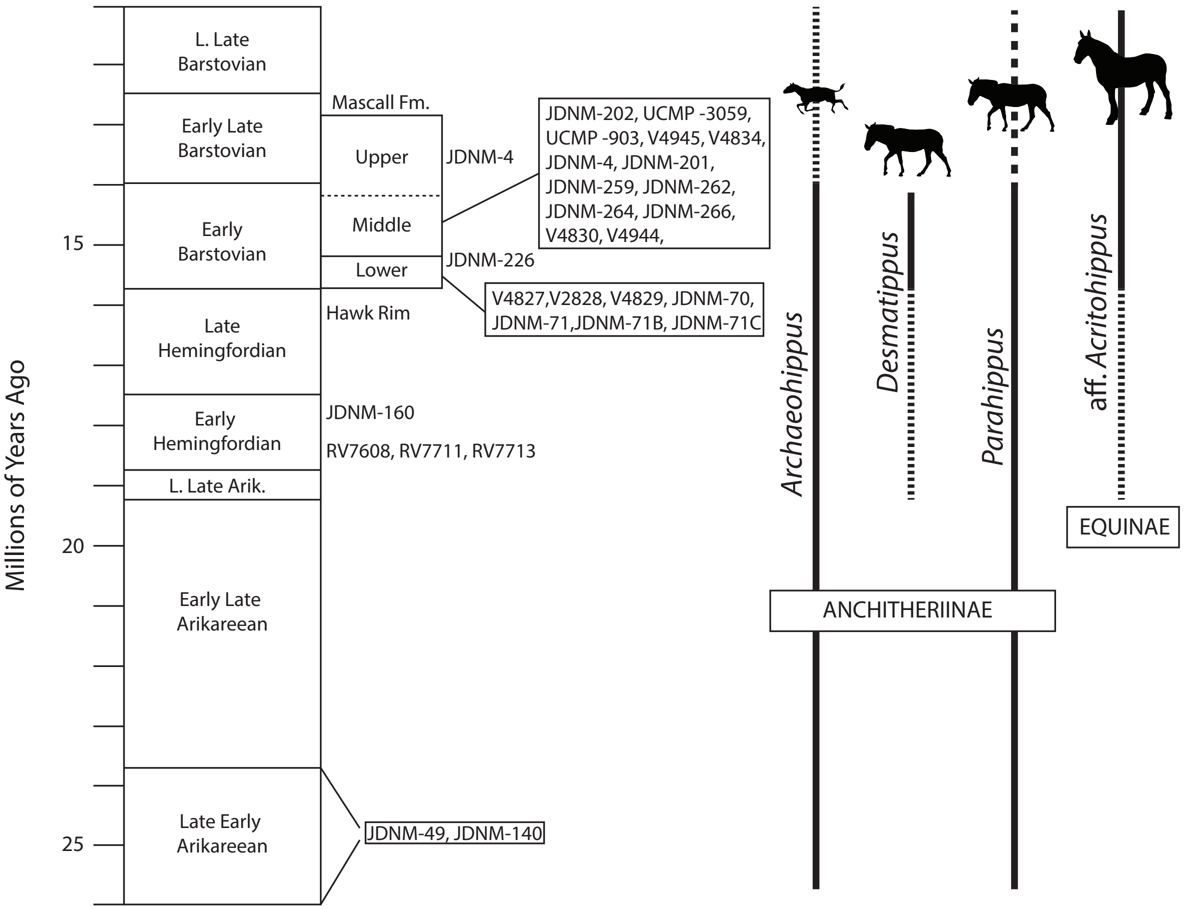

Figure 2.1 Stratigraphic ranges of each taxon and locality. Solid lines indicate stratigraphic range in Oregon, small dashed line indicates stratigraphic range in North America, large dashed line indicates uncertainty in upper stratigraphic range. Specimen localities are plotted in relation to the North American Land Mammal Ages and the Mascall Formation (divided into the lower, middle and upper units). JDNM = John Day Fossil Beds National Monument Locality; UCMP = University of California Museum of Paleontology Locality; V = University of California Museum of Paleontology.

were used. Bartlett's test was used to assess homogeneity of variances across samples. All statistical analyses were performed in R 3.0.3 for Mac OS X (R Core Team 2013).

RESULTS

Bulk $\delta^{13}C$ values for all samples analyzed are presented in Table 2.1 and Figure 2.2. *Parahippus* and *Desmatippus* have similar $\delta^{13}C$ values and given their similar tooth morphology and size, they are grouped together for subsequent analyses. The $\delta^{13}C$ values of *Archaeohippus* range from -9.42‰ to -8.52‰ with a mean of -9.01‰ (±0.299‰). The $\delta^{13}C$ values of *Parahippus*/*Desmatippus* range from -12.49‰ to -8.06‰ with a mean of -10.34‰. (±1.24‰). These values are not significantly different from aff. *Acritohippus* $\delta^{13}C$ values, which range from -12.26‰ to -8.82‰ with a mean of -10.49‰ (±0.789‰) (Table 2.1, Fig. 2.2). The $\delta^{13}C$ values of *Archaeohippus* are significantly more enriched than *Parahippus*/*Desmatippus* and aff. *Acritohippus* (ANOVA: df=59, F=11.15, $p<0.001$) (Table 2.1, Fig. 2.2). Aff. *Acritohippus* and *Parahippus*/*Desmatippus* have greater variance than *Archaeohippus* despite the latter including a larger geographic and temporal range (Bartlett's Test: $p<0.001$).

Bulk $\delta^{13}C$ values for stratigraphic subsamples for each taxon are presented in Figure 2.3. The $\delta^{13}C$ values of *Archaeohippus* are not different from the "early" to "late" time periods (two sample t-test: df=6.92, t=0.019, $p=0.99$) (Fig. 3). The same is true of *Parahippus*/*Desmatippus* (two sampled t-test: df=10.44, t=0.767, $p=0.46$) (Fig. 2.3). Aff. *Acritohippus* also has statistically similar $\delta^{13}C$ values from the lower, middle and upper units of the Mascall Formation (ANOVA: df=32, F=1.495, $p=0.239$) (Fig. 2.3).

Bulk $\delta^{18}O$ values for each taxa are presented in Table 2.1 and Figure 2.4. The $\delta^{18}O$ values of *Archaeohippus* range from -7.45‰ to -2.37‰ with a mean of -5.93‰ (±1.65‰). *Parahippus*/*Desmatippus* has $\delta^{18}O$ values ranging from -10.84‰ to -5.56‰ with a mean of -7.71‰ (±1.39‰) and aff. *Acritohippus* has $\delta^{18}O$ values ranging from -11.35‰ to -4.66‰ with a mean of -7.43‰ (±1.42‰). *Archeohippus* has significantly enriched $\delta^{18}O$ values than *Parahippus*/*Desmatippus* and aff. *Acritohippus* (ANOVA: df=59, F=4.817, $p<0.05$).

DISCUSSION

Dietary niche partitioning – All genera had $\delta^{13}C$ ratios below -8.0‰ (Fig. 2.2) indicating they consumed a C3 diet. The diet of aff. *Acritohippus* and *Parahippus*/*Desmatippus* cannot be differentiated based on $\delta^{13}C$ ratios. Aff. *Acritohippus* does not appear to have occupied more open habitats (more enriched $\delta^{13}C$ ratios) than *Parahippus*/*Desmatippus*. MacFadden (1997) eloquently demonstrated the diet partitioning of equids in relation to $\delta^{13}C$ values and tooth morphology (Fig. 2.5). Aff. *Acritohippus* plots in the upper left hand corner as a C3 hypsodont grazer while *Parahippus*/*Desmatippus* plots in the lower left hand corner as a C3 brachyodont browser. Mesowear analyses corroborate this hypothesis. Mesowear represents cumulative wear over extended periods of time, potentially representing the habitual diet of species (Damuth and Janis, 2011). *Desmatippus* and *Parahippus* have low mesowear scores, indicative of a leafy browse diet, while aff. *Acritohippus* has a higher meoswear score, reflecting a more abrasive diet (Mihlbackler et al., 2011). Aff. *Acritohippus* most likely ate abrasive C3 grasses while *Parahippus* and *Desmatippus* most likely ate leafy vegetation typical of a brachyodont herbivore. It is important to note that hypsodonty is not only driven by an abrasive diet. Hypsodonty may also be the result of increased ingestion of grit, which corresponds with habitat openness and

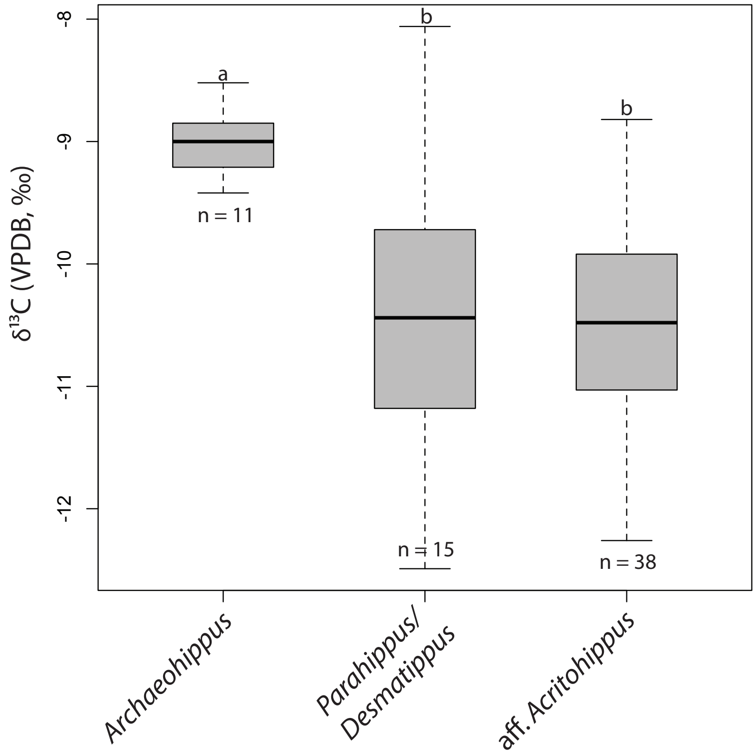

Figure 2.2 Bulk δ^{13}C ratios for *Archaeohippus*, *Parahippus*/*Desmatippus* and aff. *Acritohippus* from all time periods included in this study. For each boxplot the dark line indicates the median, the box represents the interquartile range and the dashed lines indicate the range of the values. n = the number of samples; a=significance from ANOVA with Tukey's Post-hoc Test, $p<0.05$; b=nonsignificance from Tukey's Post-hoc Test, $p>0.05$.

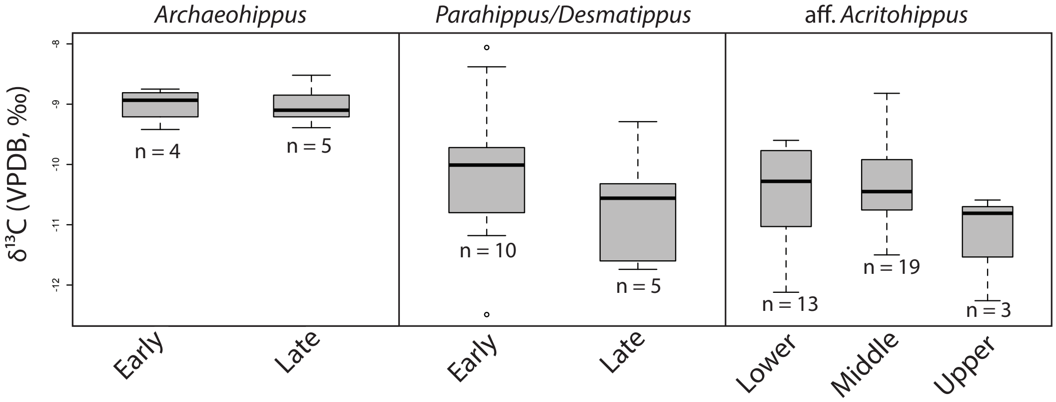

Figure 2.3 Bulk δ^{13}C ratios for each taxon at different stratigraphic ranges (see text). See Fig. 2.2 caption for explanation of boxplot conventions. Circles in boxplot indicate outliers (greater than 1.5 times the interquartile range from the median).

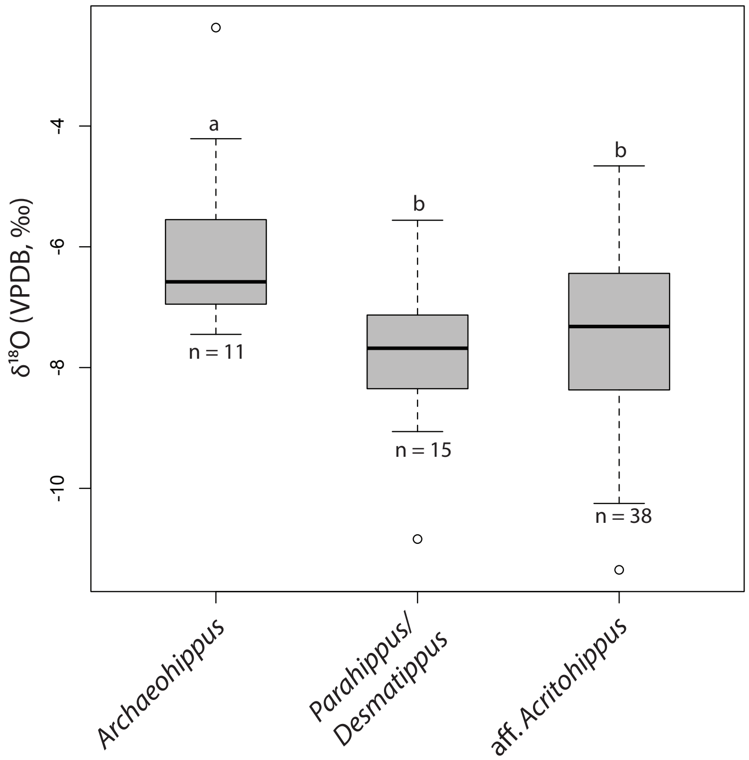

Figure 2.4 Bulk δ^{18}O ratios for *Archaeohippus*, *Parahippus*/*Desmatippus* and aff. *Acritohippus* from all time periods included in this study. See Fig. 2.2 and 2.3 captions for explanation of boxplot conventions.

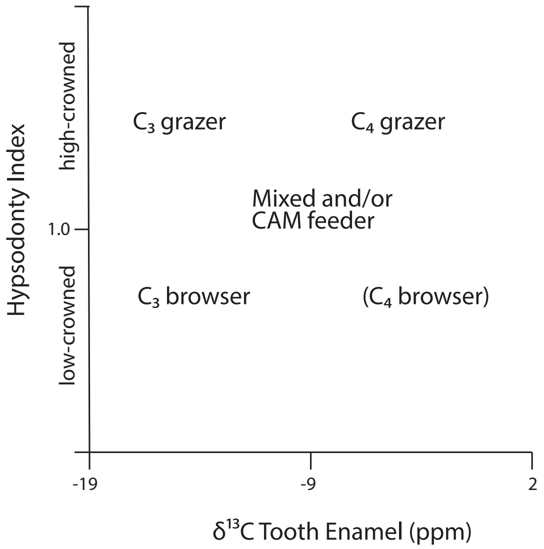

Figure 2.5 From MacFadden (1997). Plot of δ^{13}C values and versus hypsodonty index (unworn molar crownheight/molar occlusal anteroposterior length). Although a C4 browser can hypothetically exist, it is very rare in nature.

aridity (Stirton, 1947). Grazing requires feeding close to the ground, which inherently increases grit ingested and hypsodonty characterizes many open and arid habitat taxa that are not grazers, such as antilocaprids, gophers, and heteromyids (Damuth and Janis, 2011; Janis, 1988; Williams and Kay, 2001). In the Barstovian, Parahippus, *Desmatippus* and aff. *Acritohippus* apparently occupied a similar mosaic woodland habitat given their enriched $\delta^{13}C$ ratios of a C3 diet (Kohn, 2010). Using tooth morphology (brachydont vs. hypsodont) and stable carbon isotopes, Bibi (2007) also found dietary niche partitioning in bovids during the Late Miocene in a habitat in which C3 vegetation prevailed.

Archaeohippus exhibits a more isotopically enriched C3 diet than aff. *Acritohippus*, *Parahippus*, and *Desmatippus* (Fig. 2.2). Prior to the present study, the diet and habitat preference of *Archaeohippus* was unknown but hypothesized to be a small folivore browser in either a forest or an open woodland/savanna mosaic (MacFadden, 1992). The enriched $\delta^{13}C$ values reported here suggest the genus either occupied a more open, water stressed environment than the other taxa studied here; was at higher elevations than the other taxa studied here; or *Archaeohippus* was incorporating C4 vegetation into its diet. Given their low crowned tooth morphology and the absence of C4 grasses in Oregon, they most likely were not incorporating C4 grasses into their diet. And specimens of *Archaeohippus* are found in the same low lying basinal deposits as *Desmatippus*, *Parahippus*, and aff. *Acritohippus* suggesting they did not live at higher elevations. The enriched C3 diet may be the result of eating browse from the crowns of woody or herbaceous vegetation in the clearings of a woodland habitat (Quade et al., 1995; Cerling et al., 2004). Leaves at the top of a plant, towards the canopy, have enriched $\delta^{13}C$ values due to higher levels of light (Quade et al., 1995). In addition, leaves at the top of canopies have enriched $\delta^{18}O$ ratios due to higher evaporation. The $\delta^{18}O$ values of *Archaeohippus* are more enriched than *Parahippus*/*Desmatippus* and aff. *Acritohippus* (Fig. 2.4) suggesting it was browsing on crown leaf vegetation in open clearings of a woodland mosaic.

Dietary niche breadth – The $\delta^{13}C$ ratios of *Archaeohippus* have significantly less variance than the distribution of ratios for aff. *Acritohippus* (Fig. 2.2) even though specimens of *Archaeohippus* are more geographically and stratigraphically widespread (Fig. 2.1). For this reason it seems likely that *Archaeohippus* occupied a narrower dietary niche perhaps specializing on crown browse of C3 vegetation in woodland gaps. Aff. *Acritohippus*, on the other hand, had a broad dietary niche that may have included C3 grasses from a variety of habitats in both woodland and open environments. The isotopic signature of aff. *Acritohippus* ranges 3.5‰ (Fig. 2.2). Extant feral horses in southeastern Oregon, eating a C3 grass diet have a carbon isotope range of 1.3‰, most likely due to seasonal variation in food sources (Hoppe et al., 2004). Bestland et al. (2008) suggested that the Mascall Formation strata were deposited in a series of cyclical climatic changes that overturned on a 100k year time scale, in which the climate oscillated between Mediterranean climatic aspects (dry, warm summers) and continental climatic aspects (cool to cold winter). The time scale of this analysis is not fine enough to pick up diet changes associated with the 100k climatic cycles if there were any. Thus the broader stable dietary niche recorded here may be the result of seasonality, oscillating climates and time averaging. On the other hand, it may demonstrate the capability of aff. *Acritohippus* to consume a wide variety of vegetation.

Archaeohippus also had a narrower dietary niche than *Parahippus*/*Desmatippus* (Fig. 2.2). Samples of *Archaeohippus* and *Parahippus*/*Desmatippus* span similar geographic and stratigraphic ranges (Fig. 2.1), but the $\delta^{13}C$ ratios of *Parahippus*/*Desmatippus* do not have geographic or stratigraphic structure suggesting a dietary niche that is broader than *Archaeohippus* persisting across space and time (Fig. 2.3). However, the wider range of isotope values for *Parahippus*/*Desmatippus* may be due multiple species comprising the samples used in this analysis.

Stable Diets –Across the Mid-Miocene Climatic Optimum and afterward, all of the genera studied maintain their dietary preferences (Fig. 2.3). The Arikareean and Hemingfordain landscapes of Oregon have been interpreted as open habitats with bunch grass and shrublands (Retallack 2004, 2007). During the early Miocene there was wooded grassland habitat and a transition to sod grasslands. Both of these time periods are interpreted as semiarid paleoclimates, but the Hemingfordian is interpreted as having more pronounced seasonality with summer-dry conditions (Retallack 2004, 2007). During the MMCO, temperature and moisture increased (Bestland et al., 2008) and woodland habitats were dominated by broad leaved deciduous vegetation (Wolfe, 1981). After the MMCO precipitation remained stable (Bestland et al., 2008) and it is unclear to what extent temperatures or the environment shifted, however, there was a continent wide trend towards more open environments with spreading C3 grasses (Strömberg, 2005).

Archaeohippus goes extinct across North America at the end of the Late Barstovian, and in Oregon there is no evidence of the genus past the Early Barstovian. Its abundance is consistently low compared to aff. *Acritohippus* and other more hypsodont equids in Oregon. The low abundance of *Archaeohippus* combined with its specialized browse-dominated diet may have led to its extinction as more open habitats emerged in the Late Middle Miocene. The only evidence that more open habitats did indeed become more common in the region coincident with the demise of *Archaeohippus* includes the onset of sod grasses about 20 Ma in Oregon (Retallack, 1997). However, the spread and trigger of the emergence of more open habitats during this time is unclear. Bestland et al. (2008) determined that precipitation did not decrease in the Mascall Formation after the mid-Miocene Climatic Optimum. Therefore, although the effective moisture may not have changed through the Barstovian of Oregon, the grasslands may have spread, thereby changing the vegetation structure and consequently the habitat for *Archaeohippus*. In a similar vein, Koch et al. (1998) hypothesized the demise of mastodons in the Late Pleistocene was due to their narrow dietary niche breadth being exceeded as environments changed, much as I suggest here for *Archaeohippus*.

Parahippus and *Desmatippus* go extinct across the continent in the Late Barstovian, before *Archaeohippus*; however, in Oregon, just like *Archaeohippus*, there is no evidence of either genus after the Early Barstovian. These genera may have included C3 grasses (in addition to C3 browse) in their diet as grasses became more widespread, but this cannot be detected through isotopic analysis. The low crowned tooth morphology and mesowear of *Desmatippus* indicates they were not well adapted to include C3 grasses in their diet (MacFadden, 1997; Mihlbachler et al., 2011). The low crowned populations of *Desmatippus* and *Parahippus* may have suffered extinction in the Late Barstovian because habitats became more open; however, as mentioned earlier, there appears to be no significant change in precipitation during this period and the extent of spreading grasslands is unknown. Some *Parahippus* specimens were incipiently hypsodont, suggesting that some populations of this genus may have been evolving the ability to increase the proportion of C3 grasses in their diet, allowing them to persisted longer by incorporating C3 grasses into their diets; however, there is no evidence for this in Oregon. Interestingly, their broad dietary niche breadth is not correlated with stratigraphic persistence.

Aff. *Acritohippus* exhibits a dietary niche consistently dominated by C3 vegetation through the Mascall Formation from the Early Barstovian to the Late Barstovian. As expected, it did not incorporate any C4 vegetation into its diet (Fig. 2.2, 2.3), in contrast to other hypsodont equids in North America during this time (Feranec and Pagnac, 2013). In Oregon, the diet of aff. *Acritohippus* instead becomes less enriched in ^{13}C, becoming more distant from the isotopic signature that would indicate a C4 diet, through time. However, the "upper" time period in this analysis is based on three specimens, therefore, it is unclear how meaningful this signal is. The lack of C4 vegetation in the diet of aff. *Acritohippus* is not unexpected given the evidence that C4 grasses never invaded Oregon (Cerling et al. 1997; Fox and Koch, 2003; Passey et al. 2002; Retallack, 2004).

As discussed, the dietary niche of aff. *Acritohippus* is broad suggesting it had the capability to consume a variety of food sources and it may have been sorted through selection to survive changing environments. The broader dietary niche of aff. *Acritohippus* perhaps explains its high abundance and persistence into the Late Barstovian of Oregon as environments may have become more open. The fluctuating environment between Mediterranean climatic aspects and continental climatic aspects may have been able to support all three morphotypes in an open woodland habitat, but as the environment became more open through time, taxa with narrow dietary niches, such as *Archaeohippus*, went extinct while those with broader dietary niches, such as aff. *Acritohippus* survived and were more abundant.

Regional comparisons –

The δ^{13}C values of plants and in turn the isotopic signature of mammal teeth, reflecting their diet, can be influenced by a variety of factors. In general, the δ^{13}C values for these three genera fall on the enriched end of typical C3 vegetation. Plants in water stressed environments have enriched δ^{13}C values (Farquhar et al., 1989; Kohn, 2010). Although the Late Arikareean of Oregon was a period of general aridity (Retallack, 2004), the climate became warm and moist through the MMCO (17-14 Ma), the period of time during which the majority of the collected specimens were deposited (Bestland et al., 2008). None of the paleosols in Oregon during this time contain carbonate nodules (that typically form in arid conditions), indicating a moist environment (Bestland et al. 2008) and mean annual precipitation was estimated to have been approximately 750 mm/yr (Sheldon, 2003). Therefore, the enriched δ^{13}C values are most likely not due to water stress. C3 plants that grow in higher elevations are also more enriched (Tieszen et al. 1979). However, Kohn and Fremd (2007) suggest nearly constant elevations between 27 and 7 Ma in Oregon and Bestland et al. (2008) interpret the Mascall Formation and the underlying Picture-Gorge Basalts to be deposited in a low-relief, tectonically inactive area. The tectonic activity in Oregon during this time period (e.g. Hooper et al. 2002) may have resulted in regional topographic changes that influenced diversity and faunal changes at a broader spatial scale (Kent-Corson et al., 2013; Kohn and Fremd, 2008) but not at the local scale of this study. In addition, the hypothesized higher amounts of atmospheric CO_2 during the Middle Miocene would also produce enriched δ^{13}C values. Wang et al. (1994) compared the δ^{13}C ratios of equids throughout the Miocene. Specimens of taxa from the same time period (15-18 Ma) and across the continent had more enriched δ^{13}C values relative to earlier time periods, suggesting that an increase in δ^{13}C is due to increased atmospheric CO_2. The increase in δ^{13}C values during this time period may also be due to C4 input into the diet of equids (Feranec and Pagnac, 2013), however C4 grasses were not in Oregon (Cerling et al. 1997; Fox and Koch, 2003; Passey et al. 2002; Retallack, 2004). Feranec and Pagnac (2013) examined the stable isotope values of

Acritohippus from the Barstow Formation in the Basin and Range province of southern California and reported $\delta^{13}C$ values ranging from -8.8‰ to -6.2‰ and suggest incorporation (up to 20%) of C4 grasses into its diet. The difference in isotopic signatrues between the *Acritohippus* populations in southern California and Oregon further demonstrates the lack of C4 grasses in Oregon and emphasizes that the spread of C4 grasses were already abundant in California before they spread across the continent, a scenario that accords with local pockets of C4 grasses eventually expanding to become widespread in the Late Miocene. It also further exemplifies that the Pacific Northwest had a cool growing season and was more moist during the Miocene compared to other parts of the continent and supported a C3-dominated vegetation (Retallack 2007; Bestland et al. 2008). Feranec and Pagnac (2013) also sampled three genera of camels, an antilocaprid genus and a gomphothere genus from the southern Great Basin and their isotope values are similar to the values reported here. This similarity may be due to increased atmospheric CO_2 as seen with Wang et al. (1994). The presence of C4 vegetation in southern California implies a more open and summer rainfall environment. The enriched $\delta^{13}C$ values in southern California may be the result of water stress whereas the enriched $\delta^{13}C$ values in Oregon may be the result of winter rainfall or cool summers and higher elevation. Sampling of more taxa and paleosol analyses may tease these contrasting interpretations apart.

CONCLUSIONS

All equid taxa examined had isotopic signatures indicative of a C3 diet in the Late Early Miocene and Middle Miocene of Oregon. Dietary niche partitioning is evident based on carbon stable isotope analysis and tooth morphology. *Archaeohippus* had a narrow dietary niche that apparently included the crown leaves of vegetation in clearings of a woodland habitat. *Parahippus* and *Desmatippus* had an isotopically broad dietary niche and were most likely eating a variety of C3 vegetation in an open woodland mosaic environment. Aff. *Acritohippus* had an isotopically broad dietary niche as well, but its tooth morphology indicates utilization of C3 grasses in an open woodland mosaic habitat.

None of these taxa changed their diet through the Late Early and Middle Miocene, across the MMCO and subsequent cooling in Oregon. This suggests stability in dietary niches across events of environmental and climatic changes. The dietary constraints indicated by stable niches through time may be the reason why browsers such as *Archaeohippus*, *Desmatippus*, and *Parahippus* became extinct in the Middle Miocene, when the environment may have changed to favor grazing equids such as aff. *Acritohippus*. The narrower niche breadth of *Archaeohippus* may also have exacerbated its susceptibility to extinction. The diets of these taxa suggest C4 grasses were not a major component of the landscape in Oregon during the Middle Miocene as other studies have suggested. Instead, the C3 diet and high abundance of aff. *Acritohippus* as well as the enriched $\delta^{13}C$ values of *Parahippus* and *Desmatippus* suggest, the landscape during the Middle Miocene in Oregon was an open woodland environment with C3 grasses.

REFERENCES

Badgley, C., Finarelli, J.A., 2013. Diversity dynamics of mammals in relation to tectonic and climatic history: comparison of three Neogene records from North America. Paleobiology 39, 373–399.

Barnosky, A.D., 2001. Distinguishing the effects of the Red Queen and Court Jester on Miocene evolution in the Northern Rocky Mountains. Journal of Vertebrate Paleontology 21, 172-185.

Barnosky, A.D., Labar, W.J., 1989. Mid-Miocene (Barstovian) environmental and tectonic setting near Yellowstone Park, Wyoming and Montana. Geological Society of America Bulletin 101, 1448-1456.

Barnosky, A.D., Carrasco, M.A., 2002. Effects of Oligo-Miocene global climate changes on mammalian species richness in the northwestern quarter of the USA. Evolutionary Ecology Research 4, 811–841.

Berner, R.A., 1998. The carbon cycle and carbon dioxide over Phanerozoic time: the role of land plants. Philosophical Transactions of the Royal Society of London. Series B: Biological Sciences 353, 75–82.

Bestland, E.A., Forbes, M.S., Krull, E.S., Retallack, G.J., Fremd, T., 2008. Stratigraphy, paleopedology and geochemistry of the middle Miocene Mascall Formation (type area, central Oregon, USA). Paleobios 28, 41–61.

Bibi, F., 2007. Dietary niche partitioning among fossil bovids in late Miocene C_3 habitats: Consilience of functional morphology and stable isotope analysis. Palaeogeography, Palaeoclimatology, Palaeoecology 253, 529-538.

Calade, J.M., Hopkins, S.B., Davis, E.B., 2011. Turnover in burrowing rodents: The roles of competition and habitat change. Palaeogeography, Palaeoclimatology, Palaeoecology 311, 242-255.

Camp, V. E., Ross, M.E., 2004. Mantle dynamics and genesis of mafic magmatism in the intermontane Pacific Northwest. Journal of Geophysical Research 109 (B8), 1-14.

Cerling, T.E., 1991. Carbon dioxide in the atmosphere: evidence from Cenozoic and Mesozoic paleosols. American Journal of Science 29, 377-400.

Cerling, T.E., Harris, J.M., 1999. Carbon isotope fractionation between diet and bioapatite in ungulate mammals and implications for ecological and paleoecological studies. Oecologia 120, 347–363.

Cerling, T.E., Harris, J.M., MacFadden, B.J., Leakey, M.G., Quade, J., Eisenmann, V., Ehleringer, J.R., 1997. Global vegetation change through the Miocene/Pliocene boundary. Nature 389, 153–158.

Cerling, T.E., Hart, J.A., Hart, T.B., 2004. Stable isotope ecology in the Ituri Forest. Oecologia 138, 5-12.

Clementz, M.T., Koch, P.L., 2001. Differentiating aquatic mammal habitat and foraging ecology with stable isotopes in tooth enamel. Oecologia 129, 461–472.

Clementz, M. T., R. E. Fordyce, S. L. Peek, and D. L. Fox. 2012. Palaeogeography, Palaeoclimatology, Palaeoecology. Palaeogeography, Palaeoclimatology, Palaeoecology 1–13.

Cope, E.D., 1886. On two new species of three-toed horses from the Upper Miocene, with notes on the fauna of the Ticholeptus Beds. Proceedings of the American Philosophical Society 23 (123), 357-361.

Cope, E.D., 1889. A review of North American species of *Hippotherium*. Proceedings of the American Philosophical Society 26, 429-458.

Damuth, J., Janis, C.M., 2011. On the relationship between hypsodonty and feeding ecology in ungulate mammals, and its utility in palaeoecology. Biological Reviews, 86, 733–758.

Davis, E.B. 2007. Antilocapridae in Prothero, D.R. and Foss, S.E (eds.) *The Evolution of Artiodactyls*. The John Hopkins University Press, p. 227-240.

DeNiro, M.J., Epstein, S., 1978. Influence of diet on the distribution of carbon isotopes in animals. Geochimica et cosmochimica acta 42, 495–506.

DeSantis, L.R.G., Feranec, R.S., MacFadden, B.J., 2009. Effects of Global Warming on Ancient Mammalian Communities and Their Environments. PLoS ONE 4, e5750.

Dingus, L. 1990. Systematics, stratigraphy, and chronology for mammalian fossils (Late Arikareean to Hemingfordian) from the uppermost John Day formation, Warm Spring, Oregon. Paleobios 12, 1-24.

Downs, T., 1956. The Mascall fauna from the Miocene of Oregon. University of California Publications in Geological Sciences 31, 199-354.

Edwards, E.J., Osborne, C.P., Stromberg, C.A.E., Smith, S.A., C4 Grasses Consortium, Bond, W.J., Christin, P.A., Cousins, A.B., Duvall, M.R., Fox, D.L., Freckleton, R.P., Ghannoum, O., Hartwell, J., Huang, Y., Janis, C.M., Keeley, J.E., Kellogg, E.A., Knapp, A.K., Leakey, A.D.B., Nelson, D.M., Saarela, J.M., Sage, R.F., Sala, O.E., Salamin, N., Still, C.J., Tipple, B., 2010. The Origins of C4 Grasslands: Integrating Evolutionary and Ecosystem Science. Science 328, 587–591.

Ehleringer, J. R., Monson, R.K., 1993. Evolutionary and ecological aspects of photosynthetic pathway variation. Annu. Rev. Ecol. Syst. 24, 411–439.

Ehleringer, J.R., Sage, R.F., Flanagan, L.B., Pearcy, R.W., 1991. Climate change and the evolution of C4 photosynthesis. Trends in Evolution and Ecology, 6, 95-99.

Farquhar, G.D., Ehleringer, J.R., Hubick, K.T., 1989. Carbon isotope discrimination and photosynthesis. Annual review of plant biology 40, 503–537.

Feranec, R.S., Pagnac, D., 2013. Palaeogeography, Palaeoclimatology, Palaeoecology. Palaeogeography, Palaeoclimatology, Palaeoecology 388, 42–47.

Fox, D. L., Koch, P.L., 2003. Tertiary history of C4 biomass in the Great Plains, USA. Geology 31, 809-812.

Fox, D.L., Koch, P.L., 2004. Carbon and oxygen isotopic variability in Neogene paleosol carbonates: constraints on the evolution of the C4-grasslands of the Great Plains, USA. Palaeogeography, Palaeoclimatology, Palaeoecology 207, 305–329.

Honey, J.G., Harrison, J.A., Prothero, D.R., Stevens, M.S., 1998. Camelidae in Janis, C.M., Scott, K.M., and Jacobs, L.L. (eds.) *Evolution of Tertiary Mammals of North America Volume 1: Terrestrial Carnivores, Ungulates, and Ungulatelike Mammals*. Cambridge University Press, p. 439-462.

Hooper, P.R., Binger, G.B., Lees, K.R., 2002. Ages of the Steens and Columbia River flood basalts and their relationship to extension-related calc-alkalic volcanism in eastern Oregon. Geological Society of America Bulletin 114, 43–50.

Hoppe, K. A., Amundson, R., Vavra, M., McClaran, M.P., Anderson, D.L., 2004. Isotopic analysis of tooth enamel carbonate from modern North American feral horses: implications for paleoenvironmental reconstructions. Palaeogeography, Palaeoclimatology, Palaeoecology, 203, 299–311.

Hunt, R.M., Stepleton, E., 2004. Geology and paleontology of the upper John Day beds, John Day River Valley, Oregon: lithostratigraphic and biochronologic revision in the Haystack Valley and Kimberly areas (Kimberly and Mt. Misery quadrangles). Bulletin of the American Museum of Natural History, 282,1-90.

Gidley, J.W., 1906. A new genus of horse from the Mascall beds, with notes on the small collection of equine teeth in the University of California. American Museum of Natural History Bulletin 22, 385-388.

Janis C.M., 1988. An estimation of tooth volume and hypsodonty indices in ungulate mammals, and the correlation of these factors with dietary preference in Russell, D.E., Santoro, J.P., Sigogneau-Russell, D., (eds.), *Teeth revisited: Proceedings of the VIIth International Symposium on Dental Morphology*. Mémoires du Muséum national d'histoire Naturelle, Paris (serie C) 53, 367–387.

Janis, C.M., 1993. Tertiary mammal evolution in the context of changing climates, vegetation, and tectonic events. Annual Review of Ecology and Systematics, 24, 467–500

Janis, C.M., Damuth, J., Theodor, J.M., 2000. Miocene ungulates and terrestrial primary productivity: where have all the browsers gone? Proc. Natl. Acad. Sci. 97, 7899–7904.

Janis, C.M., J. Damuth, Theodor, J.M., 2002. The origins and evolution of the North American grassland the hoofed mammals. Palaeogeography, Palaeoclimatology, Palaeoecology 177, 183-198.

Janis, C.M., Damuth J., Theodor, J.M., 2004. The species richness of Miocene browsers, and implications for habitat type and primary productivity in the North American grassland biome. Palaeogeography, Palaeoclimatology, Palaeoecology 207, 371–398.

Kelly, T.S., 1995. New Miocene horses from the Caliente Formation, Cuyama Valley Badlands, California. Natural History Museum of Los Angeles Contribution in Science 455, 1-33.

Kelly, T.S., Lander, E.B., 1988. Biostratigraphy and correlation of Hemingfordian and Barstovian land mammal assemblages, Caliente Formation, Cuyama Valley area, California. In W.J.M. Bazeley (ed.) *Tertiary tectonics and sedimentation in the Cuyama Basin, San Luis Obispo, Santa Barbara, and Ventura Counties, California*. Pacific Section, Society of Economic Paleontologists and Mineralogists, Papers and Field Guide from the Cuyama Symposium and Field Trip, 1-19.

Kent-Corson, M.L., Barsnoksy, A.D., Mulch, Andreas, Carrasco, M.A., Chamberlain, C.P., 2013. Possible regional tectonic controls on mammalian evolution in western North America. Palaeogeography, Palaeoclimatology, Palaeoecology 387, 17-26.

Koch, P.L., Tuross, N., Fogel, M.L., 1997. The effects of sample treatment and diagenesis on the isotopic integrity of carbonate in biogenic hydroxylapatite. Journal of Archaeological Science 24, 417–429.

Koch, P.L., Hoppe, K.A., Webb, S.D., 1998. The isotope ecology of late Pleistocene mammals in North America Part 1. Florida. Chemical Geology 152, 119-138.

Kohn, M.J., 2010. Carbon isotope compositions of terrestrial C3 plants as indicators of (paleo)ecology and (paleo)climate. Proc. Natl. Acad. Sci. U.S.A. 107, 19691–19695.

Kohn, M.J., Fremd, T.J., 2007. Tectonic controls on isotope compositions and species diversification, John Day Basin, central Oregon. PaleoBios 27, 48-61.

Kohn, M.J., Fremd, T.J., 2008. Miocene tectonics and climate forcing of biodiversity, western United States. Geology 36, 783-786.

Kürschner, W.M., Kvaček, Z., Dilcher, D.L., 2008. The impact of Miocene atmospheric carbon dioxide fluctuations on climate and the evolution of terrestrial ecosystems. Proc. Natl. Acad. Sci. 105, 449–453.

Liu, L., Stegman, D.R., 2012. Origin of Columbia River flood basalt controlled by propagating rupture of the Farallon slab. Nature, 482, 386-390.

MacFadden, B.J. 1992. Fossil Horses: Systematics, Paleobiology, and Evolution of the Family Equidae. Cambridge University Press, New York, NY, 369p.

Macfadden, B. J. 1997. Origin and evolution of the grazing guild in new world terrestrial mammals. Trends in Ecology & Evolution 12:182–187.

MacFadden, B.J., 1998. Equidae in Janis, C.M., Scott, K.M., and Jacobs, L.L. (eds.) *Evolution of Tertiary Mammals of North America Volume 1: Terrestrial Carnivores, Ungulates, and Ungulatelike Mammals*. Cambridge University Press, p. 537-559.

MacFadden, B. J., Cerling, T.E., 1996. Mammalian herbivore communities, ancient feeding ecology, and carbon isotopes: a 10 million-year sequence from the Neogene of Florida. Journal of Vertebrate Paleontology 16:103–115.

MacFadden, B.J., Hulbert, R.C., 1988. Explosive speciation at the base of the adaptive radiation of Miocene grazing horses. Nature 336, 466–468.

McMillan, M.E., Angevine, C.L., Heller, P.L., 2002. Postdepositional tilt of the Miocene-Pliocene Ogallala Group on the western Great Plains: Evidence of late Cenozoic uplift of the Rocky Mountains. Geology 30, 63-66.

Marino, B. D., McElroy, M.B., Salawitch, R.J., Spaulding, W.G., 1992. Glacial-to-interglacial variations in the carbon isotopic composition of atmospheric CO2. Nature 357,461–466.

O'Sullivan, J.A., 2003. A new species of Archaeohippus(Mammalia, Equidae) from the Arikareean of central Florida. Journal of Vertebrate Paleontology 23, 877–885.

Pagani, M., Freeman, K.H., Arthur, M.A.,1999a. Late Miocene Atmospheric CO2 Concentrations and the Expansion of C4 Grasses. Science 285, 876–879.

Pagani, M., Arthur, M.A., Freeman, K.H., 1999b. Miocene evolution of atmospheric carbon dioxide. Paleoceanography 14, 273–292.

Passey, B. H., Cerling, T.E., Perkins, M.E., Voorhies, M.R., Harris, J.M., Tucker, S.T., 2002. Environmental Change in the Great Plains: An Isotopic Record from Fossil Horses. Journal of Geology 110,123–140.

Passey, B.H., Robinson, T.F., Ayliffe, L.K., Cerling, T.E., Sponheimer, M., Dearing, M.D., Roeder, B.L., Ehleringer, J.R., 2005. Carbon isotope fractionation between diet, breath CO2, and bioapatite in different mammals. Journal of Archaeological Science 32, 1459–1470.

Prothero, D.R., Foss, S.E. 2007. The Evolution of Artiodactyls. The John Hopkins University Press, Baltimore, MD, 367p.

Quade, J., Cerling, T.E., Andrews, P., Alpagut, B., 1995. Paleodietary reconstruction of Miocene faunas from Paşalar, Turkey using stable carbon and oxygen isotopes of fossil tooth enamel. Journal of Human Evolution 28, 373-384.

R Core Team, 2013. R: A language and environment for statistical computing. R Foundation for Statistical Computing, Vienna, Austria. URL http://www.R-project.org/.

Retallack, G., 1997. Neogene Expansion of the North American Prairie. PALAIOS 12, 380-390.

Retallack, G., 2004. Late Oligocene bunch grassland and early Miocene sod grassland paleosols from central Oregon, USA. Palaeogeography, Palaeoclimatology, Palaeoecology 207, 203–237.

Retallack, G.J., 2007. Cenozoic Paleoclimate on Land in North America. The Journal of Geology115, 271–294.

Samuels, J.X., Van Valkenburgh, B., 2009. Craniodental adaptations for digging in extinct burrowing beavers. Journal of Vertebrate Paleontology 29, 254-268.

Sheldon, N.D., 2003. Pedogenesis and geochemical alteration of the Picture Gorge subgroup, Columbia River basalts, Oregon. Geological Society of America Bulletin 115, 1377-1387.

Skrzypek, G., Kałużny, A., Wojtuń, B., Jędrysek, M.-O., 2007. The carbon stable isotopic composition of mosses: A record of temperature variation. Organic Geochemistry 38, 1770–1781.

Stirton R.A., 1947. Observations on evolutionary rates of hypsodonty. Evolution 1, 32–41.

Strömberg, C.A.E., 2005. Decoupled taxonomic radiation and ecological expansion of open-habitat grasses in the Cenozoic of North America. Proceedings of the National Academy of Sciences, 102, 11980–11984.

Tieszen, L.L., Hein, D., Qvortrup, S.A., Troughton, J.H., Imbamba, S.K., 1979. Use of δ13C values to determine vegetation selectivity in East African herbivores. Oecologia 37, 351–359.

Wang, Y., Cerling, T.E., 1994. A model of fossil tooth and bone diagenesis: Implications for paleodiet reconstruction from stable isotopes. Palaeogeography, Palaeoclimatology, Palaeoecology 107, 281-289.

Wang, Y., Cerling, T.E., MacFadden, B.J., 1994. Fossil horses and carbon isotopes: new evidence for Cenozoic dietary, habitat, and ecosystem changes in North America. Palaeogeography, Palaeoclimatology, Palaeoecology 107, 269–279.

Webb, S.D., 1977. A history of savanna vertebrates in the New World. Part I. North America. Annual Review of Ecology and Systematics, 8, 355–80

Wernicke, B., Snow, J.K., 1998. Cenozoic Tectonism in the Central Basin and Range: Motion of the Sierran-Great Valley Block. International Geology Review 40, 403–410.

Williams S.H., Kay, R.F., 2001. A comparative test of adaptive explanations for hypsodonty in ungulates and rodents. Journal of Mammalian Evolution, 8, 207–229.

Wolfe, J.A., 1981. Paleoclimatic significance of the Oligocene and Neogene floras of the northwestern United States in Niklas, K.J. (ed.) *Paleobotany, paleoecology, and evolution, Volume 2*, Praeger Publishers, New York, 79-101.

You, Y., Huber, M., Müller, R.D., Poulsen, C.J., Ribbe, J., 2009. Simulation of the Middle Miocene Climate Optimum. Geophys. Res. Lett. 36, L04702, doi:10.1029/2008GL036571.

CHAPTER 3: TESTING FOR ECOLOGICAL NICHE SHIFTS IN THE FOSSIL RECORD: A CASE STUDY EXAMINING MAMMALS FROM THE LAST GLACIAL MAXIMUM TO THE RECENT

INTRODUCTION

Studying species ecological niches through time is important for understanding both evolutionary and ecological questions (Ackerly, 2003; Orr and Smith, 1998). The ecological niche of a species is defined by the values of a suite of environmental variables in which a species can survive and reproduce (Hutchinson, 1978). Over long time scales evolutionary mechanisms such as speciation, adaptive radiations, and extinctions can be clarified through studies of niche dynamics (Brame and Stigall, 2013; Levin, 2005; Losos et al., 2003; Walls and Stigall, 2011). Over shorter time scales, delimiting the ecological niche of a species can shed light on distributional patterns, dispersal/invasion events and species-environment interactions (Broennimann et al., 2007; Brown et al., 1996; Martínez-Meyer et al., 2004). Studying ecological niches in the present or near past (tens of thousands of years) is possible given the robust occurrence datasets and environmental layers that have recently become available, which open the door for approaches such as species distribution modeling (Martínez Meyer et al., 2004; Soberón, 2007; Veloz et al., 2012). These methods utilize the geographic distribution of species and environmental parameters to construct niches. However, in deeper time (millions of years ago), while occurrence datasets are available, it is difficult to reconstruct environmental layers because of limited sampling, outcrop availability and taphonomic bias. This makes many of the quantitative approaches that are useful in studying living species unsuitable for studying niches through deep time (hundreds of thousand to millions of years) (but see Dudei and Stigall, 2010; Maguire and Stigall, 2009; Stigall, 2013; Walls and Stigall, 2011). Despite these limitations, there are sufficient data to define species ecological niches in terms of environmental space (**E**) rather than in geographic space (**G**). Environmental space is an important aspect of ecological niches that can shed light on evolutionary and ecological processes and it can be traced through long time spans (Peterson et al., 2011). Here, I explore some methods to study niche dynamics in the deeper time fossil record, when detailed, geographically widespread and empirically based environmental and climatic layers are not always available, and I provide insights into conclusions that can be drawn from such analyses.

Of particular interest at both the evolutionary (millions of years) and ecological (hundreds of years to tens of thousands of years) time scales, is whether the ecological niche of a species remains stable through time (Pearman et al., 2008a; Peterson, 2011). A large number of recent studies on this topic are driven by concerns about the assumption that niches are stable, which implicitly underlies species distribution models used to predict species' geographic ranges given projected climate change (Broennimann et al., 2007; Nogués-Bravo, 2009; Pearman et al., 2008a; Rödder and Lötters, 2009). Methods that measure niche stability through time in the recent and near past do so by calculating the amount of niche overlap of a species from two time periods (Broennimann et al., 2012; Martínez Meyer et al., 2004; Pearman et al., 2008b; Peterson and Nyári, 2007; Warren et al., 2008) or by comparing climatic response curves for niche estimates from different time periods (Rodríguez-Sánchez and Arroyo, 2008). The species niche is defined by multiple climatic variables (e.g. maximum monthly temperature, minimum precipitation) and environmental variables (e.g. vegetation cover, altitude) that are obtained from large scale, geographically widespread databases or climate models. The amount of overlap is calculated in geographic and environmental space where the greater the niche overlap, the more stable the niche is considered to be through time. When robust and geographically widespread paleoenvironmental data are available to create environmental layers, these methods have been utilized in deep time studies as well (Maguire and Stigall, 2009; Stigall, 2011). But rarely does one have the extensive correlated outcrop area needed to reconstruct environmental and climate layers through time in relation to fossil occurrences; typically, outcrops containing fossils are few and isolated. In addition modeling species climatic niches for past periods based on current environmental layers has many associated challenges (Belyea, 2007; Kozak et al., 2008; McGuire and Davis, 2013) making direct measurement of niche space via proxy data a better option for reconstructing niche space in deeper time. When an adequate number of fossiliferous outcrops are available, proxy data can be used to reconstruct niche parameters. Examples include using stable isotopes to reconstruct temperature, precipitation and diet (Cerling et al., 1997; Koch, 1998); paleosols to reconstruct paleoenvironment and precipitation (Sheldon and Tabor, 2009); plant physiognomy to reconstruct temperature and precipitation (Wilf, 1997); and morphology to reconstruct locomotor type, diet, and trophic level (Polly et al., 2011). This type of data can be studied in multivariate space, similarly to environmental space (**E**), to gain understanding of niche dynamics through time. Before doing so, however, it is important to understand what analysis of these data will reveal about niche dynamics through time. In effect, such characterizations of "niche spaces" reflect only part of the parameter space that defines the entire ecological niche. This paper examines 1) what do these niche spaces actually represent and 2) what an observed shift in niche space actually means.

In order to explore niche stability in multidimensional space in the deep time fossil record using various methods, I study the climate correlates of 15 mammals from the Last Glacial Maximum (LGM) to the Recent using data from climate models. Because climate layers are available for both time periods of interest, climate data are used to reconstruct the niche spaces instead of the proxy data typical of the fossil record in order to investigate how a lack of background environmental data in the fossil record may influence interpretations of niche stability or evolution. I limit the environmental data to the type and amount typically available in the deep time fossil record. Species niches are defined solely in terms of the bivariate space of mean annual temperature (MAT) and mean annual precipitation (MAP) derived from climate models. I purposely limit the climatic niche space of these species to MAT and MAP in order to make analyses and conclusions transferable to the terrestrial deep time fossil record. MAT and MAP are variables that can be obtained from proxy data in the geological and paleontological record (Koch, 1998; Sheldon and Tabor, 2009), unlike finer scale climatic variables typically used in more comprehensive niche characterizations of extant species. It is known that these environmental variables are not capturing all the factors important for defining species niche space through time; however, the approach and conclusions presented here are independent of the quality or type of variables being used to reconstruct the niche space.

METHODS

Terminology and Definitions – I follow the terminology and definitions outlined in Peterson et al. (2011) for occupied niche ($\mathbf{E_O}$), invadable niche ($\mathbf{E_I}$), potential niche ($\mathbf{E_P}$), fundamental niche ($\mathbf{E_A}$), and environmental space (**E**) (Fig. 3.1). The union of the invadable niche ($\mathbf{E_I}$) and the occupied niche ($\mathbf{E_O}$) is the potential niche ($\mathbf{E_P}$). The potential niche ($\mathbf{E_P}$) is conceptually similar to the realized niche of Hutchinson (1957). Species niches are constructed using known occurrences paired with environmental data; therefore analyses of niche stability through time are examining the occupied niche ($\mathbf{E_O}$) of the species which is constrained by biotic factors (**B**), dispersal limitations (**M**), and the realized environmental (**E**) (Colwell and Rangel, 2009; Hutchinson, 1957; Soberón, 2007). Due to fossil preservation biases, the occupied niche constructed from fossil occurrences may be constrained more than the occupied niche of Peterson et al. (2011) resulting in the fossil occupied niche ($\mathbf{E_{OF}}$) (See Discussion). And because the niche, in this case, is defined by climatic parameters, it is the occupied climate-niche that is constructed and analyzed.

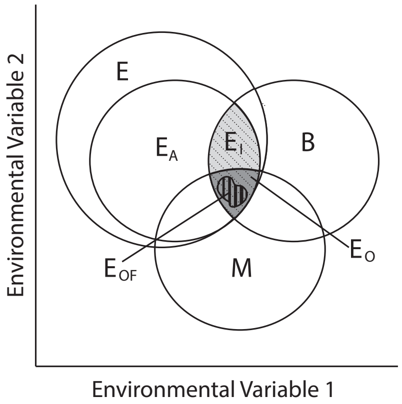

Figure 3.1 Schematic diagram from Peterson et al. (2011) demonstrating niche spaces. **E,** the available environmental space (=realized environmental space of Jackson and Overpeck (2000)); $\mathbf{E_A}$, the existing fundamental niche constrained by abiotic factors in which the species can maintain a population; **B**, biotic factors in which the species can maintain a population; **M**, niche space that is accessible to the species via dispersal and historical contingencies; $\mathbf{E_I}$, invadable niche; $\mathbf{E_O}$, occupied niche; $\mathbf{E_{OF}}$**,** occupied fossil niche. The union of $\mathbf{E_I}$ and $\mathbf{E_O}$ is the biologically reduced niche ($\mathbf{E_P}$) (=potential niche of Jackson and Overpeck (2000)) and illustrated by the cross-hatched area.

Occurrence data – Only species with at least 10 geographically distinct occurrences in the LGM were chosen for the study in order to limit the possibility of inadequate samples influencing the size and ranges of the constructed niche spaces (Table 3.1). Occurrence data for the Recent was downloaded for each species from the Global Biodiversity Information Facility (http://www.gbif.org/, April 21, 2013). This database contains specimen based and observed occurrence point records from museums, researchers, publications, and citizen scientists through out North America. Only georeferenced occurrences were used, fossil based occurrences and zoo records were removed, and the dataset was examined to remove any erroneous occurrence points. Fossil occurrences were downloaded from the Quaternary Faunal Mapping Project (FAUNMAP) accessible from the NEOMAP website (FAUNMAP Working Group, 1994; Graham & Lundelius, 2010; http://www.ucmp.berkeley.edu/neomap/, April 21, 2013). Species occurrences were downloaded from the Late Wisconsinan-age deposits. Occurrence points from both time periods were culled so that occurrences that were less resolved than the resolution of the climatic data were removed. This also removed any duplicate geographic occurrences.

Climate Data – Global mean annual temperature (MAT) and mean annual precipitation (MAP) data were downloaded from the WorldClim Global Climate Data website (Hijmans et al., 2005). LGM modeled climate data is from PMIP2 (Braconnot et al., 2007). As noted above, in order to make methods and analyses used here transferable to deep time analyses, climate data is restricted to MAT and MAP because obtaining finer scale values such as maximum monthly temperature often used in niche analyses is impossible for deep time analysis. Fossil occurrence data for the LGM time period in this study spans the Late Wisconsinan, which is a wider range of time than the climate layer for the LGM, however, the LGM climate layer from 21,000 ybp is indicative of the entire Late Wisconsinan climate.

Table 3.1 Species used in this study, along with number of recent and fossil occurrences sampled. Recent occurrence data was derived from the Global Biodiversity Information Facility (http://www.gbif.org/); fossil occurrence data as derived from the Quaternary Faunal Mapping Project (FAUNMAP, http://www.ucmp.berkeley.edu/neomap/).

Family	Species	Common name	Recent	Fossil
Soricidae	*Cryptotis parva*	North American Least Shrew	10	1957
Talpidae	*Scalopus aquaticus*	Eastern Mole	15	1639
Ochotonidae	*Ochotona princeps*	American Pika	36	5178
Leporidae	*Sylvilagus audobonii*	Audubon’s cottontail	10	2711
Sciuridae	*Tamias striatus*	Eastern chipmunk	14	2094
	Spermophilus tridecemlineatus	Thirteen-lined Ground Squirrel	23	910
Geomyidae	*Geomys bursarius*	Plains Pocket Gopher	12	2049
	Thomomys bottae	Botta’s Pocket Gopher	10	25138
Cricetidae	*Microtus pennsylvanicus*	Meadow Vole	26	12590
	Phenacomys intermedius	Western Heather Vole	28	726
	Synaptomys cooperi	Southern Bog Lemming	25	716
Canidae	*Canis latrans*	Coyote	35	4813
	Urocyon cinereoargenteus	Gray Fox	14	2180
Felidae	*Lynx rufus*	Bobcat	19	3684
Cervidae	*Odocoileus hemionus*	Mule Deer	10	2208

Niche stability measures –

Non-parametric MANOVA - For each species, the MAT and MAP at each occurrence point was extracted from the climate layer (Fig. 3.2). MAP was log transformed to produce a normal distribution. As a first order test of niche stability for each species between the two time periods, MAT and MAP from each species LGM niche and Recent niche space were compared using a Mann-Whitney U test to determine if variables shifted through time along each individual axis. Then the LGM and Recent niche spaces for each species were compared using a non-parametric MANOVA test (permutational multivariate analysis of variance) (Anderson, 2001), implemented using the *adonis* function in the Vegan R package (Oksanen et al. 2013; R Core Team 2013).

This statistical test measures the Euclidean distance between all pairs of samples in a species LGM and Recent niche space, compares the within-group and across-group distances, and uses the permutation of samples to estimate significance between the groups. A significant result indicates the two niche spaces are not equal, suggesting a shift in niche space. It does not determine the amount or direction of a detected niche shift nor can this approach determine if the fundamental niche (E_A) is shifting (i.e. niche evolution), instead of the observed (E_O) and/or realized niche (E_P), because the detected shift is not placed within a framework of the environmental space (E). To ensure results were not sensitive to sample size differences between the LGM niche space and Recent niche space (Table 3.1), the Recent niche space dataset was subsampled 100 times to be the same size as the LGM niche space dataset and perMANOVAs were rerun. All MAT and MAP points in North America from the LGM and the Recent were also compared using a non-Parametric MANOVA to determine if the environmental space (E) shifted. Because the complete environmental space dataset was too computationally large, it was subsampled 1000 times and then statistically analyzed. In addition, Hotelling's T^2 test was used to compare the MAT and MAP of the environmental space through time.

<u>Within and between climatic distances</u> – To tease apart the non-Parametric MANOVA results and place them within the context of the changing environmental space, I analyze the pairwise Euclidean climatic distances (PCD) of the niche spaces for each species three ways to understand: 1) is the variation within the LGM niche space more or less than the variation within the Recent niche space; 2) is the variation within the niche space of either time period more than the variation among the two time periods suggesting a shift in niche space; and 3) is the variation among the two time periods more than the variation among the LGM environmental space and the Recent environmental space, suggesting the shift in niche space is greater than the shift in environmental space. The within-group PCD of each niche space for each species and the among-group PCD of the two niche spaces for each species was calculated using the *dist* function in the Stats R package and the *dist2* function in the Flexclust R package (Leisch, 2006). The within- and among-group PCD of the environmental spaces for each time period was calculated in the same manner as well. For the first hypothesis, I compare the distribution of within-group PCD for the LGM niche space to the distribution of within-group PCD for the Recent niche space using a Kolmogorov-Smirnov test for each species. For the second hypothesis, I compare the distribution of the within-group PCD of each time period to the among-group PCD of the two time periods using a Kolmogorov-Smirnov test for each species. And lastly, to compare a shift in niche space to the shift in environmental space and determine if the shift observed in a species niche space through time is greater than the shift in environmental space, the among-group PCD of each species niche spaces was compared to the among-group PCD of the environmental space using a Kolmogorov-Smirnov test.

<u>Niche overlap using the D-metric</u> – There are several newly developed methods for calculating niche overlap in E space (Broennimann et al., 2012; Warren et al., 2008; 2010). These methods incorporate the environmental space to calibrate species occurrences in E space in relation to the changing environment. I utilize one of these methods as a second approach to demonstrate how incorporation of the environmental space will influence conclusions on niche stability. The amount of overlap between the past and present niche space was calculated using the D metric of Warren et al. (2008) and the framework of Broennimann et al. (2012). This framework condenses multiple niche parameters of a species and the environmental space into two dimensions using principle component analysis, thus adjusting occurrences to the environmental

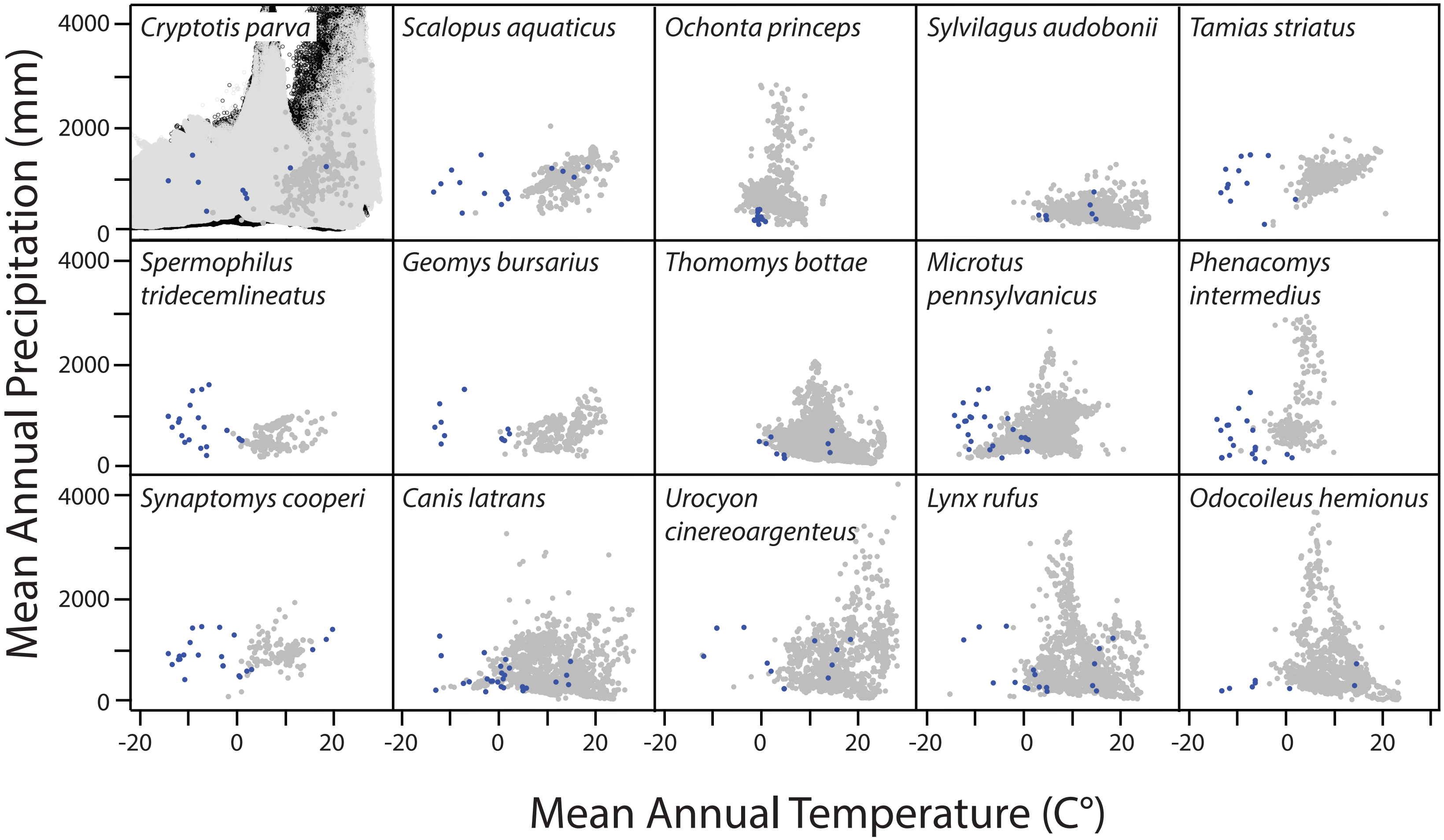

Figure 3.2 Bivariate plot of MAT and MAP values for each species occurrence in the LGM (blue) and Recent (gray) time periods. Within the *Cryptotis parva* plot are the realized environmental spaces for the LGM (black) and Recent (light gray).

space in the past and present. I utilized the "PCA-env" ordination technique of Broennimann et al. (2012), in which species occurrences are calibrated to environmental space, because this method accurately measured simulated niche overlap best in their analysis. The framework uses a kernel density function on the PCA to create an occupancy model for niche space based on the density of occurrence points. Niche overlap is calculated from the occupancy models by measuring the number of occupied cells shared by the two time periods which is translated into the D metric in which a value of 0 means no overlap and a value of 1 means complete overlap (Broennimann et al., 2012; Schoener, 1970; Warren et al., 2008). Because a kernel density function was applied to the niche space, the overlap between two niche spaces is not dependent on the resolution of the data. This is an important point when examining the niche space of species through time periods in which high-resolution environmental data are not available, or when two time periods of interest have different environmental resolution.

Using the D metric, similarity tests were conducted (Broennimann et al., 2012; Warren et al., 2008). The similarity tests determine whether the observed niche overlap is similar to the amount of overlap between the niche space of one time period and a randomly generated niche space from the occurrence points of the second time period, repeated 100 times. This test is performed in both directions. A significant *p*-value in which the observed D metric is larger than the simulated D metrics means that the observed niche overlap is more statistically similar than the observed overlap between the niche space in a time period and a randomly generated niche space from the second time period. This indicates that the niche space has not changed through time and the niche is stable. On the other hand, a significant *p*-value of an observed D metric lower than the simulated D metrics indicates the two niches are not similar and have shifted through time. If the similarity test is not significant, conclusions on stability or instability of the niche space cannot be determined. The D metric and these tests only examine the amount of overlap between the niche spaces of two time periods. It does not indicate direction of change, expansion and/or contraction. The framework developed by Broennimann et al. (2012); however, does provide a visual presentation on which direction of change can be inferred (see Fig. 3.3). The equivalency test from Warren et al. (2008) and Broennimann et al. (2012) was conducted but results are not discussed because a significant result from this test does not necessarily lead to a robust conclusion about niche shifts due to Type 1 error. Their equivalency test determines whether the amount of overlap (D metric) observed between the two time periods is statistically equivalent to the amount of overlap between two randomly generated niche spaces from the pooled occurrence datasets of both time periods, repeated 100 times. In essence this test verifies that the constructed niche spaces of a species through time indeed reflect a measure of biological reality and are indicative of actual niche spaces, rather than being a random set of points drawn from the realized environmental space.

The sample size of occurrence points for the LGM niche space is significantly lower than the occurrence points that define the recent niche space of each species (Table 3.1). Broenniman et al. (2012) state that their framework is not sensitive to differing sample sizes but given the large difference is sample sizes in this study, there is concern for skewed results for the niche overlap analysis. To accommodate for this and test the hypothesis of Broenniman et al. (2012) on sample size insensitivity, the recent occurrence dataset for each species was subsampled 100 times to be the same size as the LGM occurrence dataset. D metric analyses were then performed on all subsampled datasets for each species and compared to the non-sampled results.

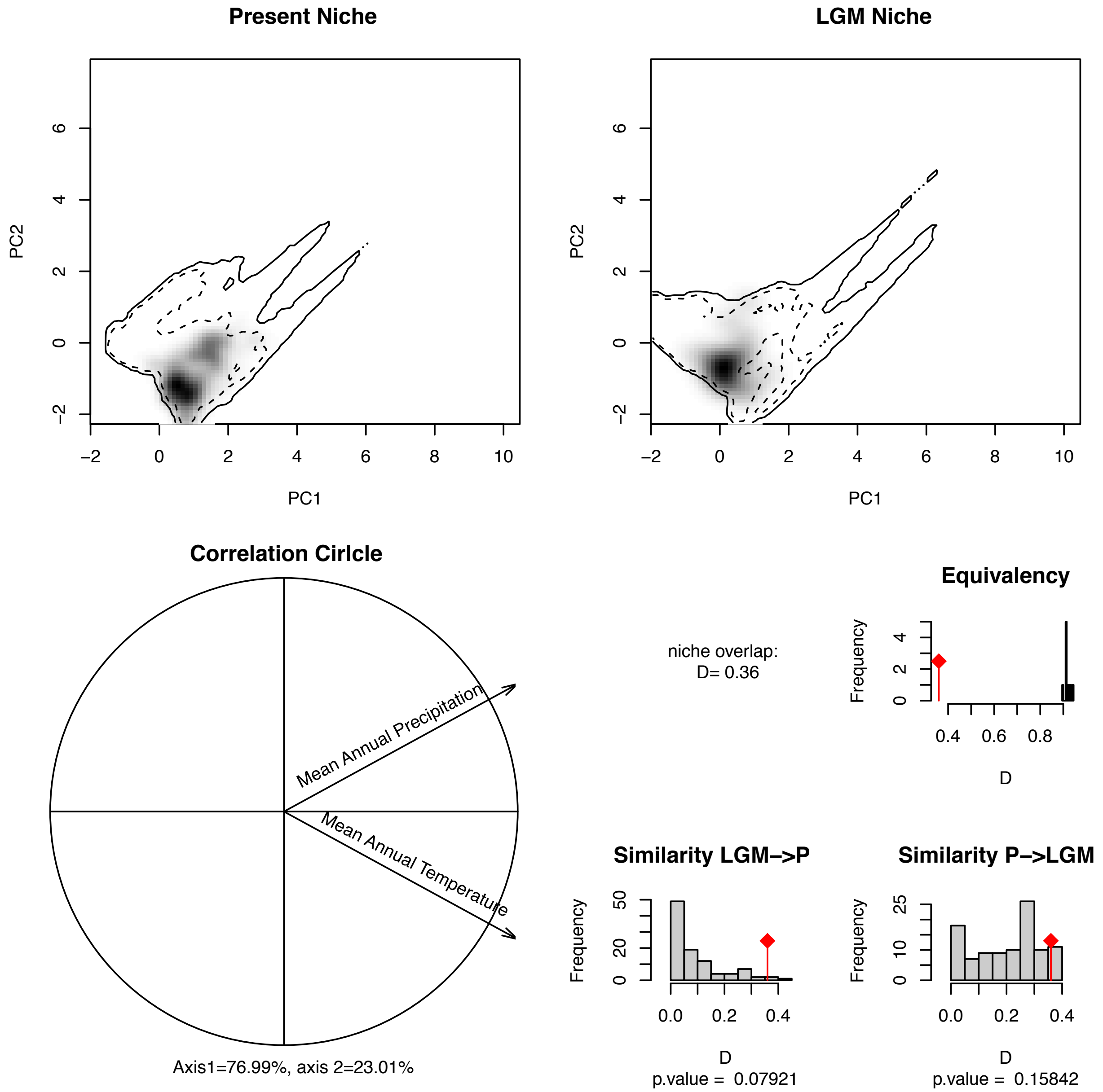

Figure 3.3 Example output of the niche overlap framework from Broenimman et al. (2012) for *Canis latrans*. PCA graphs show niche occupancy model for the Recent time period and LGM time period where darker regions represent more dense occurrences and the lines represent the realized environmental space at 50% (dashed line) and 100% (solid line). The correlation circle provides the amount of variation explained by the variables. Equivalency and similarity tests compare the observed overlap (D; red diamond) to simulated overlaps.

RESULTS

The environmental space for the LGM and recent time periods is largely similar (Fig. 3.2-*Cryptotis parva* panel); however, there are areas of climate space that existed in the LGM that do not exist in the recent. The LGM and recent environmental spaces are significantly different in multivariate space (Hotelling's T test: df=2, t=480230, p<0.001) but this result is most likely driven by spatial autocorrelation. According to the non-parametric MANOVA test on subsampled datasets, the environmental space is shifting (p<0.05). The among-group PCD of the environmental space is greater than the within-group PCD of the recent environmental space but not the LGM environmental space (Kolmogorov-Smirnov tests – within LGM and within Recent: D=0.0624, p<0.001; between LGM-Recent and within Recent: D=0.0623, p<0.001; between LGM-Recent and within LGM: D=2×10^{-4}, p=0.8928) (Fig. 3.4B).

For all species except *Sylvilagus audobonii* the LGM niche space is significantly different than the recent niche space according to the non-parametric MANOVA test (Table 3.2). However, when the recent niche spaces are subsampled to have the same number of occurrences as the LGM niche spaces, these results become non-significant for all species (Supplementary Table S3.1). Temperature values significantly shift for the majority of species according to the Mann-Whitney U tests (p<0.001; Supplementary Table S.32). The shift in temperature is consistently in the warming direction. Precipitation values are not significantly different from one time period to the next for all species except *Ochotona princeps* for which precipitation values increase (Supplementary Table S3.2). The among-group PCD for each species is greater than their within-group PCD of either time period except for *Sylivalagus audobonii, Thomomys bottae, Urocyon cinereoargenteus, Lynx rufus* and *Odocoileus hemionus* (Table 3.2, Fig. 3.4A). The species that have a larger among-group PCD than within-group PCD, do not have a larger among-group PCD than the among-group PCD of the environmental space from the LGM to the recent (Table 3.2, Fig. 3.4B).

D metric values indicate low (<0.50) overlap between species LGM niche space and recent niche space (Table 3.3). *Scalopus aquaticus*, *Sylvilagus audobonni,* and *Lynx rufus* have the highest D values and *Tamias striatus, Ochotona princeps,* and *Spermophilus tridecemlineatus* have the lowest D values. The similarity test identifies eight species that have more similar niche space through time than expected from random (*Scalopus aquaticus, Ochotona princeps, Sylvilagus audobonii, Thomomys bottae, Canis latrans, Urocyon cinereoargenteus, Lynx rufus* and *Odocoileus hemionus*). There are no species that have niche spaces significantly different from one time period to the other, that is, the differences are not more than what is expected by chance. The remaining species have non-significant similarity test results.

Subsampling the recent occurrences so that they are equal in number to the LGM occurrences generated similar results overall (Table 3.3). There are a few exceptions to this generalization. Five species (*Scalopus aquaticus, Ochotona princeps, Canis latrans, Lynx rufus,* and *Odocoileus hemionus*) that had significantly similar niche space through time according to the similarity test from the recent to the LGM have non-significant results more than 50% of the time when the recent time period is subsampled. On the other hand, two species (*Sylvilagus audobonii* and *Canis latrans*) that had non-significant similarity test results on the raw data, have significantly similar niches through time with the subsampled dataset over 50% of the time. This results in both species having similar niches through time according to the similarity test in both directions.

Table 3.2 Results of the permutational multivariate analysis of variance (**perMANOVA**) where a significant value indicates the two niche spaces are not similar; results of the pairwise climatic distance comparison in which a significant value indicates: **LGM-Recent** – the within-group pairwise climatic distance for the LGM and the Recent are different, **LGM** - the among-group pairwise climatic distance is greater than the within-group LGM pairwise climatic distance, **Recent** - the among-group pairwise climatic distance is greater than the within-group Recent pairwise climatic distance, and **Env. Space** - the among-group pairwise climatic distance of the niche space is greater than (^) or less than (‘) the among-group pairwise climatic distance of the environmental space from the LGM to the Recent. $p<0.05$*, $p<0.01$**, $p<0.001$***. *P*-values were adjusted using a Bonnferoni correction.

Family	Species	perMANOVA	LGM-Recent	LGM	Recent	Env. Space
Soricidae	*Cryptotis parva*	0.015*	<0.001***	4.45E-03**	<0.001***	<0.001***’
Talpidae	*Scalopus aquaticus*	0.015*	<0.001***	0.023*	<0.001***	<0.001***’
Ochotonidae	*Ochotona princeps*	0.015*	<0.001***	<0.001***	<0.001***	<0.001***’
Leporidae	*Sylvilagus audobonii*	0.554	0.149	1	<0.001***	<0.001***’
Sciuridae	*Tamias striatus*	0.015*	1	<0.001***	<0.001***	<0.001***’
	Spermophilus tridecemlineatus	0.015*	<0.001***	<0.001***	<0.001***	<0.001***’
Geomyidae	*Geomys bursarius*	0.015*	<0.001***	4.45E-03**	<0.001***	<0.001***’
	Thomomys bottae	0.015*	1.41E-02**	1	<0.001***	<0.001***’
Cricetidae	*Microtus pennsylvanicus*	0.015*	1	<0.001***	<0.001***	<0.001***’
	Phenacomys intermedius	0.015*	<0.001***	<0.001***	<0.001***	<0.001***’
	Synaptomys cooperi	0.015*	<0.001***	<0.001***	<0.001***	<0.001***’
Canidae	*Canis latrans*	0.015*	<0.001***	<0.001***	<0.001***	<0.001***’
	Urocyon cinereoargenteus	0.015*	<0.001***	1	<0.001***	<0.001***’
Felidae	*Lynx rufus*	0.015*	<0.001***	1	<0.001***	<0.001***’
Cervidae	*Odocoileus hemionus*	0.015*	<0.001***	0.595	<0.001***	<0.001***’

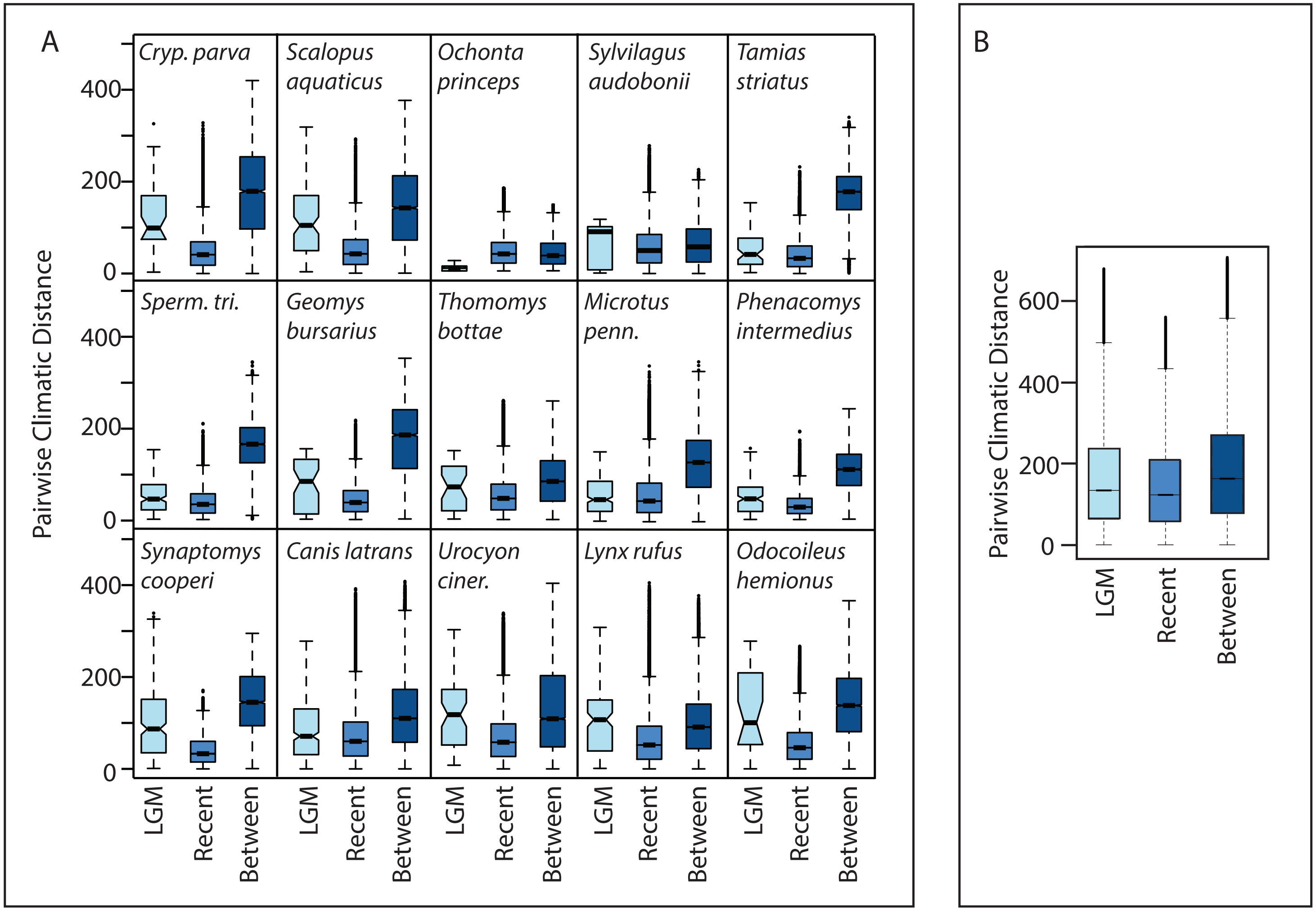

Figure 3.4 A) Boxplots of pairwise climatic distance distributions for the within-group LGM niche space, the within- group Recent niche space, and the among-group LGM-Recent shift for each species. B) Boxplots of the pairwise climatic distance distributions for the environmental space. For each boxplot the dark line indicates the median, the box represents the interquartile range, the dashed lines indicate the range of the values and the open circles are outliers.

Table 3.3 Observed amount of niche overlap (**D** metric) calculated using the niche overlap analysis of Broenimman et al. (2012) on all occurrences of the LGM and the Recent time periods. **Similarity** test results for the LGM to Recent followed by Recent to LGM where ns=non-significant, *p*<0.05*, *p*<0.01**, *p*<0.001***. **Subsampled** results give the number of subsampled simulated niche overlap analyses that produced the same result as the non-subsampled analyses in the previous column. *P*-values were adjusted using a Bonnferoni correction.

Family	**Species**	**D**	**Similarity**	**Subsampled**
Soricidae	*Cryptotis parva*	0.293	ns/ns	97/99
Talpidae	*Scalopus aquaticus*	0.409	***/***	61/12
Ochotonidae	*Ochotona princeps*	0.124	ns/***	100/11
Leporidae	*Sylvilagus audobonii*	0.492	*/ns	88/29
Sciuridae	*Tamias striatus*	0.107	ns/ns	100/100
	Spermophilus tridecemlineatus	0.138	ns/ns	100/100
Geomyidae	*Geomys bursarius*	0.191	ns,ns	100/100
	Thomomys bottae	0.374	*/ns	84/65
Cricetidae	*Microtus pennsylvanicus*	0.218	ns/ns	100/100
	Phenacomys intermedius	0.205	ns/ns	100/100
	Synaptomys cooperi	0.229	ns/ns	85/99
Canidae	*Canis latrans*	0.360	***/ns	26/90
	Urocyon cinereoargenteus	0.371	*/ns	51/93
Felidae	*Lynx rufus*	0.414	***/*	83/40
Cervidae	*Odocoileus hemionus*	0.273	ns/***	96/47

DISCUSSION

In this study, comparison of niche spaces assumes the constructed niche space represents the entire observed niche (E_O) of that particular species for a particular time period (Fig. 3.1). Low sample sizes representing the LGM niche space may violate this assumption. The fossil record by its nature can be an incomplete representation of a species entire distribution or niche space. I recognize that the LGM niche space may be a subset of the actual observed niche given the limited occurrence points. Fossilization potential, geologic setting, and taphonomic processes can bias occurrences. These biases will limit the number of occurrences and may prejudice them towards certain environments in which preservation potential is high. For example, body fossils are less likely to preserve in moist habitats due to the higher likelihood of decomposition before burial in these environments (Behrensmeyer et al., 2000). Therefore, the observed niche space (E_O) for proxy constructed niche spaces in deep time is further restricted to the observed fossil niche space (E_{OF}) (Fig. 3.1). Interpretations of niche spaces through time constructed from fossil occurrences must bear this in mind when interpreting results. Where terrestrial fossils are found, studies have shown that fossil deposits accurately represent the surrounding faunal community (Terry, 2010; Western and Behrensmeyer, 2009) and given robust sampling across a species entire distribution in the fossil record, one can approach the observed niche space. Another aspect of the fossil record that needs to be addressed when examining niche spaces of species is time averaging. In this study, occurrences from the LGM were pooled from the Late Wisconsinan, which spans 10,000 to 35,000 years ago in the FAUNMAP database. A time averaged niche space may represent a compilation of multiple observed fossil niche spaces. This compilation of several E_{OF} spaces may approach a better understanding of the occupied niche space (E_O), potential niche space (E_P) and even the fundamental niche space (E_A); however, this needs to be examined more fully before conclusions can be drawn.

When a species is faced with environmental changes, it either adapts to the changes, goes extinct or shifts its geographic range so that it tracks its niche (Peterson et al., 2011). The first option, adaptation will result in the evolution of the niche space while the latter option will result in a stable niche (niche conservatism) through time. Niche shifts over evolutionary time scales are often interpreted as niche evolution (e.g. Brame and Stigall, 2013). However, conclusions about niche evolution are contingent on the type of niche being analyzed. A shift in fundamental niche space implies evolution of the niche and adaptation of the species. On the other hand, a shift in the observed niche space (E_O) or potential niche space (E_P) does not imply evolution (here I use the term potential niche space (E_P) conceptually as the realized niche space). Change in the species biotic interactions (B), dispersal capabilities (M) or a change in the environment (E) can cause an observable shift in these niche spaces but it does not necessarily mean the niche is evolving (Jackson and Overpeck, 2000; Peterson et al., 2011). If a shift in the occupied niche space is detected, it can be due to a variety of conditions resulting in contrasting, or at least different conclusions about niche evolution (Fig. 3.5). If the environmental space is not changing but the occupied niche (for the purposes of this discussion E_O=E_{OF}) is shifting, then the occupied niche space can either be moving within the fundamental niche space or it can expand outside the fundamental niche space with respect to a given time period (Fig. 3.5A). The former does not imply evolution, but the latter does. If the occupied niche space does shift and the environment space shifts as well, the occupied niche space can track the potential niche space, or it can shift in a different direction or magnitude great enough so that it changes the estimate of the fundamental niche - in which case, the niche would have evolved (Fig. 3.5B). All scenarios that conclude the niche is evolving must know the size and shape of the fundamental niche as well as the environmental space. Given the data available in deep time records (and in fact, even for current records), the fundamental niche and the environmental space are difficult to reconstruct, making it challenging to ever robustly document niche evolution. Nogues-Bravo (2009) concluded the same when using species distribution modeling and climatic envelopes to determine niche evolution through time. But given a reconstructed niche space based on environmental variables, it is tractable to test for shifts in the occupied niche space.

Some of the species examined here occupy different climatic space in the LGM than they do today (Fig. 3.2). This is especially true of the smaller bodies species: *Cryptotis parva, Scalopus aquaticus, Tamias striatus, Spermophilus tridecemlineatus, Geomys busarius, Phenacomys intermedius,* and *Synaptomys cooperi*. When environmental space is ignored in analyses, most species occupy significantly different occupied niche spaces through time (perMANOVA - Table 3.2). But when the occurrence dataset for the recent time period is subsampled to be of equal size to the LGM time period, results become non-significant. This suggests that this test is sensitive to sample sizes and caution is needed when interpreting results of analyses that contain small sample sizes (at least less than 40 occurrences per time period). The environmental space is significantly different through time according to the non-parametric

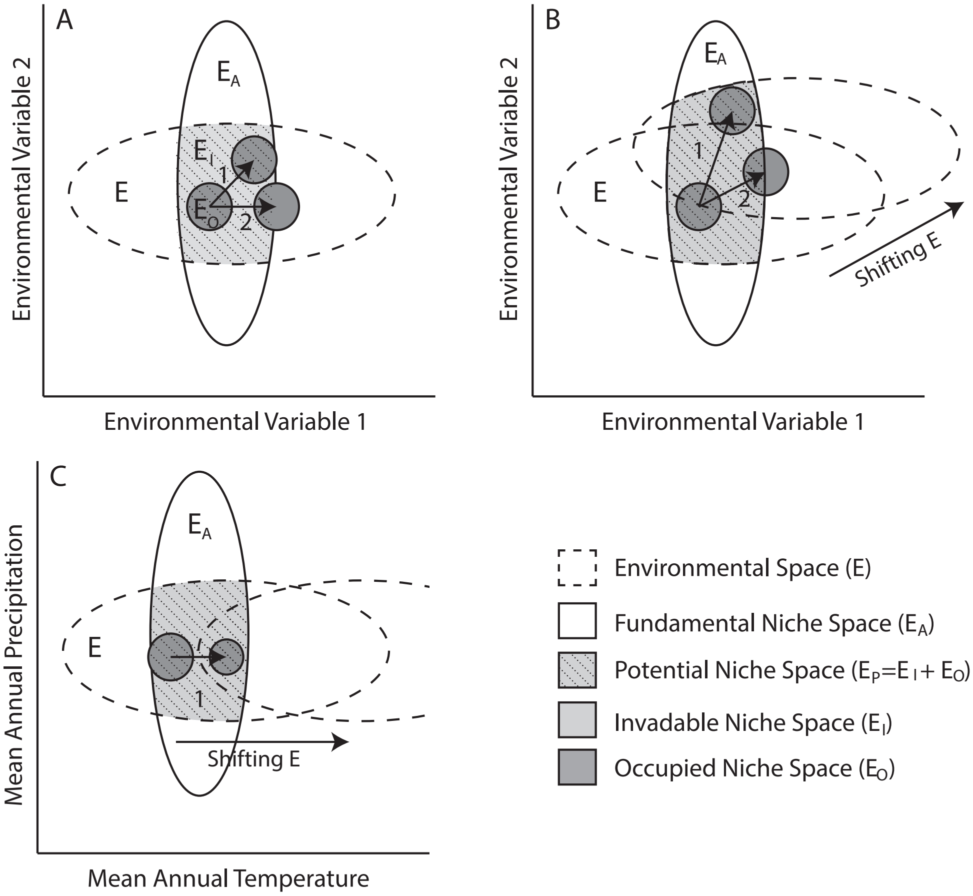

Figure 3.5 Schematic diagrams demonstrating the types of niche spaces and niche stability vs. niche evolution. For simplicity M, B, and E_{OF} are not included. A) Environmental space is not changing, scenario (1) the occupied niche is shifting within the fundamental niche space, scenario (2) the occupied niche is shifting outside the fundamental niche space. B) Environmental space is changing, scenario (1) the occupied niche tracks the potential niche space, scenario (2) the occupied niche shifts along with the environmental space and with great enough distance and/or magnitude to expand outside the fundamental niche space. C) Proposed scenario for species with shifting niche space from the LGM to the Recent where the environmental space is shifting to the right along the temperature axis and the occupied niche is shrinking in variance and tracking the potential niche space. In all scenarios, the (1) does not involve niche evolution and the (2) does involve niche evolution.

MANOVA. From the perMANOVA analysis, it cannot be determined if the species niche space is shifting more than the environmental space; however, closer examination of the pairwise climatic distances can provide insight into how niches are shifting in relation to the shifting environmental space. The results for pairwise climatic distances identify five species (*Sylvilagus audobonni, Thomomys bottae, Urocyon cinereoargenteus, Lynx rufus* and *Odocoileus hemionus*) that do not have greater among-group PCD than within-group PCD for each time period, suggesting they do not shift their occupied niche space from the LGM to the recent (Table 3.2,

Fig. 3.4A). This result stems from the broader niche space of these species in the LGM so that the change observed between the two time periods is not more than the within-group PCD of their LGM niche space. The large variance within the LGM for these species may be due to time averaging; alternatively, the large variance in the LGM may be because these species actually had wider realized climatic niche breadths during this time. The lynx (*L. rufus*) and the gray fox (*U. cinereoargenteus*) have large geographic ranges and this may result in an apparently stable broad realized niche space through time (Brown et al., 1996). But all species have greater pairwise climatic distances in the LGM than the Recent (Table 3.2, Fig. 3.4A, except for *Sylvilagus audobonii, Tamias straitus* and *Microtus pennsylvanicus*), leading to the conclusion that the LGM niche spaces show higher variance due to time averaging, rather than providing robust information on the niche breadth of species. The fact that the distribution of among-group PCD for each species in this study was always greater than the distribution of the within-group PCD observed for the Recent time period, may be due to the large sample sizes in the Recent time period because a slight difference in the among-group PCD and the within-group PCD of the Recent time period will result in a statistically significant difference because of the large sample size.

When the difference in climatic niche space occupied by the species in the respective time periods is placed within the environmental space changes, conflicting interpretations about niche stability emerge. The environmental space shifts in multivariate space but again this may be due to large sample sizes causing a slight difference between the two time periods to results in statistical significance or this may be due to spatial autocorrelation. According to the pairwise climatic distance analysis, the environmental space does not exhibit a statistically significant shift from the LGM to the Recent. Regardless of the significance of a shift in environmental space, and even though the majority of species demonstrate a shift in niche space via pairwise climatic distance comparison, the shift in their niche space is not larger than the shift in environmental space from the LGM to the Recent (Table 3.2, Fig. 3.4). Species occupy significantly different temperature distributions from the LGM to the Recent, therefore it is probably the shift in environmental space along the temperature axis from the LGM to the Recent that causes the potential niche space of many of the species to shift along that axis (Fig. 3.5C). Thus, although the niche space of these species is changing, it is not changing more than the environmental space suggesting their occupied niches are shifting and/or tracking the potential niche space as the environmental space shifts.

These results are somewhat in concordance with the results from the niche overlap analysis. No species demonstrate a shift in niche space when the occurrence data are calibrated to the environmental space. In addition, this analysis recognizes niche stability through time for 8 of the 15 species. These include *Sylvilagus audobonni, Thomomys bottae, Urocyon cinereoargenteus, Lynx rufus* and *Odocoileus hemionus*, species that were also concluded to be stable in the pairwise climatic distance analysis. And one of the species, *Scalopus aquaticus,* had lower significance in the pairwise climatic distance analysis. Although the non-parametric MANOVA and pairwise climatic distance methods recognize some species are shifting their occupied niches and tracking the potential niche space, the overlap niche analysis suggests species niches are not changing. This begs the question as to what niche is being analyzed in the niche overlap method. Veloz et al. (2012) interpret their results using this method as shifting realized niches because the observed shifts in niche space are not unidirectional on an evolutionary trajectory. Broenniman et al. (2012) does not identify what type of niche is being analyzed. Because a shift in occupied niche space is apparent in the non-parametric MANOVA and pairwise climatic distance analyses and not apparent in the niche overlap method, I conclude that the niche space being measured in the niche overlap analysis is closer to the fundamental niche space rather than the realized or potential niche space and that species are shifting their realized niche space (observed in the non-parametric MANOVA and pairwise climatic distance analyses) and not shifting their fundamental niche space (observed in the niche overlap analysis).

A species with a stable niche through time and across periods of environmental change, must migrate in order to track its niche space in geographic space (Peterson et al. 2011). The majority of species examined here are shifting their realized niches but not changing their fundamental niche. Therefore, they are not evolving their niche and adapting. We would expect then, that these species will have geographic range shifts to accommodate for the changing environment and stable niche spaces. Future work examining the amount and direction of geographic range shifts for each of the species will shed light on this assumption.

The overlap analysis is sensitive to sample size for some of the species. In general these species demonstrated niche stability when subsampling was not applied. Subsampling the recent occurrences for these species results in non-significant results therefore suggesting that when sample sizes are low, the analysis cannot tease apart niche stability or niche shifts. According to Broennimann et al. (2012), the niche overlap framework is not sensitive to differing sample size. This statement may be true when examining extant systems with sufficient data in which differences in sample size may be small. But when this framework is applied to the fossil record, sample size does matter. In essence, sample sizes need to be large enough to obtain significant results. When occurrence data is low, such as with fossil data, the niche overlap framework loses statistical power and results become non-significant. This also highlights a warning that the sample sizes of the LGM niche spaces are not robust enough to use this analysis and therefore results from this analysis may not be reliable. Perhaps no shifts in niche space were detected using this method because sample sizes were too low. Indeed many of the species returned non-significant results indicating perhaps there was not enough data to make conclusions on niche stability versus niche shifts.

When only the LGM niche and the Recent niche are examined and the environment space is ignored, the occupied niche space has significantly shifted for the majority of species. In some instances, the pairwise climatic distance method suggests that some species are not significantly shifting their niche space but this may be due to high variance in the LGM niche space as a result of time averaging. When environmental space is incorporated, it is apparent that the occupied niche space, although shifting, is not shifting more than the environmental space. Therefore, species are shifting their potential or realized niches but not evolving their fundamental niche space. The niche overlap method confirms this result, indicating that none of the species are significantly changing their niche space when it is calibrated to the environmental space. In addition, this analysis identifies several species that have significantly similar niche spaces through time. Some of these species are the same species identified by the pairwise climatic distance analysis as not shifting their occupied niche space. This implies that the pairwise climatic distance method can identify taxa that have stable occupied niche spaces through time. In addition, the pairwise climatic distance method can identify instances of shifting realized niche space through time. Species that demonstrate a shift in realized niche space according to the pairwise climatic distance method, have non-significant results in the niche overlap method. Non-significance in the niche overlap method does not mean that the niches are similar through time; it only means that given the data, the niche spaces are neither significantly different nor similar. Therefore, conclusions cannot be drawn. This may be due to low sample sizes in the

LGM or a common product of the method. Non-significant results are common in other studies using this method (Veloz et al. 2012; Saupe et al. 2013).

The nonparametric MANOVA test is sensitive to changes in niche space. Testing for a shift in niche space using an analysis of variance statistical method may lead to conclusions of shifting niche space even though the niche space has remained the same (e.g. *Lynx rufus* Fig. 3.2, Table 3.2). And small sample sizes may lead to Type 2 error. Nogues-Bravo et al. (2008) found Kruskal-Wallis tests comparing species climatic niches in multivariate space was also highly sensitive to changes in niche space. Although the pairwise climatic distance analysis is also highly sensitive to changes in niche space, the shift can be compared to the variation among the time periods as well as to the environmental space through time to tease apart shifting realized niche space versus niche evolution.

An observed shift in the occupied niche space in the deep time fossil record over a long time period (e.g. hundreds of thousand to millions of years) implies a considerable change in climatic space given time averaging. Because a time-averaged niche space likely incorporates several occupied niche spaces or realized niche spaces and therefore begins to approach the fundamental niche space, such observed shifts likely indicate important changes for the species. However, to firmly document that an observed niche (whatever parameters are used to characterize it) is shifting so much so that it is evolving, the environmental space must be known as well as the complete shape and defining parameters of the fundamental niche. In practice this is seldom achievable.

CONCLUSIONS

Studying ecological niche shifts in deep time (e.g. hundreds of thousand to millions of years) can provide insights into evolutionary and ecological processes. Niches are studied in deep time either in univariate space or when adequate spatial environmental data is available, by using species distribution modeling to measure niche overlap in geographic and climatic space. In most deep time study systems there is not enough spatial environmental data to create environmental layers for species distribution modeling; however, there is sufficient data to reconstruct a species niche in multivariate climate space or E space. Given these multivariate niche constructions, niche stability can be examined through time; however, explicitly defining and caution in interpreting what kind of niche is shifting (occupied, realized, fundamental, climatic, etc.) is essential. Without available environmental space data, conclusions about niche stability in multivariate deep time studies are limited to potential or realized niche shifts. Actual niche evolution, or change in the fundamental niche can seldom, if ever, be resolved. Determining whether a species' realized niche is shifting or not is valuable to understanding the extent to which the species may withstand a variety of climatic conditions. Combined, the realized niches as determined at several different time periods, will better predict the species fundamental niche and niche breadth. Lastly, a directional shift of a realized niche through long time periods (millions of years) can indicate potential evolution (Veloz et al., 2012). On a shorter time scale (centuries to millennia), a shift in realized niche space is important for predicting species distributions based on projected climate change. The current realized niche space of the mammalian species studied here is small relative to the realized niche space defined by combining Pleistocene with recent climatic niches, and therefore predictions based only on the current niche space will likely under-predict the species potential range of environmental tolerances. This implies that when using species distribution modeling, it is important to look into the fossil record to reconstruct past realized niches of species and incorporate this data into models.

REFERENCES

Ackerly, D.D., 2003. Community Assembly, Niche Conservatism, and Adaptive Evolution in Changing Environments. Int. J Plant Sci. 164, S165–S184.

Anderson, M.J., 2001. A new method for non-parametric multivariate analysis of variance. Austral Ecology 26, 32–46.

Behrensmeyer, A.K., Kidwell, S.M., Gastaldo, R.A., 2000. Taphonomy and paleobiology. Paleobiology 26, 103–147.

Belyea, L.R., 2007. Revealing the Emperor's new clothes: niche-based palaeoenvironmental reconstruction in the light of recent ecological theory. The Holocene 17, 683–688.

Braconnot, P., Otto-Bliesner, B., Harrison, S., Joussaume, S., Peterchmitt, J.-Y., Abe-Ouchi, A., Crucifix, M., Driesschaert, E., Fichefet, T., Hewitt, C.D., 2007. Results of PMIP2 coupled simulations of the Mid-Holocene and Last Glacial Maximum–Part 1: experiments and large-scale features. Climate of the Past 3, 261–277.

Brame, H., Stigall, A.L., 2013. Controls on niche stability in geologic time: congruent responses to biotic and abiotic environmental changes among Cincinnatian (Late Ordovician) marine invertebrates. Paleobiology 40, 70-90.

Broennimann, O., Fitzpatrick, M.C., Pearman, P.B., Petitpierre, B., Pellissier, L., Yoccoz, N.G., Thuiller, W., Fortin, M.-J., Randin, C., Zimmermann, N.E., Graham, C.H., Guisan, A., 2012. Measuring ecological niche overlap from occurrence and spatial environmental data. Global Ecology and Biogeography 21, 481–497.

Broennimann, O., Treier, U.A., Müller-Schärer, H., Thuiller, W., Peterson, A.T., Guisan, A., 2007. Evidence of climatic niche shift during biological invasion. Ecology Letters 10, 701–709.

Brown, J.H., Stevens, G.C., Kaufman, D.M., 1996. The geographic range: size, shape, boundaries, and internal structure. Annual Review of Ecology and Systemics 27, 597–623.

Cerling, T.E., Harris, J.M., Ambrose, S.H., Leakey, M.G., Solounias, N., 1997. Dietary and environmental reconstruction with stable isotope analyses of herbivore tooth enamel from the Miocene locality of Fort Ternan, Kenya. Journal of Human Evolution 33, 635–650.

Colwell, R.K., Rangel, T.F., 2009. Hutchinson's duality: the once and future niche. Proceedings of the National Academy of Sciences 106, 19651–19658.

Dudei, N.L., Stigall, A.L., 2010. Using ecological niche modeling to assess biogeographic and niche response of brachiopod species to the Richmondian Invasion (Late Ordovician) in the Cincinnati Arch. Palaeogeography, Palaeoclimatology, Palaeoecology 296, 28–43.

FAUNMAP Working Group, 1994. FAUNMAP: A database documenting late Quaternary distributions of mammal species in the United States. Illinois State Museum Scientific Papers 25, 1-690.

Graham, R.W., Lundelius, E.L., Jr., 2010. FAUNMAP II: New data for North America with temporal extension for the Blancan, Irvingtonian and early Rancholabrean. FAUNMAP II Database, version 1.0, http://www.ucmp.berkeley.edu/neomap/

Hijmans, R.J., Cameron, S.E., Parra, J.L., Jones, P.G., Jarvis, A., 2005. Very high resolution interpolated climate surfaces for global land areas. International Journal of Climatology 25, 1965-1978.

Hutchinson, G.E., 1957. Concluding Remarks. Cold Spring Harbor Symposia on Quantitative Biology 22, 415–427.

Hutchinson, G.E., 1978. An Introduction to Population Ecology. Yale University Press, New Haven, CT, 271 pp.

Jackson, S.T., Overpeck, J.T., 2000. Responses of plant populations and communities to environmental changes of the late Quaternary. Paleobiology 26, 194–220.

Koch, P.L., 1998. Isotopic reconstruction of past continental environments. Annual Review of Earth and Planetary Sciences 26, 573–613.

Kozak, K.H., Graham, C.H., Wiens, J.J., 2008. Integrating GIS-based environmental data into evolutionary biology. Trends in Ecology & Evolution 23, 141–148.

Leisch, F., 2006. A Toolbox for K-Centroids Cluster Analysis. Computation Statistics and Data Analysis 51 (2), 526-544.

Levin, D.A., 2005. Niche shifts: The primary driver of novelty within angiosperm genera. Systematic Botany 30, 9–15.

Losos, J.B., Leal, M., Glor, R.E., De Queiroz, K., Hertz, P.E., Rodríguez Schettino, L., Lara, A.C., Jackman, T.R., Larson, A., 2003. Niche lability in the evolution of a Caribbean lizard community. Nature 424, 542–545.

Maguire, K.C., Stigall, A.L., 2009. Using ecological niche modeling for quantitative biogeographic analysis: a case study of Miocene and Pliocene Equinae in the Great Plains. Paleobiology 35, 587–611.

Martínez-Meyer, E., Peterson, A.T., Hargrove, W.W., 2004. Ecological niches as stable distributional constraints on mammal species, with implications for Pleistocene extinctions and climate change projections for biodiversity. Global Ecology and Biogeography 13, 305–314.

McGuire, J.L., Davis, E.B., 2013. Using the palaeontological record of Microtusto test species distribution models and reveal responses to climate change. Journal of Biogeography 40, 1490–1500.

Nogués-Bravo, D., 2009. Predicting the past distribution of species climatic niches. Global Ecology and Biogeography 18, 521–531.

Nogués-Bravo, D., Rodríguez, J., Hortal, J., Batra, P., Araújo, M.B., 2008. Climate change, humans, and extinction of the woolly mammoth. PLoS Biology 6, e79.

Oksanen, J., F.G. Blanchet, R. Kindt, P. Legendre, P.R. Minchin, R.B. O'Hara, G.L. Simpson, P. Solymos, M. Henry, H. Stevens and H. Wagner 2103. vegan: Community Ecology Package. R package version 2.0-9.

Orr, M.R., Smith, T.B., 1998. Ecology and speciation. Trends in Ecology & Evolution 13, 502–506.

Pearman, P.B., Guisan, A., Broennimann, O., Randin, C.F., 2008a. Niche dynamics in space and time. Trends in Ecology & Evolution 23, 149–158.

Pearman, P.B., Randin, C.F., Broennimann, O., Vittoz, P., Knaap, W.O.V.D., Engler, R., Lay, G.L., Zimmermann, N.E., Guisan, A., 2008b. Prediction of plant species distributions across six millennia. Ecol Letters 11, 357–369.

Peterson, A.T., 2011. Ecological niche conservatism: a time-structured review of evidence. Journal of Biogeography 38, 817–827.

Peterson, A.T., Nyári, Á.S., 2007. Ecological niche conservatism and Pleistocene refugia in the Thrush-like Mourner, *Schiffornis sp.*, in the neotropics.. Evolution 62, 173-183.

Peterson, A.T., Soberón, J., Pearson, R.G., Anderson, R.P., Martínez-Meyer, E., Nakamura, M., Araújo, M.B., 2011. Ecological Niches and Geographic Distributions, Princeton University Press, Princeton, NJ, 314 pp.

Polly, P.D., Eronen, J.T., Fred, M., Dietl, G.P., Mosbrugger, V., Scheidegger, C., Frank, D.C., Damuth, J., Stenseth, N.C., Fortelius, M., 2011. History matters: ecometrics and integrative climate change biology. Proceedings of the Royal Society B: Biological Sciences 278, 1131–1140.

R Core Team 2013. R: A language and environment for statistical computing. R Foundation for Statistical Computin, Vienna, Austria. URL http://www.R-project.org/.

Rodríguez-Sánchez, F., Arroyo, J., 2008. Reconstructing the demise of Tethyan plants: climate-driven range dynamics of *Laurus* since the Pliocene. Global Ecology and Biogeography 17, 685–695.

Rödder, D., Lötters, S., 2009. Niche shift versus niche conservatism? Climatic characteristics of the native and invasive ranges of the Mediterranean house gecko (*Hemidactylus turcicus*). Global Ecology and Biogeography 18, 674–687.

Saupe, E.E., Hendricks, J.R., Portell, R.W., Dowsett, J.J., Haywood, A., Hunter, S., Lieberman, B.S., 2013. Macroevolutionary consequences of profound climate change on niche evolution: An examination of marine mollusks over the past 3 million years. Geological Society of America Abstract with Programs 45, 91.

Schoener, T.W., 1970. Nonsynchronous spatial overlap of lizards in patchy habitats. Ecology 51, 408-418.

Sheldon, N.D., Tabor, N.J., 2009. Quantitative paleoenvironmental and paleoclimatic reconstruction using paleosols. Earth Science Reviews 95, 1–52.

Soberón, J., 2007. Grinnellian and Eltonian niches and geographic distributions of species. Ecology Letters 10, 1115–1123.

Stigall, A.L., 2011. Using ecological niche modelling to evaluate niche stability in deep time. Journal of Biogeography 39, 772–781.

Stigall, A.L., 2013. Analysing links between biogeography, niche stability and speciation: the impact of complex feedbacks on macroevolutionary patterns. Palaeontology 56, 1225–1238.

Terry, R.C., 2010. On raptors and rodents: testing the ecological fidelity and spatiotemporal resolution of cave death assemblages. Paleobiology 36, 137–160.

Veloz, S.D., Williams, J.W., Blois, J.L., He, F., Otto-Bliesner, B., Liu, Z., 2012. No-analog climates and shifting realized niches during the late quaternary: implications for 21st-century predictions by species distribution models. Global Change Biology 18, 1698–1713.

Walls, B.J., Stigall, A.L., 2011. Analyzing niche stability and biogeography of Late Ordovician brachiopod species using ecological niche modeling. Palaeogeography, Palaeoclimatology, Palaeoecology 299, 15–29.

Warren, D.L., Glor, R.E., Turelli, M., 2008. Environmental niche equivalency versus conservatism: Quantitative approaches to niche evolution. Evolution 62, 2868–2883.

Warren, D.L., Glor, R.E., Turelli, M., 2010. ENMTools: a toolbox for comparative studies of environmental niche models. Ecography 33, 607-611.

Western, D., Behrensmeyer, A.K., 2009. Bone Assemblages Track Animal Community Structure over 40 Years in an African Savanna Ecosystem. Science 324, 1061–1064.

Wilf, P., 1997. When are leaves good thermometers? A new case for leaf margin analysis. Paleobiology 23, 373–390.

APPENDIX A: CHAPTER 1 SUPPLEMENTARY DATA FILES

1. LA-ICPMS U-Pb geochronologic analyses (NPS Report J8R07110010)

	Corrected isotope ratios										Apparent ages (Ma)			
Analysis	207Pb* / 235U*	±2σ (%)	206Pb* / 238U	±2σ (%)	error corr.	238U / 206Pb*	±2σ (%)	207Pb* / 206Pb*	±2σ (%)	error corr.	207Pb* / 235U	±2σ (Ma)	**206Pb* / 238U***	**±2σ (Ma)**
KCM61023a — Kangaroo Tuff														
KCMJUNE1023a_8 12/2/2011 1:42:35 PM	0.1403	11.9	0.003087	5.9	0.5	324.0	5.9	0.3297	10.3	0.00	133	15	**19.9**	**1.2**
KCMJUNE1023a_9 12/2/2011 1:44:20 PM	0.0434	17.3	0.002242	4.5	0.26	446.1	4.5	0.1405	16.7	0.00	43	7	**14.4**	**0.7**
KCMJUNE1023a_10 12/2/2011 1:46:05 PM	0.0249	9.0	0.002084	4.9	0.54	479.9	4.9	0.0867	7.6	0.00	25	2	**13.4**	**0.7**
KCMJUNE1023a_12 12/2/2011 1:49:37 PM	0.0109	17.0	0.002059	5.1	0.3	485.6	5.1	0.0384	16.2	0.00	11	2	**13.3**	**0.7**
KCMJUNE1023a_4 12/2/2011 1:35:30 PM	0.0126	19.9	0.002054	7.5	0.38	486.8	7.5	0.0443	18.4	0.00	13	3	**13.2**	**1.0**
KCMJUNE1023a_7 12/2/2011 1:40:48 PM	0.0134	48.3	0.002025	4.6	0.1	493.7	4.6	0.0479	48.0	0.00	13	6	**13.0**	**0.6**
KCMJUNE1023a_11 12/2/2011 1:47:51 PM	0.0134	12.3	0.00195	4.9	0.4	512.8	4.9	0.0497	11.2	0.00	13	2	**12.6**	**0.6**
KCMJUNE1023a_6 12/2/2011 1:39:03 PM	0.0107	41.7	0.001924	4.1	0.1	519.7	4.1	0.0402	41.5	0.00	11	4	**12.4**	**0.5**
KCMJUNE1023a_5 12/2/2011 1:37:16 PM	0.0100	24.6	0.001849	4.1	0.17	540.8	4.1	0.0392	24.2	0.00	10	2	**11.9**	**0.5**
KCM71040 — Koala Tuff														
ECM11S_175B 9/13/2011 3:28:56 PM	3.4535	11.1	0.033354	8.6	0.78	30.0	8.6	0.7509	7.0	0.00	1517	87	**211.5**	**17.9**
ECM11S_179B 9/13/2011 3:35:58 PM	1.2854	25.9	0.017773	10.0	0.38	56.3	10.0	0.5245	23.9	0.00	839	148	**113.6**	**11.2**
ECM11S_182 9/13/2011 3:45:02 PM	0.8079	17.7	0.013445	11.5	0.65	74.4	11.5	0.4358	13.5	0.00	601	80	**86.1**	**9.8**
ECM11S_171 9/13/2011 3:21:55 PM	0.8190	9.1	0.012001	5.6	0.62	83.3	5.6	0.4950	7.2	0.00	608	42	**76.9**	**4.3**
ECM11S_173 9/13/2011 3:25:25 PM	0.1396	27.7	0.006589	11.8	0.43	151.8	11.8	0.1536	25.1	0.00	133	34	**42.3**	**5.0**
ECM11S_189 9/13/2011 3:57:21 PM	0.0341	19.6	0.006384	5.6	0.28	156.6	5.6	0.0387	18.8	0.00	34	7	**41.0**	**2.3**
ECM11S_187 9/13/2011 3:53:50 PM	0.1005	85.6	0.006347	8.8	0.1	157.6	8.8	0.1148	85.1	0.00	97	79	**40.8**	**3.6**
ECM11S_184 9/13/2011 3:48:33 PM	0.1610	14.6	0.005639	5.9	0.41	177.3	5.9	0.2070	13.3	0.00	152	21	**36.2**	**2.1**
ECM11S_179A 9/13/2011 3:35:58 PM	0.0363	101.4	0.005617	18.7	0.18	178.0	18.7	0.0469	99.7	0.00	36	36	**36.1**	**6.7**
ECM11S_174 9/13/2011 3:27:11 PM	0.0386	23.5	0.004865	7.5	0.32	205.5	7.5	0.0576	22.3	0.00	38	9	**31.3**	**2.3**
ECM11S_181 9/13/2011 3:43:16 PM	0.0326	9.9	0.00481	3.7	0.37	207.9	3.7	0.0491	9.2	0.00	33	3	**30.9**	**1.1**
ECM11S_176 9/13/2011 3:30:42 PM	0.0199	56.6	0.004447	6.9	0.12	224.9	6.9	0.0325	56.2	0.00	20	11	**28.6**	**2.0**
ECM11S_188 9/13/2011 3:55:36 PM	0.0220	64.1	0.00443	10.8	0.17	225.7	10.8	0.0360	63.2	0.00	22	14	**28.5**	**3.1**
ECM11S_180 9/13/2011 3:37:44 PM	0.0143	40.7	0.004326	9.6	0.24	231.2	9.6	0.0240	39.5	0.00	14	6	**27.8**	**2.7**
ECM11S_177 9/13/2011 3:32:27 PM	0.4606	720.2	0.002541	10.9	0.02	393.6	10.9	1.3147	720.1	0.00	385	2306	**16.4**	**1.8**
ECM11S_175A 9/13/2011 3:28:56 PM	0.0190	65.8	0.002234	13.4	0.2	447.5	13.4	0.0617	64.4	0.00	19	12	**14.4**	**1.9**
ECM11S_183 9/13/2011 3:46:48 PM	0.0150	18.5	0.002063	5.2	0.28	484.7	5.2	0.0528	17.7	0.00	15	3	**13.3**	**0.7**
KCM081182 — Mascall Tuff														
KCM081182_1 10/18/2012 12:34:34 PM	0.6907	78.8	0.042183	61.7	0.78	23.7	61.7	0.1188	48.9	0.00	533	327	**266.3**	**161.1**
KCM081182_11 10/18/2012 12:58:27 PM	0.1195	101.9	0.029836	8.9	0.09	33.5	8.9	0.0291	101.5	0.00	115	111	**189.5**	**16.6**
KCM081182_28 10/18/2012 1:34:08 PM	-0.4693	112.3	0.029209	31.6	0.28	34.2	31.6	-0.1165	107.7	0.00	-643	-1008	**185.6**	**57.9**
KCM081182_10 10/18/2012 12:49:42 PM	0.0571	162.3	0.028988	16.7	0.1	34.5	16.7	0.0143	161.5	0.00	56	89	**184.2**	**30.3**
KCM081182_21 10/18/2012 1:22:21 PM	0.1534	88.4	0.024418	24.5	0.28	41.0	24.5	0.0456	84.9	0.00	145	119	**155.5**	**37.6**
KCM081182_3 10/18/2012 12:37:56 PM	0.1627	29.8	0.021636	16.7	0.56	46.2	16.7	0.0545	24.7	0.00	153	42	**138.0**	**22.8**
KCM081182_6 10/18/2012 12:42:59 PM	0.6365	70.3	0.0213	45.7	0.65	46.9	45.7	0.2167	53.4	0.00	500	278	**135.9**	**61.5**
KCM081182_2 10/18/2012 12:36:15 PM	0.2716	25.0	0.021257	14.0	0.56	47.0	14.0	0.0927	20.8	0.00	244	54	**135.6**	**18.7**
KCM081182_23 10/18/2012 1:25:43 PM	0.0337	95.3	0.021104	18.9	0.2	47.4	18.9	0.0116	93.4	0.00	34	32	**134.6**	**25.1**
KCM081182_7 10/18/2012 12:44:39 PM	-0.2886	403.9	0.020071	15.6	0.04	49.8	15.6	-0.1043	403.6	0.00	-346	-1664	**128.1**	**19.8**
KCM081182_14 10/18/2012 1:03:30 PM	0.0397	9.9	0.005534	8.3	0.84	180.7	8.3	0.0520	5.3	0.00	40	4	**35.6**	**3.0**
KCM081182_15 10/18/2012 1:05:10 PM	0.0356	10.6	0.005354	7.6	0.71	186.8	7.6	0.0482	7.4	0.00	35	4	**34.4**	**2.6**

KCM081182_25	10/18/2012 1:29:05 PM	0.0337	28.1	0.005255	8.5	0.3	190.3	8.5	0.0465	26.8	0.00	34	9	**33.8**	**2.9**
KCM081182_29	10/18/2012 1:35:49 PM	0.0344	34.4	0.004952	9.6	0.28	201.9	9.6	0.0504	33.1	0.00	34	12	**31.8**	**3.0**
KCM081182_4	10/18/2012 12:39:37 PM	0.0187	31.6	0.004393	11.5	0.36	227.7	11.5	0.0308	29.4	0.00	19	6	**28.3**	**3.2**
JB12L1_21	4/12/2012 2:02:27 PM	0.0436	15.6	0.004225	5.5	0.35	236.7	5.5	0.0749	14.7	0.00	43	7	**27.2**	**1.5**
JB12L1_22	4/12/2012 2:03:57 PM	0.0256	6.9	0.004064	4.1	0.59	246.1	4.1	0.0457	5.6	0.00	26	2	**26.1**	**1.1**
JB12L1_30	4/12/2012 2:19:17 PM	0.0257	7.4	0.003958	4.4	0.59	252.6	4.4	0.0470	6.0	0.00	26	2	**25.5**	**1.1**
KCM081182_27	10/18/2012 1:32:27 PM	0.0263	17.8	0.003738	9.5	0.54	267.5	9.5	0.0511	15.0	0.00	26	5	**24.1**	**2.3**
KCM081182_24	10/18/2012 1:27:24 PM	0.0956	84.5	0.003298	25.4	0.3	303.3	25.4	0.2103	80.6	0.00	93	75	**21.2**	**5.4**
KCM081182_26	10/18/2012 1:30:46 PM	0.0326	32.3	0.002954	9.2	0.28	338.6	9.2	0.0800	31.0	0.00	33	10	**19.0**	**1.7**
KCM081182_17	10/18/2012 1:08:32 PM	0.0037	55.4	0.002768	13.9	0.25	361.3	13.9	0.0096	53.6	0.00	4	2	**17.8**	**2.5**
JB12L1_27	4/12/2012 2:14:45 PM	0.0278	25.5	0.002676	7.4	0.29	373.6	7.4	0.0753	24.4	0.00	28	7	**17.2**	**1.3**
KCM081182_16	10/18/2012 1:06:51 PM	0.0193	33.8	0.002659	11.9	0.35	376.1	11.9	0.0525	31.7	0.00	19	6	**17.1**	**2.0**
KCM081182_12	10/18/2012 1:00:08 PM	-0.0937	411.6	0.002599	14.8	0.04	384.8	14.8	-0.2614	411.3	0.00	-100	-432	**16.7**	**2.5**
KCM081182_8	10/18/2012 12:46:20 PM	0.0136	32.7	0.002587	10.2	0.31	386.6	10.2	0.0381	31.0	0.00	14	4	**16.7**	**1.7**
KCM081182_5	10/18/2012 12:41:18 PM	0.0032	77.4	0.002554	9.5	0.12	391.5	9.5	0.0090	76.9	0.00	3	2	**16.4**	**1.6**
KCM081182_20	10/18/2012 1:13:35 PM	0.0091	51.8	0.00255	9.5	0.18	392.2	9.5	0.0258	51.0	0.00	9	5	**16.4**	**1.6**
JB12L1_25	4/12/2012 2:11:44 PM	0.0194	9.1	0.002408	3.7	0.41	415.3	3.7	0.0586	8.3	0.00	20	2	**15.5**	**0.6**
JB12L1_23	4/12/2012 2:05:27 PM	0.0250	15.5	0.002386	4.9	0.32	419.1	4.9	0.0760	14.7	0.00	25	4	**15.4**	**0.8**
KCM081182_13	10/18/2012 1:01:49 PM	0.0195	98.8	0.002378	14.4	0.15	420.5	14.4	0.0595	97.7	0.00	20	19	**15.3**	**2.2**
JB12L1_26	4/12/2012 2:13:15 PM	0.0161	8.8	0.002373	3.6	0.41	421.5	3.6	0.0493	8.1	0.00	16	1	**15.3**	**0.5**
KCM081182_22	10/18/2012 1:24:02 PM	0.0136	35.5	0.002343	8.5	0.24	426.8	8.5	0.0422	34.4	0.00	14	5	**15.1**	**1.3**
KCM081182_19	10/18/2012 1:11:54 PM	0.0173	26.3	0.00232	10.3	0.39	430.9	10.3	0.0542	24.2	0.00	17	5	**14.9**	**1.5**
JB12L1_29	4/12/2012 2:17:46 PM	0.0189	28.2	0.002302	5.3	0.19	434.5	5.3	0.0596	27.7	0.00	19	5	**14.8**	**0.8**
JB12L1_24	4/12/2012 2:06:58 PM	0.0149	17.0	0.002281	3.2	0.19	438.5	3.2	0.0475	16.7	0.00	15	3	**14.7**	**0.5**
JB12L1_28	4/12/2012 2:16:15 PM	-0.0033	143.0	0.00225	9.1	0.06	444.4	9.1	-0.0108	142.7	0.00	-3	-5	**14.5**	**1.3**
KCM081182_9	10/18/2012 12:48:01 PM	0.0147	21.3	0.002186	6.7	0.32	457.4	6.7	0.0487	20.2	0.00	15	3	**14.1**	**0.9**

Secondary Standards

AUSZ2 86	12/18/2012 4:43:09 PM	0.0402	21.4	0.006057	5.3	0.25	165.1	5.3	0.0481	20.7	0.00	40	8	**38.9**	**2.1**
AUSZ2 87	12/18/2012 4:44:49 PM	0.0349	17.7	0.006167	5.5	0.31	162.2	5.5	0.0410	16.9	0.00	35	6	**39.6**	**2.2**
AUSZ2 88	12/18/2012 5:27:10 PM	0.0337	19.2	0.006078	6.0	0.31	164.5	6.0	0.0402	18.3	0.00	34	6	**39.1**	**2.3**
AUSZ2 89	12/18/2012 5:28:51 PM	0.0373	14.7	0.006043	4.5	0.31	165.5	4.5	0.0448	14.0	0.00	37	5	**38.8**	**1.8**
AUSZ2 90	12/18/2012 6:11:12 PM	0.0318	21.8	0.006081	4.4	0.2	164.4	4.4	0.0380	21.4	0.00	32	7	**39.1**	**1.7**
AUSZ2 91	12/18/2012 6:12:52 PM	0.0406	16.5	0.006106	4.9	0.29	163.8	4.9	0.0483	15.8	0.00	40	7	**39.2**	**1.9**
AUSZ2 92	12/18/2012 6:57:07 PM	0.0285	21.2	0.006052	4.4	0.2	165.2	4.4	0.0341	20.8	0.00	29	6	**38.9**	**1.7**
AUSZ2 93	12/18/2012 6:58:48 PM	0.0336	38.8	0.005968	2.6	0.07	167.6	2.6	0.0409	38.7	0.00	34	13	**38.4**	**1.0**
AusZ2_37	4/12/2012 5:51:49 PM	0.0448	15.8	0.006008	4.2	0.26	166.5	4.2	0.0541	15.2	0.00	45	7	**38.6**	**1.6**
AusZ2_38	4/12/2012 5:53:08 PM	0.0400	10.7	0.006104	3.8	0.35	163.8	3.8	0.0475	10.1	0.00	40	4	**39.2**	**1.5**
AusZ2_39	4/12/2012 6:10:28 PM	0.0464	11.5	0.006045	3.8	0.33	165.4	3.8	0.0557	10.8	0.00	46	5	**38.8**	**1.5**
AusZ2_40	4/12/2012 6:11:47 PM	0.0428	11.8	0.006045	4.0	0.34	165.4	4.0	0.0514	11.1	0.00	43	5	**38.9**	**1.6**
AusZ2_41	4/12/2012 6:29:14 PM	0.0453	10.0	0.005791	4.0	0.4	172.7	4.0	0.0568	9.2	0.00	45	4	**37.2**	**1.5**
AusZ2_42	4/12/2012 6:30:33 PM	0.0418	12.0	0.005999	4.8	0.4	166.7	4.8	0.0505	10.9	0.00	42	5	**38.6**	**1.9**
AusZ2_46	10/18/2012 12:31:05 PM	0.0467	25.3	0.006058	6.4	0.25	165.1	6.4	0.0560	24.5	0.00	46	11	**38.9**	**2.5**
AusZ2_47	10/18/2012 12:32:46 PM	0.0514	20.1	0.006177	8.0	0.4	161.9	8.0	0.0603	18.5	0.00	51	10	**39.7**	**3.2**
AusZ2_48	10/18/2012 12:53:14 PM	0.0370	20.9	0.006403	7.4	0.35	156.2	7.4	0.0419	19.5	0.00	37	8	**41.1**	**3.0**
AusZ2_49	10/18/2012 12:54:55 PM	0.0310	28.5	0.005995	7.4	0.26	166.8	7.4	0.0375	27.5	0.00	31	9	**38.5**	**2.8**

AusZ2_50	10/18/2012 1:17:08 PM	0.0433	17.0	0.005657	8.8	0.52	176.8	8.8	0.0555	14.5	0.00	43	7	**36.4**	**3.2**
AusZ2_51	10/18/2012 1:18:48 PM	0.0344	29.2	0.005894	8.1	0.28	169.7	8.1	0.0423	28.1	0.00	34	10	**37.9**	**3.0**
AusZ2_52	10/18/2012 1:37:38 PM	0.0285	30.5	0.006044	8.6	0.28	165.5	8.6	0.0342	29.3	0.00	28	9	**38.8**	**3.3**
AusZ2_53	10/18/2012 1:39:19 PM	0.0382	23.1	0.006255	6.8	0.29	159.9	6.8	0.0443	22.1	0.00	38	9	**40.2**	**2.7**
R33_214	9/13/2011 12:42:01 PM	0.4995	9.9	0.067033	3.1	0.32	14.9	3.1	0.0540	9.4	0.00	411	33	**418**	**13**
R33_215	9/13/2011 12:43:47 PM	0.4770	10.2	0.066892	3.6	0.35	14.9	3.6	0.0517	9.5	0.00	396	33	**417**	**14**
R33_216	9/13/2011 1:49:31 PM	0.5155	10.5	0.067042	3.8	0.36	14.9	3.8	0.0558	9.8	0.00	422	36	**418**	**15**
R33_217	9/13/2011 1:51:16 PM	0.4693	11.6	0.066077	4.6	0.4	15.1	4.6	0.0515	10.6	0.00	391	38	**412**	**18**
R33_218	9/13/2011 2:56:59 PM	0.4786	11.9	0.06761	3.6	0.3	14.8	3.6	0.0513	11.3	0.00	397	39	**422**	**15**
R33_219	9/13/2011 2:58:44 PM	0.4980	12.4	0.070232	2.9	0.23	14.2	2.9	0.0514	12.1	0.00	410	42	**438**	**12**
R33_220	9/13/2011 4:06:16 PM	0.5838	10.5	0.06854	3.9	0.37	14.6	3.9	0.0618	9.8	0.00	467	39	**427**	**16**
R33_221	9/13/2011 4:08:02 PM	0.5023	11.6	0.066992	4.5	0.38	14.9	4.5	0.0544	10.8	0.00	413	40	**418**	**18**
FC1_54	4/12/2012 1:31:55 PM	1.9306	4.0	0.183039	3.5	0.89	5.5	3.5	0.0765	1.8	0.00	1092	27	**1084**	**35**
FC1_55	4/12/2012 1:33:25 PM	1.9020	2.5	0.18277	1.8	0.72	5.5	1.8	0.0755	1.7	0.00	1082	16	**1082**	**18**
FC1_56	4/12/2012 2:20:54 PM	1.9809	3.1	0.187803	2.7	0.87	5.3	2.7	0.0765	1.5	0.00	1109	21	**1109**	**27**
FC1_57	4/12/2012 2:22:24 PM	1.9085	2.8	0.183862	2.5	0.89	5.4	2.5	0.0753	1.3	0.00	1084	19	**1088**	**25**
Orapa_222	9/13/2011 12:29:43 PM	8.2717	1198.8	0.019146	12.6	0.01	52.2	12.6	3.1335	1198.7	0.00	2261	10859	**122**	**15**
Orapa_223	9/13/2011 12:31:29 PM	-9.2897	918.3	0.013793	19.6	0.02	72.5	19.6	-4.8846	918.1	0.00	#NUM!	10449	**88**	**17**
Orapa_224	9/13/2011 12:33:14 PM	-3.7677	521.4	0.017325	24.8	0.05	57.7	24.8	-1.5773	520.8	0.00	#NUM!	7207	**111**	**27**
Orapa_225	9/13/2011 4:09:48 PM	0.7925	88.6	0.017956	23.8	0.27	55.7	23.8	0.3201	85.3	0.00	593	398	**115**	**27**
Orapa_226	9/13/2011 4:11:34 PM	-1.1269	155.4	0.012544	17.1	0.11	79.7	17.1	-0.6516	154.5	0.00	#NUM!	14009	**80**	**14**
Orapa_227	9/13/2011 4:13:19 PM	0.3820	66.2	0.015646	14.1	0.21	63.9	14.1	0.1771	64.6	0.00	329	186	**100**	**14**
Orapa 82	12/18/2012 4:29:43 PM	0.4671	102.4	0.016243	12.7	0.12	61.6	12.7	0.2086	101.6	0.00	389	331	**104**	**13**
Orapa 83	12/18/2012 4:31:23 PM	1.1512	241.9	0.013069	17.0	0.07	76.5	17.0	0.6388	241.3	0.00	778	1314	**84**	**14**
Orapa 84	12/18/2012 4:33:03 PM	0.3282	94.9	0.012913	13.1	0.14	77.4	13.1	0.1843	94.0	0.00	288	238	**83**	**11**
Orapa 85	12/18/2012 4:34:44 PM	-408.8573	####	0.0128	13.3	0	78.1	13.3	-231.6627	####	0.00	#NUM!	####	**82**	**11**
Orapa_33	10/18/2012 12:20:57 PM	0.4210	47.8	0.018397	16.4	0.34	54.4	16.4	0.1660	44.9	0.00	357	144	**118**	**19**
Orapa_34	10/18/2012 12:22:38 PM	0.0962	60.9	0.015021	19.6	0.32	66.6	19.6	0.0464	57.6	0.00	93	54	**96**	**19**
Orapa_35	10/18/2012 12:24:19 PM	-0.0881	64.3	0.014657	16.3	0.25	68.2	16.3	-0.0436	62.2	0.00	-94	-63	**94**	**15**
Primary Standards															
PL_190	9/13/2011 12:35:00 PM	0.4045	5.4	0.053365	3.5	0.66	18.7	3.5	0.0550	4.1	0.00	345	16	**335**	**12**
PL_191	9/13/2011 12:36:45 PM	0.4074	5.4	0.054577	4.1	0.76	18.3	4.1	0.0541	3.5	0.00	347	16	**343**	**14**
PL_192	9/13/2011 12:38:30 PM	0.3924	6.1	0.054887	4.1	0.67	18.2	4.1	0.0519	4.5	0.00	336	17	**344**	**14**
PL_193	9/13/2011 12:40:16 PM	0.3754	6.4	0.052079	4.3	0.67	19.2	4.3	0.0523	4.8	0.00	324	18	**327**	**14**
PL_194	9/13/2011 1:03:19 PM	0.3849	6.0	0.053763	3.8	0.63	18.6	3.8	0.0519	4.6	0.00	331	17	**338**	**12**
PL_195	9/13/2011 1:05:04 PM	0.3951	5.7	0.053848	4.1	0.73	18.6	4.1	0.0532	3.9	0.00	338	16	**338**	**14**
PL_196	9/13/2011 1:24:39 PM	0.3915	6.5	0.053132	4.7	0.72	18.8	4.7	0.0534	4.5	0.00	335	19	**334**	**15**
PL_197	9/13/2011 1:26:24 PM	0.3885	6.7	0.053225	4.5	0.68	18.8	4.5	0.0529	4.9	0.00	333	19	**334**	**15**
PL_198	9/13/2011 1:45:59 PM	0.4037	7.0	0.053991	5.1	0.72	18.5	5.1	0.0542	4.8	0.00	344	20	**339**	**17**
PL_199	9/13/2011 1:47:45 PM	0.3960	5.9	0.053317	3.8	0.65	18.8	3.8	0.0539	4.4	0.00	339	17	**335**	**13**
PL_200	9/13/2011 2:10:49 PM	0.3915	4.9	0.054439	3.6	0.73	18.4	3.6	0.0522	3.3	0.00	335	14	**342**	**12**
PL_201	9/13/2011 2:12:35 PM	0.3952	5.5	0.052827	3.6	0.65	18.9	3.6	0.0543	4.2	0.00	338	16	**332**	**12**
PL_202	9/13/2011 2:32:09 PM	0.4096	7.1	0.055716	5.3	0.75	17.9	5.3	0.0533	4.7	0.00	349	21	**350**	**18**
PL_203	9/13/2011 2:33:54 PM	0.3871	5.2	0.053141	3.6	0.7	18.8	3.6	0.0528	3.7	0.00	332	15	**334**	**12**
PL_204	9/13/2011 2:53:27 PM	0.3950	4.9	0.052669	3.0	0.62	19.0	3.0	0.0544	3.8	0.00	338	14	**331**	**10**
PL_205	9/13/2011 2:55:13 PM	0.3835	5.8	0.052601	3.4	0.59	19.0	3.4	0.0529	4.7	0.00	330	16	**330**	**11**

PL_206	9/13/2011 3:18:16 PM	0.3873	5.4	0.054999	3.9	0.73	18.2	3.9	0.0511	3.6	0.00	332	15	**345**	**13**
PL_207	9/13/2011 3:20:02 PM	0.4040	6.1	0.054197	3.8	0.63	18.5	3.8	0.0541	4.7	0.00	345	18	**340**	**13**
PL_208	9/13/2011 3:39:38 PM	0.4031	6.4	0.054167	3.5	0.56	18.5	3.5	0.0540	5.3	0.00	344	19	**340**	**12**
PL_209	9/13/2011 3:41:23 PM	0.3809	5.2	0.052875	3.7	0.71	18.9	3.7	0.0523	3.6	0.00	328	15	**332**	**12**
PL_210	9/13/2011 3:59:14 PM	0.3943	5.3	0.053301	3.1	0.58	18.8	3.1	0.0536	4.3	0.00	337	15	**335**	**10**
PL_211	9/13/2011 4:00:59 PM	0.3891	5.2	0.053111	4.0	0.78	18.8	4.0	0.0531	3.3	0.00	334	15	**334**	**13**
PL_212	9/13/2011 4:02:45 PM	0.3953	5.5	0.053972	4.0	0.73	18.5	4.0	0.0531	3.8	0.00	338	16	**339**	**13**
PL_213	9/13/2011 4:04:30 PM	0.3987	5.7	0.053838	3.7	0.64	18.6	3.7	0.0537	4.4	0.00	341	16	**338**	**12**
PL 62	12/18/2012 4:36:25 PM	0.3892	5.5	0.053304	3.9	0.71	18.8	3.9	0.0530	3.9	0.00	334	16	**335**	**13**
PL 63	12/18/2012 4:38:06 PM	0.3922	5.2	0.05369	2.7	0.52	18.6	2.7	0.0530	4.4	0.00	336	15	**337**	**9**
PL 64	12/18/2012 4:39:46 PM	0.4011	5.0	0.054184	3.1	0.62	18.5	3.1	0.0537	3.9	0.00	342	14	**340**	**10**
PL 65	12/18/2012 4:41:27 PM	0.3875	4.4	0.053548	3.5	0.79	18.7	3.5	0.0525	2.7	0.00	333	12	**336**	**11**
PL 66	12/18/2012 5:03:27 PM	0.3986	4.4	0.053338	3.0	0.68	18.7	3.0	0.0542	3.2	0.00	341	13	**335**	**10**
PL 67	12/18/2012 5:05:08 PM	0.4018	4.6	0.053937	3.2	0.69	18.5	3.2	0.0540	3.3	0.00	343	13	**339**	**10**
PL 68	12/18/2012 5:23:48 PM	0.3883	4.4	0.053831	2.6	0.6	18.6	2.6	0.0523	3.5	0.00	333	13	**338**	**9**
PL 69	12/18/2012 5:25:28 PM	0.4013	5.3	0.052951	3.3	0.63	18.9	3.3	0.0550	4.1	0.00	343	15	**333**	**11**
PL 70	12/18/2012 5:47:29 PM	0.3862	5.4	0.053758	3.7	0.69	18.6	3.7	0.0521	3.9	0.00	332	15	**338**	**12**
PL 71	12/18/2012 5:49:10 PM	0.3877	5.5	0.054708	3.2	0.58	18.3	3.2	0.0514	4.5	0.00	333	16	**343**	**11**
PL 72	12/18/2012 6:07:49 PM	0.3844	4.3	0.052991	3.3	0.77	18.9	3.3	0.0526	2.8	0.00	330	12	**333**	**11**
PL 73	12/18/2012 6:09:30 PM	0.3945	3.8	0.053493	2.5	0.66	18.7	2.5	0.0535	2.8	0.00	338	11	**336**	**8**
PL 74	12/18/2012 6:31:38 PM	0.4093	3.9	0.053347	2.8	0.72	18.7	2.8	0.0557	2.7	0.00	348	11	**335**	**9**
PL 75	12/18/2012 6:33:19 PM	0.3953	4.1	0.054202	2.3	0.57	18.4	2.3	0.0529	3.4	0.00	338	12	**340**	**8**
PL 80	12/18/2012 6:53:44 PM	0.3947	4.6	0.053309	2.9	0.64	18.8	2.9	0.0537	3.5	0.00	338	13	**335**	**10**
PL 81	12/18/2012 6:55:25 PM	0.3889	4.1	0.053952	2.4	0.6	18.5	2.4	0.0523	3.2	0.00	334	12	**339**	**8**
PL_36	10/18/2012 12:26:01 PM	0.3995	7.9	0.053522	5.9	0.75	18.7	5.9	0.0541	5.2	0.00	341	23	**336**	**19**
PL_37	10/18/2012 12:27:42 PM	0.3869	8.0	0.054156	5.8	0.73	18.5	5.8	0.0518	5.5	0.00	332	23	**340**	**19**
PL_38	10/18/2012 12:29:22 PM	0.3960	7.4	0.053565	6.1	0.83	18.7	6.1	0.0536	4.2	0.00	339	21	**336**	**20**
PL_39	10/18/2012 12:51:32 PM	0.4007	7.6	0.053554	6.1	0.8	18.7	6.1	0.0543	4.5	0.00	342	22	**336**	**20**
PL_40	10/18/2012 12:56:37 PM	0.3792	7.0	0.052567	5.7	0.82	19.0	5.7	0.0523	4.0	0.00	326	19	**330**	**18**
PL_41	10/18/2012 1:15:25 PM	0.3989	7.9	0.05478	6.3	0.81	18.3	6.3	0.0528	4.7	0.00	341	23	**344**	**21**
PL_42	10/18/2012 1:20:31 PM	0.3991	8.0	0.053956	6.7	0.84	18.5	6.7	0.0536	4.3	0.00	341	23	**339**	**22**
PL_43	10/18/2012 1:41:01 PM	0.3933	6.9	0.05324	4.9	0.71	18.8	4.9	0.0536	4.9	0.00	337	20	**334**	**16**
PL_44	10/18/2012 1:42:42 PM	0.3872	6.9	0.052547	4.8	0.7	19.0	4.8	0.0534	4.9	0.00	332	20	**330**	**16**
PL_45	10/18/2012 1:44:22 PM	0.3982	7.0	0.054765	5.7	0.82	18.3	5.7	0.0527	4.0	0.00	340	20	**344**	**19**
PL_27	4/12/2012 5:47:50 PM	0.3981	4.4	0.053622	3.3	0.76	18.6	3.3	0.0538	2.8	0.00	340	13	**336.7**	**10.9**
PL_28	4/12/2012 5:49:09 PM	0.3850	3.9	0.052946	3.1	0.78	18.9	3.1	0.0527	2.5	0.00	331	11	**332.6**	**10.0**
PL_29	4/12/2012 5:50:28 PM	0.3978	4.2	0.054589	3.2	0.76	18.3	3.2	0.0528	2.7	0.00	340	12	**342.6**	**10.5**
PL_30	4/12/2012 6:07:48 PM	0.3942	3.5	0.053343	2.7	0.77	18.7	2.7	0.0536	2.2	0.00	337	10	**335.0**	**8.9**
PL_31	4/12/2012 6:09:07 PM	0.4040	4.1	0.053224	3.4	0.83	18.8	3.4	0.0550	2.3	0.00	345	12	**334.3**	**11.2**
PL_32	4/12/2012 6:13:08 PM	0.3899	4.0	0.053955	2.8	0.71	18.5	2.8	0.0524	2.8	0.00	334	11	**338.8**	**9.3**
PL_33	4/12/2012 6:14:27 PM	0.3838	4.3	0.053989	2.8	0.65	18.5	2.8	0.0516	3.2	0.00	330	12	**339.0**	**9.1**
PL_34	4/12/2012 6:25:15 PM	0.4004	4.0	0.053631	2.8	0.71	18.6	2.8	0.0541	2.8	0.00	342	12	**336.8**	**9.3**
PL_35	4/12/2012 6:26:34 PM	0.3980	3.6	0.054041	3.0	0.83	18.5	3.0	0.0534	2.0	0.00	340	10	**339.3**	**9.9**
PL_36	4/12/2012 6:27:53 PM	0.3873	4.2	0.053251	3.1	0.74	18.8	3.1	0.0528	2.8	0.00	332	12	**334.4**	**10.1**
PL_38	4/12/2012 1:27:23 PM	0.3995	3.4	0.054188	2.9	0.84	18.5	2.9	0.0535	1.8	0.00	341	10	**340.2**	**9.5**
PL_39	4/12/2012 1:28:53 PM	0.3936	2.6	0.054283	2.2	0.88	18.4	2.2	0.0526	1.2	0.00	337	7	**340.8**	**7.5**
PL_40	4/12/2012 1:30:23 PM	0.3884	3.4	0.052547	2.9	0.87	19.0	2.9	0.0536	1.7	0.00	333	10	**330.1**	**9.5**

PL_41	4/12/2012 1:50:13 PM	0.3957	3.7	0.053642	3.1	0.85	18.6	3.1	0.0535	1.9	0.00	338	11	**336.8**	**10.2**
PL_42	4/12/2012 1:51:43 PM	0.3894	2.7	0.053172	2.2	0.83	18.8	2.2	0.0531	1.5	0.00	334	8	**334.0**	**7.2**
PL_43	4/12/2012 2:08:36 PM	0.4023	3.0	0.054611	2.5	0.82	18.3	2.5	0.0534	1.7	0.00	343	9	**342.8**	**8.2**
PL_44	4/12/2012 2:10:06 PM	0.3910	3.9	0.053488	3.1	0.79	18.7	3.1	0.0530	2.4	0.00	335	11	**335.9**	**10.1**
PL_45	4/12/2012 2:23:55 PM	0.3876	3.4	0.05346	2.9	0.85	18.7	2.9	0.0526	1.8	0.00	333	10	**335.7**	**9.5**
PL_46	4/12/2012 2:25:25 PM	0.3956	3.1	0.053738	2.5	0.82	18.6	2.5	0.0534	1.8	0.00	338	9	**337.4**	**8.4**
PL_47	4/12/2012 2:26:55 PM	0.3958	3.2	0.053479	2.6	0.81	18.7	2.6	0.0537	1.9	0.00	339	9	**335.8**	**8.6**

2. ID-TIMS U-Th-Pb isotopic data (NPS Report J8R07110010)

	Compositional Parameters						Radiogenic Isotope Ratios								
Sample	$\frac{Th}{U}$	^{206}Pb* x10^{-13} mol	mol % ^{206}Pb*	$\frac{Pb^*}{Pb_c}$	Pb$_c$ (pg)	$\frac{^{206}Pb}{^{204}Pb}$	$\frac{^{208}Pb}{^{206}Pb}$	$\frac{^{207}Pb}{^{206}Pb}$	% err	$\frac{^{207}Pb}{^{235}U}$	% err	$\frac{^{206}Pb}{^{238}U}$	% err	corr. coef.
(a)	(b)	(c)	(c)	(c)	(c)	(d)	(e)	(e)	(f)	(e)	(f)	(e)	(f)	
KCM61023a — Kangaroo Tuff														
z1	**0.597**	**0.1153**	**97.20%**	**10.8**	**0.27**	**655**	**0.196**	**0.047092**	**1.501**	**0.013669**	**1.600**	**0.002105**	**0.115**	**0.871**
z2	**0.785**	**0.0291**	**85.52%**	**2.0**	**0.41**	**127**	**0.271**	**0.049456**	**9.615**	**0.014452**	**10.090**	**0.002119**	**0.559**	**0.858**
z3	**0.743**	**0.0497**	**93.19%**	**4.5**	**0.30**	**269**	**0.256**	**0.049345**	**3.810**	**0.014346**	**4.042**	**0.002109**	**0.254**	**0.920**
z4	**0.667**	**0.0263**	**81.94%**	**1.5**	**0.48**	**102**	**0.235**	**0.050558**	**13.499**	**0.014716**	**14.074**	**0.002111**	**0.735**	**0.794**
z5	**0.753**	**0.0637**	**94.77%**	**5.9**	**0.29**	**351**	**0.253**	**0.048175**	**2.877**	**0.014023**	**3.056**	**0.002111**	**0.196**	**0.919**
z6	**0.691**	**0.0356**	**90.66%**	**3.1**	**0.30**	**196**	**0.244**	**0.050762**	**5.539**	**0.014792**	**5.849**	**0.002113**	**0.355**	**0.881**
z7	**0.585**	**0.2190**	**97.75%**	**13.4**	**0.42**	**814**	**0.191**	**0.046820**	**1.216**	**0.013584**	**1.298**	**0.002104**	**0.103**	**0.809**
z8	**0.965**	**0.0804**	**94.64%**	**6.0**	**0.38**	**342**	**0.320**	**0.047616**	**3.053**	**0.013825**	**3.240**	**0.002106**	**0.211**	**0.896**
KCM081182 — Mascall Tuff														
z1 (23)	0.614	0.0148	77.01%	1.0	0.37	78	0.198	0.052884	25.275	0.017695	25.447	0.002427	0.538	0.329
z2 (24)	0.979	0.0323	46.16%	0.3	3.13	34	0.316	0.053170	12.719	0.020065	13.073	0.002737	1.117	0.354
z3 (26)	**1.078**	**0.3483**	**98.69%**	**26.1**	**0.38**	**1373**	**0.348**	**0.046575**	**0.339**	**0.015254**	**0.382**	**0.002375**	**0.090**	**0.644**
z4 (28)	**0.934**	**0.0316**	**53.05%**	**0.4**	**2.32**	**38**	**0.301**	**0.050899**	**10.817**	**0.016771**	**11.226**	**0.002390**	**0.815**	**0.528**
z5 (29)	0.684	0.0325	85.36%	1.8	0.46	123	0.221	0.050472	5.198	0.016645	5.433	0.002392	0.347	0.694
z6 (9)	**0.709**	**0.3955**	**98.12%**	**16.5**	**0.63**	**959**	**0.229**	**0.046675**	**0.483**	**0.015290**	**0.529**	**0.002376**	**0.082**	**0.664**
z7 (22)	0.474	0.0257	82.19%	1.4	0.46	101	0.153	0.048386	9.839	0.015994	10.070	0.002397	0.398	0.591
WNMF081158 — Hawk Rim														
z1 (2)	**0.453**	**0.1208**	**95.29%**	**6.0**	**0.50**	**383**	**0.146**	**0.046708**	**1.414**	**0.016237**	**1.513**	**0.002521**	**0.121**	**0.838**
z2 (8)	**0.346**	**0.0652**	**91.50%**	**3.1**	**0.50**	**212**	**0.112**	**0.048152**	**2.794**	**0.016767**	**2.957**	**0.002525**	**0.177**	**0.925**
z3 (39)	**0.381**	**0.0477**	**88.26%**	**2.2**	**0.53**	**154**	**0.123**	**0.048338**	**4.792**	**0.016867**	**4.969**	**0.002531**	**0.262**	**0.688**
z4 (36)	**0.354**	**0.0648**	**87.41%**	**2.0**	**0.77**	**143**	**0.114**	**0.047802**	**3.547**	**0.016661**	**3.761**	**0.002528**	**0.245**	**0.877**
z5 (31)	**0.344**	**0.1215**	**95.22%**	**5.7**	**0.51**	**378**	**0.111**	**0.047043**	**1.527**	**0.016373**	**1.625**	**0.002524**	**0.141**	**0.716**
z6 (25)	**0.358**	**0.0916**	**92.99%**	**3.8**	**0.57**	**258**	**0.116**	**0.047545**	**2.047**	**0.016567**	**2.186**	**0.002527**	**0.152**	**0.919**
z7 (44)	**0.477**	**0.0978**	**93.99%**	**4.7**	**0.52**	**300**	**0.154**	**0.048090**	**1.813**	**0.016763**	**1.936**	**0.002528**	**0.148**	**0.845**
z8 (45)	**0.359**	**0.1104**	**92.75%**	**3.7**	**0.72**	**249**	**0.116**	**0.048355**	**1.994**	**0.016845**	**2.130**	**0.002527**	**0.155**	**0.886**

Sample (a)	Isotopic Ages $\frac{^{207}Pb}{^{206}Pb}$ (g)	± (f)	$\frac{^{207}Pb}{^{235}U}$ (g)	± (f)	$\frac{^{206}Pb}{^{238}U}$ (g)	± (f)
KCM61023a — Kangaroo Tuff						
z1	**54**	**36**	**13.79**	**0.22**	**13.557**	**0.015**
z2	**170**	**224**	**14.57**	**1.46**	**13.648**	**0.076**
z3	**164**	**89**	**14.46**	**0.58**	**13.578**	**0.034**
z4	**221**	**311**	**14.83**	**2.07**	**13.595**	**0.099**
z5	**108**	**68**	**14.14**	**0.43**	**13.595**	**0.026**
z6	**230**	**128**	**14.91**	**0.87**	**13.610**	**0.048**
z7	**40**	**29**	**13.70**	**0.18**	**13.551**	**0.014**
z8	**80**	**72**	**13.94**	**0.45**	**13.560**	**0.028**
KCM081182 — Mascall Tuff						
z1 (23)	324	573	17.81	4.49	15.625	0.084
z2 (24)	336	288	20.17	2.61	17.619	0.197
z3 (26)	**28**	**8**	**15.37**	**0.06**	**15.294**	**0.014**
z4 (28)	**236**	**249**	**16.89**	**1.88**	**15.387**	**0.125**
z5 (29)	217	120	16.76	0.90	15.400	0.053
z6 (9)	**33**	**12**	**15.41**	**0.08**	**15.298**	**0.012**
z7 (22)	118	231	16.11	1.61	15.436	0.061
WNMF081158 — Hawk Rim						
z1 (2)	**34**	**34**	**16.35**	**0.25**	**16.232**	**0.020**
z2 (8)	**107**	**66**	**16.88**	**0.50**	**16.259**	**0.029**
z3 (39)	**116**	**113**	**16.98**	**0.84**	**16.294**	**0.043**
z4 (36)	**90**	**84**	**16.78**	**0.63**	**16.275**	**0.040**
z5 (31)	**51**	**36**	**16.49**	**0.27**	**16.252**	**0.023**
z6 (25)	**77**	**49**	**16.68**	**0.36**	**16.271**	**0.025**
z7 (44)	**104**	**43**	**16.88**	**0.32**	**16.277**	**0.024**
z8 (45)	**117**	**47**	**16.96**	**0.36**	**16.267**	**0.025**

Weighted Mean Calculations

$^{206}Pb/^{238}U$ ± random (+tracer) [+l]			**MSWD**	**prob. Fit**
13.564	± 0.009 (0.016) [0.022]	**± 2s int.**	**2.78**	0.0068
	± 0.018 (0.022) [0.027]	**± 95% c.i.***	**n =**	8

*** 95% conf. int. = 2s * Student's T * (MSWD)^0.5**

$^{206}Pb/^{238}U$ ± random (+tracer) [+l]			**MSWD**	**prob. Fit**
15.297	± 0.009 (0.012) [0.020]	**± 2s int.**	**1.12**	0.325
	± 0.015 (0.017) [0.024]	**± 95% c.i.***	**n =**	3

*** 95% conf. int. = 2s * Student's T * (MSWD)^0.5**

t

$^{206}Pb/^{238}U$ ± random (+tracer) [+l]			**MSWD**	**prob. Fit**
16.260	± 0.009 (0.012) [0.021]	**± 2s int.**	**2.13**	0.037
	± 0.016 (0.018) [0.025]	**± 95% c.i.***	**n =**	8

*** 95% conf. int. = 2s * Student's T * (MSWD)^0.5**

(a) z1, z2 etc. are labels for CL-imaged zircon grains annealed and chemically abraded after Mattinson (2005); the number in parentheses represents the LA-ICPMS spot analysis for the associated grain.

(b) Model Th/U ratio calculated from radiogenic 208Pb/206Pb ratio and 207Pb/235U age.

(c) Pb* and Pbc represent radiogenic and common Pb, respectively; mol % ^{206}Pb* with respect to radiogenic, blank and initial common Pb.

(d) Measured ratio corrected for spike and fractionation only. Fractionation estimated at 0.15 +/- 0.03 %/a.m.u. for Daly analyses, based on analysis of NBS-981 and NBS-982.

(e) Corrected for fractionation, spike, and common Pb; up to 1 pg of common Pb was assumed to be procedural blank: 206Pb/204Pb = 18.042 ± 0.61%; 207Pb/204Pb = 15.537 ± 0.52%; 208Pb/204Pb = 37.686 ± 0.63% (all uncertainties 1-sigma).

Excess over blank was assigned to initial common Pb, using the Stacey and Kramers (1975) two-stage Pb isotope evolution model at the nominal sample age.

(f) Errors are 2-sigma, propagated using the algorithms of Schmitz and Schoene (2007).

(g) Calculations are based on the decay constants of Jaffey et al. (1971). 206Pb/238U and 207Pb/206Pb ages corrected for initial disequilibrium in 230Th/238U using Th/U [magma] = 3.

3: Systematic Paleontology of previously reported taxa from the type Mascall Fauna.

Class MAMMALIA Linnaeus, 1758
Order CARNIVORA Bowdich, 1821
Family CANIDAE Fischer, 1817
Genus TEPHROCYON Merriam, 1906
Tephrocyon rurestris Condon, 1896

Occurrence – Cottonwood Creek, UCMP V4834, JDNM-4*, JDNM-71.
Holotype – From Cottonwood Creek: skull with right C1(broken), P1 alveoli, left and right P2-M2 (left P3 broken) and mandible with canine, p1 alveoli and left and right p2-m3, OU 23077 (Wang et al., 1999: fig. 68).
Referred material–From Cottonwood Creek: partial dentary with p4-m1, UO 24191; maxillary fragment with P4, UO 24192; left P4, M1-2, right P4, and left m2 and m3, YPM 12713 (Downs, 1956L fig. 12a). From V4834: partial left m1, UCMP 39297 (Downs, 1956: fig. 12c). From JDNM-4*: left p4 through m2, JODA 1336; partial m1, JODA 2318; right dentary with p4-m, JODA 2396. From JDNM-71: right upper M1, JODA 6644.
Comments – These specimens were originally identified as *Tomarctus rurestris* and then recombined to *Tephrocyon rurestris* according to Wang et al. (1999). The complete description of the holotype and species description are presented in Wang et al. (1999).

Family MUSTELIDAE Fischer, 1817
Genus LEPTARCTUS Leidy, 1857
Leptarctus oregonensis Stock, 1930

Occurrence – CIT 113, JDNM-262, UCMP V4824, UCMP V4825, JDNM-71.
Holotype – From CIT 113: Left partial maxilla with P4 and M1, right partial maxilla with P4, upper right M1, incisor, nasals, zygomatic arches, occipital crest, CIT 206.
Referred material –From JDNM-262: partial skull including the cranial cavity, zygomatic arches, and complete palate with left and right M1, UO 10869. From V4824: right P4 , UCMP 39102. From V4825: dentary fragment with right m1 and the two roots of p4, JODA 3335. From JDNM-71: left second phalanx, JODA 7500.
Comments – This species is well documented from the Mascall in Stock (1930) and Downs (1956). UO 10869, recovered from the Mascall Tuff during road excavation is added to the referred material list here. JODA 7500 extends the known range of the species to the lower Mascall unit. CIT 206 dimensions of the individual teeth are P4: ap=6.03, t=4.81; ap=6.3, t=5.18; M1: ap=7.12, t=6.2; ap=6.9, t=6.51; I: ap=2.38, t=1.8. The locality for the type specimen (CIT 113) is described by Stock (1930) as “Mascall deposits north of the east for of the John Day River, approximately, 1.5 miles northwest of Dayville, Oregon.

Carnivora indet.

Occurrence – UCMP V4830, V4834, UCMP -903, JDNM-262.

Referred Material – From UCMP V4830: lower canine, UCMP 33107. From V4834: axis, JODA 15606. From -903: distal section of a metatarsal or metacarpal, UCMP 2067. From JDNM-262: vertebra, JODA 15340.
Description and Comments – UCMP 33107 and UCMP 2067 are described in Downs (1956). The length of JODA 15340 is 27.36 mm. This specimen was recovered from the Mascall Tuff, *in situ.*

Order PERRISODACTYL Owen, 1848
Family EQUIDAE Gray, 1821
Genus ARCHAEOHIPPUS Gidley, 1906
Archaeohippus ultimus Cope, 1886

Occurrence – CIT 113, Cottonwood Creek, UCMP -3059, UCMP -903.
Holotype – From Cottonwood Creek: "nearly complete superior dentition with palate and sides of skull to the middle of the orbits and top of skull to above the infraorbital foramen" Cope (1886), AM 8174.
Referred material – From Cottonwood Creek: "part of ramus with roots of one premolar and part of another" Downs (1956), USNM 18746; single lower premolar, USNM 3909. From CIT 113: lower premolar, CIT 424. From unknown locality from the "Condon Collection": lower premolars, YPM 14258, 14259. From -3059: lower right molar, UCMP 31987; lower left molar, UCMP 26643; left lower dp4, JODA 41195. From -903: right M3 and left P3, UCMP 1689; partial dentary with p3 through p4, UCMP 1700. From JDNM-4: right dentary fragment with m2 and m3, JODA 7010; right dentary fragment with p4-m2, JODA 7368; right lower molar, JODA 14141; right lower molar, JODA 14620; left M2, JODA JXA610-103
Comments – All specimens are described in Downs (1956) except UCMP 41195 and JODA specimens. Measurements for JODA material: JODA 41195 ap=14.35 mm and t=8.95 mm; JODA 7010 m2 ap=11.03 mm, t=7.85 mm and m3 ap=15.19 mm, t=7.06 mm; JODA 7368 p4 ap=11.66 mm, t=8.38 mm, m1 ap=11.34 mm, t=9.18 mm and m2 ap=11.03 mm, t=7.59 mm; JODA 14141 ap=13.29 mm, t=7.09 mm; JODA 14620 ap=13.39 mm, t=7.21 mm; JODA JXS610-103 ap=13.85 mm, t=16.07 mm. The lower molars have metaconid and metastylid separate and well developed hypoconulid. YPM 14258 and 14259 are listed from Mascall Ranch in the YPM database and Downs (1956) states they are most likely from the Mascall Formation.

Order ARDIODACTYLA Owen, 1848
Family MERYCOIDODONTIDAE Thorpe, 1923

Occurrence – JDNM-4*, V4834 Mascall 20
Referred Material – From JDNM-4*: left m1 and partial m2 in jaw fragment, JODA 2361. From V4834: canine, JODA 4264; astragulus, UCMP 39313.
Comments – JODA 2362 is too large for *Ticholeptus* and lacks significant diagnostic material (length = 18.09, width = 12.59). JODA 4264 is a complete canine however not diagnosable to genus or species. UCMP 39313 was reported by Downs (1956) (ap=8.0 mm and t=6.6 mm).

Family CAMELIDAE

Genus MIOLABIS Hay, 1899
Miolabis transmontanus Cope, 1879

Occurrence – Cottonwood Creek, JDNM-4*
Referred Material – Cottonwood Creek: nearly complete cranium, AM8196; JDNM-4*: nearly complete mandible, JODA 1326.
Comments – AM 8196 is the type specimen for *Miolabis transmontanus* named by Cope (=*Protolabis transmontanus*). Honey et al. (1998) used this specimen as the type for the genus. The skull was found by Charles Sternberg in the Cottonwood Creek area. Measurements for AM 8196 are presented in Cope (1879) and Downs (1956), and figured in Cope (1886). JODA 1326 is assigned to this species based on the following: no p1, premolars stouter and less compressed than *Protolabis*, p2 shortened and simplified, p3 is shortened with a high, central protoconid, p4 has enlarged hypoconid, molars low crowned, however they do not have strong metastylids (this may be due to the extreme wear of the teeth), m3 less anteroposteriorly expanded relative to m2 than in *Protolabis*. Measurements for JODA 1326: m3 ap=28.24, mm t=13.7 mm; m2 ap=18.98 mm, t=14.9 mm; m1 ap=15.14 mm, t=12.31 mm; p4 ap=13.37 mm, t=7.29 mm; p3 ap=13.47 mm, t=5.87 mm; p2 ap=9.18 mm, t=4.94 mm; canine ap=8.91 mm; i3 ap=7.03 mm, t=5.22 mm; i2 ap=8.45 mm, t=5.16 mm; i1 ap=8.04 mm, t=5.35 mm; diastema=39.76 mm. JODA 1326 may be the mandible to the skull found by Sternberg. Both specimens have heavily worn teeth however it is unclear where JODA 1326 was found.

Family PALEOMERYCIDAE Lydekker, 1883
Genus DROMOMERYX Frick, 1937
Dromomeryx borealis Cope, 1878

Occurrence – UCMP -3059, V4835, V4831, V4832, CIT 184, Cottonwood Creek
Referred Material – From UCMP -3059: partial skull with complete horns and post cranial elements, UCMP 1486; P4, UCMP 29985. From V4835: left partial mandible with p2-m2 and parts of three lumbar vertebrae, UCMP 39185; P4, UCMP 39301. From V4831: m1, UCMP 39293. From V4832: partial calcaneum and distal tibia, UCMP 39305. From CIT 184: horn with partial cranium and orbit, CIT 799. From Cottonwood Creek: right P3 and M3, USNM 5515; left P2-M3, right P3-M3, left p3-m1, m3 and postcranial material, USNM 5516; i1-i3, canine, partial mandible with right p2-m3 and postcranial material, USNM 5517; left M1-M2 and right P4-M2 and distal tibia, AMNH 8204; isolated M1 and M1-M3, AMNH 1486.
Comments - All specimens are described in Downs (1956). Downs (1956) also lists several specimens assigned to this taxon that have uncertain provenance, but states they are most likely from the Mascall.

Order RODENTIA Bowditch, 1821
Family HETEROMYIDAE Gray 1868
Genus PRODIPODOMYS Hibbard, 1939
Prodipodomys mascallensis Downs, 1956

Occurrence – V4830, V4833, CIT 1869
Holotype – From V4830: left dentary with i1, p4-m3, UCMP 39094

Referred Material – From V4833: partial maxilla with partial palate, left P4 and M1, UCMP 39895. From CIT 1869: p4 and m1; CIT 4002B.

Description – All material is described in Downs (1956). For UCMP 39094 and CIT 4002B the p4 has an x-pattern and 2 roots, the m1 and m2 are subequal with an H-pattern, and the m3 is small. Downs originally assigned the type specimen to *P. mascallensis*. It was reassigned to *Mojavemys mascallensis* by Lindsay (1972) and Barnosky (1986). Korth (1979) and Whistler (1984) suggested it should be assigned to *Cupidinimus* but did not provide evidence for doing so. Wahlert (1991) used *P. mascallensis* for comparison with *Harrymys* and suggested that it was a candidate to include in *Harrymys* based on the R shaped lower molars. It is assigned to *Prodipodomys mascallensis* by Flynn et al. (2008). UCMP 39895 is assigned here to this taxon but may belong to *Cupidinimus halli* based on the following: the protocone on P4 is distinct and does not attach to the hypostyle lingually; however, it connects to the metacone-hypocone complex more lingually than other species in the genus. There is no accessory cusp on the P4. The P4 is slightly wider than the M1. Downs (1956) assigned this tentatively to *Peridiomys* cf. *oregonensis* but was unsure if it belonged to Heteromyinae or Perognathinae. The hypsodonty of the premolar and first molar place it within Dipodomyinae (Flynn et al. 2008). Korth (1997) discusses the taxonomic confusion surrounding *P. mascallensis* because its cheek teeth are smaller and higher crowned than *Peridiomys,* it is stratigraphically much younger than the otherwise first occurrence of *Prodipodomys* in the Hemphillian, and it is much smaller with lophate, lower crowned molars than any species of *Mojavemys*, suggesting it may represent an as yet unnamed genus of heteromyid.

APPENDIX B: CHAPTER 3 SUPPLEMENTARY DATA FILES

S3.1. Results of the permutational multivariate analysis of variance when the Recent occurrence dataset is subsampled to be the same size as the LGM occurrence data set. *P*-values were adjusted using a Bonnferoni correction.

Simulation	***Canis latrans***	***Cryp. parva***	***Geomys burs.***	***Lynx rufus***	***Micro. penn.***	***Och. princeps***	***Odo. hem.***	***Phen. inter.***	***Scal. aqua.***	***Sperm. trid.***	***Sylv. aud.***	***Syn. coop.***	***Tamias stria.***	***Thom. bott.***	***Uro. cin.***
1	0.1	0.1	0.1	1	0.1	0.1	1	0.1	0.1	0.1	1	0.1	0.1	0.7	1
2	0.1	0.2	0.1	0.2	0.1	0.1	1	0.1	0.2	0.1	1	0.1	0.1	1	0.4
3	0.1	0.1	0.1	1	0.1	0.1	1	0.1	0.1	0.1	1	0.1	0.1	1	0.1
4	0.1	0.2	0.1	1	0.1	0.1	1	0.1	0.1	0.1	1	0.1	0.1	1	1
5	0.1	0.4	0.1	1	0.1	0.1	1	0.1	0.1	0.1	1	0.1	0.1	1	1
6	0.1	0.2	0.1	0.3	0.1	0.1	1	0.1	0.1	0.1	1	0.1	0.1	0.4	0.1
7	0.1	0.1	0.1	1	0.1	0.1	1	0.1	0.1	0.1	1	0.1	0.1	1	0.6
8	0.1	0.1	0.1	1	0.1	0.1	0.6	0.1	0.1	0.1	1	0.1	0.1	0.5	0.5
9	0.1	0.2	0.1	1	0.1	0.1	1	0.1	0.1	0.1	1	0.1	0.1	1	1
10	0.1	0.2	0.1	0.3	0.1	0.1	1	0.1	0.1	0.1	1	0.1	0.1	0.4	0.2
11	0.1	0.3	0.1	1	0.1	0.1	1	0.1	0.1	0.1	1	0.1	0.1	1	0.6
12	0.1	0.1	0.1	1	0.1	0.1	1	0.1	0.1	0.1	1	0.1	0.1	0.1	0.4
13	0.1	0.1	0.1	1	0.1	0.1	1	0.1	0.2	0.1	1	0.1	0.1	1	1
14	0.1	0.1	0.1	0.1	0.1	0.1	1	0.1	0.1	0.1	1	0.1	0.1	1	0.4
15	0.1	0.1	0.1	1	0.1	0.1	1	0.1	0.1	0.1	1	0.1	0.1	0.3	0.5
16	0.1	0.1	0.1	1	0.1	0.1	1	0.1	0.1	0.1	1	0.1	0.1	0.3	1
17	0.1	0.3	0.1	1	0.1	0.1	1	0.1	0.1	0.1	1	0.1	0.1	1	0.3
18	0.1	0.3	0.1	1	0.1	0.1	1	0.1	0.1	0.1	1	0.1	0.1	0.5	0.1
19	0.1	0.2	0.1	1	0.1	0.1	0.7	0.1	0.1	0.1	1	0.1	0.1	1	0.4
20	0.1	0.1	0.1	1	0.1	0.1	1	0.1	0.1	0.1	1	0.1	0.1	0.2	0.3
21	0.1	0.1	0.1	1	0.1	0.1	1	0.1	0.1	0.1	1	0.1	0.1	0.7	1
22	0.1	0.1	0.1	1	0.1	0.1	1	0.1	0.1	0.1	1	0.1	0.1	0.4	0.2
23	0.1	0.3	0.1	1	0.1	0.1	1	0.1	0.1	0.1	1	0.1	0.1	0.5	0.5
24	0.1	0.1	0.1	1	0.1	0.1	1	0.1	0.1	0.1	1	0.1	0.1	1	1
25	0.1	0.1	0.1	1	0.1	0.1	1	0.1	0.1	0.1	1	0.1	0.1	0.3	0.1

Simulation	***Canis latrans***	***Cryp. parva***	***Geomys burs.***	***Lynx rufus***	***Micro. penn.***	***Och. princeps***	***Odo. hem.***	***Phen. inter.***	***Scal. aqua.***	***Sperm. trid.***	***Sylv. aud.***	***Syn. coop.***	***Tamias stria.***	***Thom. bott.***	***Uro. cin.***
26	0.1	0.2	0.1	1	0.1	0.1	1	0.1	0.3	0.1	1	0.1	0.1	1	0.2
27	0.1	0.2	0.1	1	0.1	0.1	1	0.1	0.1	0.1	1	0.1	0.1	0.8	0.4
28	0.1	0.3	0.1	1	0.1	0.1	1	0.1	0.1	0.1	1	0.1	0.1	0.4	1
29	0.1	0.3	0.1	0.7	0.1	0.2	1	0.1	0.1	0.1	1	0.1	0.1	1	0.4
30	0.1	0.1	0.1	1	0.1	0.1	1	0.1	0.1	0.1	1	0.1	0.1	0.2	0.4
31	0.1	0.1	0.1	1	0.1	0.1	1	0.1	0.1	0.1	1	0.1	0.1	0.3	0.2
32	0.1	0.2	0.1	1	0.1	0.1	1	0.1	0.1	0.1	1	0.1	0.1	1	1
33	0.1	0.2	0.1	1	0.1	0.1	1	0.1	0.1	0.1	1	0.1	0.1	1	0.4
34	0.1	0.2	0.1	1	0.1	0.1	1	0.1	0.1	0.1	1	0.1	0.1	0.3	1
35	0.1	0.2	0.1	1	0.1	0.1	1	0.1	0.1	0.1	1	0.1	0.1	0.8	1
36	0.1	0.1	0.1	1	0.1	0.2	1	0.1	0.2	0.1	1	0.1	0.1	1	1
37	0.1	0.1	0.1	1	0.1	0.1	1	0.1	0.1	0.1	1	0.1	0.1	0.9	0.2
38	0.1	0.1	0.1	1	0.1	0.1	1	0.1	0.1	0.1	1	0.1	0.1	1	0.2
39	0.1	0.5	0.1	1	0.1	0.1	1	0.1	0.1	0.1	1	0.1	0.1	0.5	0.1
40	0.1	0.1	0.1	1	0.1	0.3	1	0.1	0.1	0.1	1	0.1	0.1	1	0.9
41	0.1	0.3	0.1	1	0.1	0.1	1	0.1	0.1	0.1	1	0.1	0.1	1	0.3
42	0.1	0.6	0.1	1	0.1	0.1	1	0.1	0.1	0.1	1	0.1	0.1	0.1	0.1
43	0.1	0.1	0.1	0.3	0.1	0.1	1	0.1	0.1	0.1	1	0.1	0.1	1	0.6
44	0.1	0.3	0.1	1	0.1	0.1	1	0.1	0.1	0.1	1	0.1	0.1	1	0.3
45	0.1	0.1	0.1	1	0.1	0.1	1	0.1	0.1	0.1	1	0.1	0.1	1	0.9
46	0.1	0.1	0.1	1	0.1	0.1	0.9	0.1	0.1	0.1	1	0.1	0.1	0.7	0.9
47	0.1	0.1	0.1	1	0.1	0.1	1	0.1	0.3	0.1	1	0.1	0.1	1	0.5
48	0.1	0.1	0.1	1	0.1	0.1	1	0.2	0.1	0.1	1	0.1	0.1	0.7	0.4
49	0.1	0.3	0.1	1	0.1	0.1	1	0.1	0.1	0.1	1	0.1	0.1	1	0.1
50	0.1	0.1	0.1	1	0.1	0.1	1	0.1	0.1	0.1	1	0.1	0.1	0.3	0.4
51	0.1	0.1	0.1	1	0.1	0.1	1	0.1	0.1	0.1	1	0.1	0.1	0.9	0.1
52	0.1	0.1	0.1	0.3	0.1	0.1	1	0.1	0.1	0.1	1	0.1	0.1	0.1	0.6
53	0.1	0.4	0.1	1	0.1	0.1	1	0.1	0.1	0.1	1	0.1	0.1	1	0.3
54	0.1	0.2	0.1	1	0.1	0.1	0.8	0.1	0.1	0.1	1	0.1	0.1	1	0.2

Simulation	*Canis latrans*	*Cryp. parva*	*Geomys burs.*	*Lynx rufus*	*Micro. penn.*	*Och. princeps*	*Odo. hem.*	*Phen. inter.*	*Scal. aqua.*	*Sperm. trid.*	*Sylv. aud.*	*Syn. coop.*	*Tamias stria.*	*Thom. bott.*	*Uro. cin.*
55	0.1	0.2	0.1	1	0.1	0.1	1	0.1	0.1	0.1	1	0.1	0.1	0.3	0.8
56	0.1	0.1	0.1	0.5	0.1	0.1	1	0.1	0.1	0.1	1	0.1	0.1	0.1	0.1
57	0.1	0.1	0.1	0.9	0.1	0.1	1	0.1	0.1	0.1	1	0.1	0.1	1	0.8
58	0.1	0.2	0.1	1	0.1	0.1	1	0.1	0.1	0.1	0.2	0.1	0.1	0.3	0.4
59	0.1	0.1	0.1	0.3	0.1	0.1	1	0.1	0.1	0.1	1	0.1	0.1	1	0.2
60	0.1	0.2	0.1	1	0.1	0.1	1	0.1	0.1	0.1	1	0.1	0.1	0.4	0.2
61	0.1	0.1	0.1	0.9	0.1	0.1	1	0.1	0.1	0.1	1	0.1	0.1	0.7	0.3
62	0.1	0.5	0.1	1	0.1	0.1	1	0.1	0.2	0.1	1	0.1	0.1	0.1	1
63	0.1	0.1	0.1	1	0.1	0.1	1	0.1	0.2	0.1	1	0.1	0.1	1	1
64	0.1	0.1	0.1	1	0.1	0.1	1	0.1	0.2	0.1	1	0.1	0.1	1	1
65	0.1	0.1	0.1	1	0.1	0.1	0.9	0.1	0.1	0.1	1	0.1	0.1	1	0.3
66	0.1	0.1	0.1	1	0.1	0.1	1	0.1	0.1	0.1	1	0.1	0.1	0.5	0.3
67	0.1	0.2	0.1	1	0.1	0.1	1	0.1	0.2	0.1	1	0.1	0.1	0.1	0.5
68	0.1	0.1	0.1	0.2	0.1	0.1	1	0.1	0.1	0.1	1	0.1	0.1	1	0.2
69	0.1	0.1	0.1	1	0.1	0.1	1	0.1	0.1	0.1	1	0.1	0.1	1	0.5
70	0.1	0.1	0.1	1	0.1	0.1	1	0.1	0.1	0.1	1	0.1	0.1	0.5	0.3
71	0.1	0.1	0.1	1	0.1	0.1	1	0.1	0.1	0.1	1	0.1	0.1	0.3	0.7
72	0.1	0.2	0.1	1	0.1	0.5	1	0.1	0.1	0.1	1	0.1	0.1	0.2	1
73	0.1	0.1	0.1	0.3	0.1	0.1	1	0.1	0.2	0.1	1	0.1	0.1	1	0.3
74	0.1	0.2	0.1	0.5	0.1	0.1	1	0.1	0.1	0.1	1	0.1	0.1	1	1
75	0.1	0.1	0.1	1	0.1	0.1	0.9	0.1	0.1	0.1	1	0.1	0.1	1	0.7
76	0.1	0.1	0.1	1	0.1	0.1	1	0.1	0.1	0.1	0.1	0.1	0.1	0.8	0.3
77	0.1	0.1	0.1	1	0.1	0.1	1	0.1	0.1	0.1	1	0.1	0.1	0.4	1
78	0.1	0.2	0.1	1	0.1	0.1	1	0.1	0.1	0.1	1	0.1	0.1	0.1	0.1
79	0.1	0.1	0.1	0.7	0.1	0.1	1	0.1	0.1	0.1	1	0.1	0.1	1	0.5
80	0.1	0.2	0.1	1	0.1	0.1	1	0.1	0.1	0.1	1	0.1	0.1	0.3	0.8
81	0.1	0.2	0.1	1	0.1	0.1	1	0.1	0.2	0.1	1	0.1	0.1	0.6	0.1
82	0.1	0.4	0.1	1	0.1	0.1	0.7	0.1	0.1	0.1	1	0.1	0.1	0.1	0.1
83	0.1	0.1	0.1	0.2	0.1	0.1	1	0.1	0.1	0.1	1	0.1	0.1	1	1

Simulation	***Canis latrans***	***Cryp. parva***	***Geomys burs.***	***Lynx rufus***	***Micro. penn.***	***Och. princeps***	***Odo. hem.***	***Phen. inter.***	***Scal. aqua.***	***Sperm. trid.***	***Sylv. aud.***	***Syn. coop.***	***Tamias stria.***	***Thom. bott.***	***Uro. cin.***
84	0.1	0.2	0.1	1	0.1	0.1	1	0.1	0.1	0.1	1	0.1	0.1	0.3	0.3
85	0.1	0.3	0.1	1	0.1	0.1	1	0.1	0.1	0.1	1	0.1	0.1	1	0.5
86	0.1	0.1	0.1	1	0.1	0.1	1	0.1	0.1	0.1	1	0.1	0.1	0.9	0.5
87	0.1	0.4	0.1	0.8	0.1	0.1	1	0.1	0.1	0.1	1	0.1	0.1	1	0.5
88	0.1	0.6	0.1	1	0.1	0.1	1	0.1	0.1	0.1	1	0.1	0.1	0.4	1
89	0.1	0.2	0.1	1	0.1	0.1	1	0.1	0.1	0.1	1	0.1	0.1	1	0.5
90	0.1	0.1	0.1	1	0.1	0.1	1	0.1	0.1	0.1	1	0.1	0.1	1	0.5
91	0.1	0.1	0.1	1	0.1	0.1	1	0.1	0.1	0.1	1	0.1	0.1	1	0.2
92	0.1	0.2	0.1	1	0.1	0.1	1	0.1	0.1	0.1	1	0.1	0.1	1	0.5
93	0.1	0.1	0.1	1	0.1	0.1	1	0.1	0.1	0.1	1	0.1	0.1	1	0.2
94	0.1	0.1	0.1	1	0.1	0.1	1	0.1	0.1	0.1	1	0.1	0.1	1	0.1
95	0.1	0.1	0.1	1	0.1	0.1	1	0.1	0.1	0.1	1	0.1	0.1	1	0.9
96	0.1	0.1	0.1	1	0.1	0.1	1	0.1	0.1	0.1	1	0.1	0.1	1	0.3
97	0.1	0.2	0.1	1	0.1	0.1	1	0.1	0.1	0.1	1	0.1	0.1	0.8	0.1
98	0.1	0.2	0.1	1	0.1	0.1	1	0.1	0.1	0.1	1	0.1	0.1	1	0.5
99	0.1	0.2	0.1	1	0.1	0.1	1	0.1	0.1	0.1	1	0.1	0.1	1	0.2
100	0.1	0.2	0.1	0.2	0.1	0.1	0.7	0.1	0.1	0.1	1	0.1	0.1	0.6	0.7

S3.2 Significant differences in species MAT and MAP values using Mann Whitney U Tests. $p<0.05$*, $p<0.01$**, $p<0.001$***.. *P*-values were adjusted using a Bonnferoni correction.

Family	**Species**	**MAT**	**MAP**
Soricidae	*Cryptotis parva*	<0.001***	1
Talpidae	*Scalopus aquaticus*	<0.001***	1
Ochotonidae	*Ochotona princeps*	<0.001***	<0.001***
Leporidae	*Sylvilagus audobonii*	0.925	1
Sciuridae	*Tamias striatus*	<0.001***	1
	Spermophilus tridecemlineatus	<0.001***	1
Geomyidae	*Geomys bursarius*	<0.001***	1
	Thomomys bottae	0.0112*	1
Cricetidae	*Microtus pennsylvanicus*	<0.001***	1
	Phenacomys intermedius	<0.001***	0.068
	Synaptomys cooperi	<0.001***	1
Canidae	*Canis latrans*	<0.001***	1
	Urocyon cinereoargenteus	0.004**	1
Felidae	*Lynx rufus*	0.011*	1
Cervidae	*Odocoileus hemionus*	0.080	0.060